

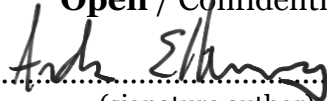


FACULTY OF SCIENCE AND TECHNOLOGY  
MASTER THESIS

Study programme / specialisation:  
Marine and Offshore Technology

The spring semester, 2022

Author:  
Andre Eltervaag

**Open / Confidential**  
  
.....  
(signature author)

Course coordinator:  
Professor Yihan Xing

Supervisor(s):  
Associate Prof. Lin Li  
Prof. Emeritus Sverre Haver

Thesis title:  
Long Term Response Analyses of a Jacket  
Structure with Focus on a Peak Over  
Threshold Approach

Credits (ECTS): 30

Keywords:  
Peak Over Threshold, Jacket structure,  
Modified all sea state, Time-domain  
simulation, Long term analysis

Pages: 106  
+ appendix: 11

Stavanger, 15.06.2022  
date/year

---



## ACKNOWLEDGMENT

I would like to express my gratitude to my supervisor, Associate Professor Lin Li, for helping me during this last chapter of the master's program at the University of Stavanger. Thank you for the interest you have taken in my work and for all guidance in the subject.

I also wish to extend my gratitude to Professor Emeritus Sverre Haver, who has been my co-supervisor for the thesis. Thank you for sharing your knowledge and for the inspiring conversations on the thesis topic.

Lastly, a final thanks goes to the University of Stavanger, for giving me the opportunity to take the Master's degree within Marine and Offshore Technology.

## ABSTRACT

This thesis investigates the use of long term analysis to estimate the q-probability responses of a non-linear problem. The structure subjected to the investigations is a realistic jacket found in the Norwegian Continental Shelf (NCS) with slightly increased deck mass to increase the dynamic behaviour. The following responses are investigated, airgap, deck displacement, overturning moment and base shear. The long term analysis q-probability responses are obtained using the peak over threshold (POT) method and a modified all sea state approach. Hindcast data from a reference site in the Norwegian Sea is used with over 61 years of metocean data.

The responses from the jacket structure follow a Gumbel distribution. Therefore, the maximum response for each 3-hour simulation is obtained, and Gumbel's location and shape parameters are assessed for each sea state by method of moments. The unknown sea states between the simulated sea states are known by an interpolation function named spline. As a result, a response surface is obtained as the short term variability for the 3-hour maximum responses.

The modified all sea state method uses the joint distribution of all 3-hour sea states over 8 metres (m). The probability density of the joint distribution of sea states is multiplied by the short term response surfaces to obtain the long term distribution of a 3-hour maximum response. The q-probability values correspond to a 100-year and 10.000-year response value.

The POT approach is implemented as the long term distribution of a response given the most probable maximum response for a random storm. Each storm is sequenced by 3-hour storm steps which are assumed stationary. The long term analysis is achieved by multiplying the conditional distribution of storm maximum response given the most probable maximum response with the long term distribution of most probable maximum responses. The q-probability is the same as for modified all sea state.

The long term analysis results demonstrate that for a jacket structure, the q-probability responses are less conservatively estimated by the POT. This implies that for design work, the

responses obtained by the POT following the guidelines for q-probability will have a better cost-optimized design without disregarding or compromising the safety.

# TABLE OF CONTENTS

<b>ACKNOWLEDGMENT .....</b>	<b>I</b>
<b>ABSTRACT .....</b>	<b>II</b>
<b>1. INTRODUCTION.....</b>	<b>1</b>
1.1 BACKGROUND.....	1
1.2 OBJECTIVE.....	3
1.3 THESIS OUTLINE.....	4
<b>2. WAVE DATA AND MODELLING .....</b>	<b>7</b>
2.1 HINDCAST DATASET.....	9
2.2 SITE-SPECIFIC HINDCAST ANALYSIS .....	11
2.3 JOINT DISTRIBUTION OF SEA STATES .....	13
2.3.1 <i>Marginal distribution of <math>H_s</math></i> .....	14
2.3.2 <i>Conditional distribution of <math>T_p</math> given <math>H_s</math></i> .....	17
2.3.3 <i>Contour lines</i> .....	20
<b>3. PEAK OVER THRESHOLD APPROACH.....</b>	<b>25</b>
3.1 STORMS.....	28
<b>4. JACKET STRUCTURE.....</b>	<b>31</b>
4.1 MODEL.....	31
4.2 DECK DISPLACEMENT NODE .....	35
<b>5. USFOS SIMULATION .....</b>	<b>36</b>
5.1 TIME-DOMAIN SIMULATIONS .....	36
5.2 WAVE GENERATION .....	38
5.3 LOAD GOVERN RESPONSE .....	43
5.4 SPOOL TO A PEAK ELEVATION .....	45
5.5 DYNAMIC AND STATIC BEHAVIOUR OF RESPONSES.....	47
<b>6. JACKET ASSESSMENT.....</b>	<b>50</b>
6.1 AIRGAP ANALYSIS.....	50
6.2 TIME-DOMAIN SIMULATIONS .....	55
6.2.1 <i>Simulations</i> .....	55
6.2.2 <i>Distribution of 3-hour extremes</i> .....	57
6.2.3 <i>Response surface for Gumbel parameters</i> .....	59

<b>7.</b>	<b>LONG TERM ANALYSIS MODIFIED ALL SEA STATE .....</b>	<b>63</b>
7.1	MODIFIED ALL SEA STATE APPROACH .....	63
7.1.1	<i>Modified marginal distribution of <math>H_s</math></i> .....	64
7.1.2	<i>Conditional distribution of <math>T_p</math> given modified <math>H_s</math></i> .....	66
7.1.3	<i>Contour lines based on modified <math>H_s</math> values</i> .....	68
7.1.4	<i>Long term analysis</i> .....	69
<b>8.</b>	<b>LONG TERM ANALYSIS POT .....</b>	<b>71</b>
8.1	SHORT TERM MODELLING .....	71
8.2	LONG TERM ANALYSIS .....	77
8.2.1	<i>Long term analysis of mpm storm max, <math>X</math></i> .....	77
8.2.2	<i>Long term analysis of <math>X</math></i> .....	81
8.3	THRESHOLD SENSITIVITY STUDY.....	83
<b>9.</b>	<b>COMPARISON BETWEEN LONG TERM ANALYSES METHODS POT AND MODIFIED ALL SEA STATE .....</b>	<b>86</b>
<b>10.</b>	<b>CONCLUSION .....</b>	<b>88</b>
10.1	FUTURE WORK .....	89
	<b>REFERENCES.....</b>	<b>91</b>
	<b>APPENDICES.....</b>	<b>93</b>
<b>A</b>	<b>SCATTER DIAGRAM .....</b>	<b>94</b>
<b>B</b>	<b>MODIFIED SCATTER DIAGRAM.....</b>	<b>95</b>
<b>C</b>	<b>RESULTS FROM MODIFIED ALL SEA STATE.....</b>	<b>96</b>
C.1	AIRGAP .....	96
C.2	DECK DISPLACEMENT .....	97
C.3	OVERTURNING MOMENT .....	98
C.3	BASE SHEAR .....	99
<b>D</b>	<b>RESULTS FROM POT.....</b>	<b>100</b>
D.1	AIRGAP.....	100
D.2	DECK DISPLACEMENT .....	101
D.3	OVERTURNING MOMENT .....	102
D.4	BASE SHEAR .....	103

# LIST OF FIGURES

FIGURE 1: LOAD LEVEL FOR THE SAME SYSTEM UNDERGOING AN ABRUPT CHANGE FOR AN ANNUAL EXCEEDANCE PROBABILITY LOWER THAN  $ALS(10 - 4)[3]$ ..... 2

FIGURE 2: DATA CONTAINED IN A HINDCAST DATABASE..... 7

FIGURE 3: MAP OF HINDCAST LOCATION. LATITUDE 67.05, LONGITUDE 7.00 IN THE NORWEGIAN SEA. OBTAINED FROM GOOGLE MAPS. .... 9

FIGURE 4: SCATTER PLOT OF HINDCAST DATA, WITH UNCORRECTED AND CORRECTED DATA COMPARED IN THE SAME PLOT (TOTAL SEA). .... 10

FIGURE 5: WAVE PROPAGATION DIRECTION FOR ALL EVENTS IN THE HINDCAST DATASET. EACH BIN IS 30° ... 11

FIGURE 6: HISTOGRAM OF WAVE HEIGHT AND WAVE PERIOD COMPARING THE PERCENTAGE OF OCCURRENCES PER BIN. EACH BIN IS OF A LENGTH SCALE OF 1 UNIT. .... 12

FIGURE 7: MARGINAL DISTRIBUTION OF  $H_s$  FITTED WITH A 3-PARAMETER WEIBULL DISTRIBUTION. .... 14

FIGURE 8:  $H_s$  VALUES FROM THE EKOFISK AREA FITTED WITH 3-PARAMETER WEIBULL DISTRIBUTION AND COMPARED TO THE ORIGINAL SAMPLE FROM THE NORWEGIAN SEA. .... 16

FIGURE 9: OBTAINING LINE ESTIMATE FOR THE POINT ESTIMATE. THIS IS DONE FOR PARAMETERS  $\mu(h)$  AND  $\sigma(h)$ . .... 18

FIGURE 10: THE 90 % BAND FOR  $T_p$  AND THE CONDITIONAL MEAN FROM HINDCAST DATA FROM THE REFERENCE SITE. .... 19

FIGURE 11: OBTAINED CIRCLE IN STANDARD GAUSSIAN SPACE FOR THE VARIABLES  $u_1$  AND  $u_2$ . .... 22

FIGURE 12: TRANSFORMATION FROM STANDARD GAUSSIAN SPACE TO PHYSICAL SPACE WITH CONTOUR LINE CORRESPONDING TO AN ANNUAL EXCEEDANCE PROBABILITY OF  $10 - 4$ . .... 23

FIGURE 13: CONTOUR LINES BASED ON THE JOINT DISTRIBUTION OF  $H_s$  AND  $T_p$ . THE CONTOUR LINES HAVE AN ANNUAL EXCEEDANCE PROBABILITY CORRESPONDING TO A 100-YEAR AND 10.000-YEAR RETURN PERIOD. THERE ARE ADDED DNV WAVE HEIGHT LIMIT TO THE CONTOUR PLOT. .... 24

FIGURE 14: A RANDOM STORM EXTRACTED OVER A THRESHOLD OF 9 M. .... 28

FIGURE 15: POLARHISTOGRAM OF WAVE DIRECTION WITH DIFFERENT WAVE HEIGHTS AS THE INPUT PARAMETER. .... 29

FIGURE 16: HISTOGRAM OF WAVE HEIGHT AND WAVE PERIOD COMPARING THE PERCENTAGE OF OCCURRENCES PER BIN. EACH BIN IS OF LENGTH SCALE 1 UNIT, WITH AN 8 M THRESHOLD. .... 30

FIGURE 17: JACKET STRUCTURE REPLICA FROM THE NORTH SEA. THE STRUCTURE IS IN THE USFOS SOFTWARE. .... 33

FIGURE 18: FRONT AND SIDE VIEW OF THE JACKET STRUCTURE. .... 33

FIGURE 19: DECK DISPLACEMENT MEASUREMENT ON NODE 145. .... 35

FIGURE 20: TRUE WHEELER STRETCHING ON A LINEAR WAVE. THE TWO GRAPHS ARE FROM THE SAME TIME-DOMAIN SIMULATION OF DIFFERENT WAVES. THE WAVES ARE NEGATIVE DUE TO THE ORIENTATION OF THE COORDINATE SYSTEM. .... 39



FIGURE 21: RAYLEIGH LINEAR CREST VERSUS FORRISTALL SECOND-ORDER CREST MODEL. THE SIMULATED SEEDS FROM THE TIME-DOMAIN SIMULATION ARE ADDED USING THE SAME SEA STATE..... 40

FIGURE 22: JONSWAP SPECTRUM FOR  $H_s = 14.9\text{ m}$ ,  $T_p = 16.4\text{ s}$  AND  $\gamma = 2.4$ ..... 42

FIGURE 23: SPOOL WAVE FUNCTION FOUND IN USFOS SOFTWARE. A GRAPHIC DESCRIPTION OF HOW THE FUNCTION WORKS[25]..... 45

FIGURE 24: COMPARISON OF DYNAMIC AND STATIC DECK DISPLACEMENT. THE THREE FIGURES DISPLAY A DYNAMIC SECOND-ORDER RESPONSE, DYNAMIC LINEAR RESPONSE AND STATIC LINEAR RESPONSE. THE LINEAR RESPONSES HAVE ALSO WHEELER STRETCHING. .... 47

FIGURE 25: SURFACE ELEVATION FOR SECOND-ORDER WAVE AND LINEAR WAVE + WHEELER STRETCHING. ... 49

FIGURE 26: SIMULATED SEA STATES FOR TIME-DOMAIN SIMULATION OF THE JACKET STRUCTURE..... 56

FIGURE 27: GUMBEL DISTRIBUTION OF 3-HOUR MAXIMUM RESPONSES. THE SELECTED SEA STATE IS  $H_s = 16\text{ m}$ ,  $T_p = 19\text{ s}$ . FIGURE (A) RESPONSE IS BASE SHEAR, (B) IS DECK DISPLACEMENT AND (C) IS OVERTURNING MOMENT..... 58

FIGURE 28: DECK DISPLACEMENT RESPONSE SURFACE FOR  $\alpha G$  AND  $\beta G$ ..... 59

FIGURE 29: BASE SHEAR RESPONSE SURFACE FOR  $\alpha G$  AND  $\beta G$  ..... 59

FIGURE 30: OVERTURNING MOMENT RESPONSE SURFACE FOR  $\alpha G$  AND  $\beta G$  ..... 60

FIGURE 31: THE EVOLUTION OF GUMBEL RESPONSE PARAMETERS A AND B FOR THE RESPONSES DECK DISPLACEMENT, BASE SHEAR AND OVERTURNING MOMENT. THE EVOLUTION IS CONSIDERING AN INCREASING  $H_s$  RANGE AND FIXED  $T_p$ ..... 60

FIGURE 32: THE EVOLUTION OF GUMBEL RESPONSE PARAMETERS  $\alpha$  AND  $\beta$  FOR THE RESPONSES DECK DISPLACEMENT, BASE SHEAR AND OVERTURNING MOMENT. THE EVOLUTION IS CONSIDERING AN INCREASING  $T_p$  RANGE AND FIXED  $H_s$ ..... 61

FIGURE 33: FITTED MARGINAL DISTRIBUTION FOR  $H_s$  EQUAL AND OVER 8 M TO A 3-PARAMETER WEIBULL DISTRIBUTION. THE DISTRIBUTION IS SEEN IN THE GUMBEL SCALE..... 65

FIGURE 34: NON-LINEAR FITTING OF LOG-NORMAL PARAMETER  $\mu$  FOR MODIFIED  $H_s$  VALUES. .... 66

FIGURE 35: NON-LINEAR FITTING OF LOG-NORMAL PARAMETER  $\sigma^2$  FOR MODIFIED  $H_s$  VALUES..... 67

FIGURE 36: A 90 PERCENTILE OF  $T_p$ , BASED ON FITTED  $T_p$  DATA..... 67

FIGURE 37: CONTOUR LINES BASED ON THE JOINT DISTRIBUTION OF MODIFIED SEA STATES. .... 69

FIGURE 38: CUMULATIVE DENSITY FUNCTION FOR EACH STORM STEP IN A GIVEN STORM. THE FUNCTIONS FOR EACH STEP ARE MULTIPLIED TO A STORM MAXIMUM, SEEN AS A STIPPLED LINE IN THE FIGURE. .... 72

FIGURE 39: CUMULATIVE DENSITY FUNCTION OF THE EXACT STORM, DISPLAYING ITS MOST PROBABLE MAXIMUM. .... 74

FIGURE 40:  $\beta$  VALUES FOR ALL THE STORMS OVER THE THRESHOLD OF 8 M. .... 75

FIGURE 41: COMPARES THE EXACT AND APPROXIMATED STORM DISTRIBUTION IN A GUMBEL PROBABILITY PAPER FOR RANDOM STORMS IN THE DATASET. THE EXACT DISTRIBUTION IS FROM THE OVERTURNING MOMENT RESPONSE..... 76

FIGURE 42: PROBABILITY PLOT IN WEIBULL SCALE, WHERE A FITTED 3-PARAMETER WEIBULL DISTRIBUTION IS COMPARED TO AN EMPIRICAL SAMPLE OF  $X$  VALUES. .... 79

FIGURE 43: PROBABILITY PLOT IN GUMBEL SCALE, WHERE A FITTED 3-PARAMETER WEIBULL DISTRIBUTION IS COMPARED TO AN EMPIRICAL SAMPLE OF  $X$ VALUES. .... 80

FIGURE 44: DISTRIBUTION FUNCTION FOR THE LONG TERM ANALYSIS OF OVERTURNING MOMENT. THE THRESHOLD IS 8 M. .... 81

FIGURE 45: DISTRIBUTION FUNCTION FOR THE LONG TERM ANALYSIS OF AN OVERTURNING MOMENT IN A GUMBEL PROBABILITY PAPER. THE THRESHOLD IS 8 M..... 82

FIGURE 46: RELATIVE CONTRIBUTION FOR THE CREST HEIGHT TO EXCEED ULS (LEFT FIGURE) AND ALS (RIGHT FIGURE) PROBABILITIES GIVEN THE SEA STATES IN THE MODIFIED ALL SEA STATE APPROACH. .... 96

FIGURE 47: RELATIVE CONTRIBUTION FOR THE DECK DISPLACEMENT EXCEEDED ULS (LEFT FIGURE) AND ALS (RIGHT FIGURE) PROBABILITIES GIVEN THE SEA STATES IN THE MODIFIED ALL SEA STATE APPROACH. ... 97

FIGURE 48: RELATIVE CONTRIBUTION FOR THE OVERTURNING MOMENT TO EXCEED ULS (LEFT FIGURE) AND ALS (RIGHT FIGURE) PROBABILITIES GIVEN THE SEA STATES IN THE MODIFIED ALL SEA STATE APPROACH. .... 98

FIGURE 49: RELATIVE CONTRIBUTION FOR THE BASE SHEAR TO EXCEED ULS (LEFT FIGURE) AND ALS (RIGHT FIGURE) PROBABILITIES GIVEN THE SEA STATES IN THE MODIFIED ALL SEA STATE APPROACH. .... 99

**LIST OF TABLES**

TABLE 1: THE THREE LARGEST  $H_s$  VALUES IN THE SAMPLE. .... 15

TABLE 2: SIGNIFICANT WAVE HEIGHT VALUES FOR THE 3-PARAMETER WEIBULL WHEN EXTRAPOLATED TO THE DESIGN CRITERION. .... 16

TABLE 3: PARAMETERS FOR THE LINE ESTIMATE FOR  $\mu$  AND  $\sigma^2$ . .... 18

TABLE 4: EXTREME SEA STATES OBTAINED FROM ALL SEA STATES. .... 19

TABLE 5: STORMS AND STORM EVENTS EXTRACTED OVER VARIOUS THRESHOLDS..... 29

TABLE 6: SUMMARY OF INFORMATION REGARDING THE JACKET STRUCTURE USED IN THIS THESIS[17]. .... 32

TABLE 7: THE TWO FIRST EIGENMODES OF THE JACKET STRUCTURE. THE PERIODS ARE OBTAINED FROM USFOS WITH ADDED GRAVITY. .... 34

TABLE 8: SUMMARY OF THE OBSERVED POPULATION (LINEAR CREST) VERSUS A FORRISTALL SECOND-ORDER CREST MODEL. THE SEA STATE IS  $H_s = 16 m$  AND  $T_p = 19 s$ . .... 41

TABLE 9: OVERVIEW OF THE CHOSEN COEFFICIENTS IN THE MORRISONS EQUATION FOR  $CD$  AND  $CM$  ..... 44

TABLE 10: DIFFERENCES BETWEEN DYNAMIC AND STATIC SIMULATIONS OF THE SAME SEA STATE AND SEED. 48

TABLE 11: DIFFERENCES BETWEEN DYNAMIC RESPONSES SIMULATED WITH A SECOND-ORDER WAVE THEORY AND SIMULATION PERFORMED WITH LINEAR WAVES + WHEELER STRETCHING. THE SEA STATE AND SEED ARE THE SAME FOR BOTH. .... 48

TABLE 12: SELECTED SEA STATES TO SIMULATE RESPONSES IN THE TIME DOMAIN. .... 56

TABLE 13: LONG TERM EXTRAPOLATION OF  $H_s$  TO TARGET PROBABILITY..... 65

TABLE 14: VALUES FROM THE 90% BAND OF ULS AND ALS VALUES .....	68
TABLE 15: MOST PROBABLE MAXIMUM OVERTURNING MOMENT CORRESPONDING TO ULS AND ALS VALUES AT THRESHOLD 8 M.....	80
TABLE 16: CHARACTERISTIC MOST SIGNIFICANT VALUES FOR THE OVERTURNING MOMENT GIVEN ULS AND ALS FOR DIFFERENT THRESHOLDS. ....	83
TABLE 17: SENSITIVITY STUDY OF THE STORMS BY THRESHOLD.....	83
TABLE 18: $\beta v$ VALUES FOR ALL RESPONSES GIVEN DIFFERENT THRESHOLDS.....	84
TABLE 19: COMPARISON FOR THRESHOLD ANALYSIS OF ALS RESPONSES OF THE JACKET STRUCTURE.....	84
TABLE 20: COMPARISON TABLE OF RESPONSES PREDICTED BY POT AND MODIFIED ALL SEA STATE. THE THRESHOLD IS 8 M. ....	86
TABLE 21: COMPARISON TABLE OF RESPONSES PREDICTED BY POT AND MODIFIED ALL SEA STATE. THE THRESHOLD IS 9 M. ....	86
TABLE 22: SCATTER DIAGRAM FOR ALL $H_s$ AND $T_p$ VALUES. DATA IS OBTAINED FROM HINDCAST. ....	94
TABLE 23: MODIFIED SCATTER DIAGRAM FOR ALL $H_s$ AND $T_p$ VALUES OVER THE THRESHOLD OF 8 M. DATA IS OBTAINED FROM HINDCAST. ....	95
TABLE 24: CHARACTERISTIC CREST HEIGHT VALUES FROM THE LONG TERM ANALYSIS IN MODIFIED ALL SEA STATE APPROACH. THE CHARACTERISTIC VALUES ARE FOUND IN Q-PROBABILITIES ULS AND ALS. ....	96
TABLE 25: CHARACTERISTIC DECK DISPLACEMENT VALUES FROM THE LONG TERM ANALYSIS IN MODIFIED ALL SEA STATE APPROACH. THE CHARACTERISTIC VALUES ARE FOUND IN Q-PROBABILITIES ULS AND ALS. ....	97
TABLE 26: CHARACTERISTIC OVERTURNING MOMENT VALUES FROM THE LONG TERM ANALYSIS IN MODIFIED ALL SEA STATE APPROACH. THE CHARACTERISTIC VALUES ARE FOUND IN Q-PROBABILITIES ULS AND ALS. .....	98
TABLE 27: CHARACTERISTIC BASE SHEAR VALUES FROM THE LONG TERM ANALYSIS IN MODIFIED ALL SEA STATE APPROACH. THE CHARACTERISTIC VALUES ARE FOUND IN Q-PROBABILITIES ULS AND ALS.....	99
TABLE 28: SUMMARY OF CREST RESPONSE VALUES IN A POT APPROACH. ....	100
TABLE 29: SUMMARY OF DECK DISPLACEMENT RESPONSE VALUES IN A POT APPROACH.....	101
TABLE 30: SUMMARY OF OVERTURNING MOMENT RESPONSE VALUES IN A POT APPROACH. ....	102
TABLE 31: SUMMARY OF BASE SHEAR RESPONSE VALUES IN A POT APPROACH. ....	103

## **ABBREVIATIONS**

ULS – Ultimate Limit State

ALS – Accident Limit State

POT – Peak over threshold

pdf – probability density function

cdf – cumulative density function

MoM – Method of Moments

CoG – Centre of Gravity

JONSWAP – Joint North Sea Wave Project

DNV – Det Norske Veritas

NCS – Norwegian Continental Shelf

## NOMENCLATURE

$H_s$  = Significant wave height

$T_p$  = Spectral peak period

t = time

$S_d$  = Design load

$R_d$  = Design resistance

$\gamma_G$  = Partial safety factor for variable load

$x_G$  = Characteristic response for variable load

$\gamma_Q$  = Partial safety factor variable for functional load

$x_Q$  = Characteristic response for variable functional load

$\gamma_E$  = Partial safety factor for environmental load

$x_E$  = Characteristic response for environmental load

$\gamma_D$  = Partial safety factor for deformation load

$x_D$  = Characteristic response for deformation load

$R_k$  = Characteristic resistance

$\gamma_M$  = Material factor

rnd = Random number generator [0,1]

$T_p^*$  = Corrected spectral peak period

$f_{H_s T_p}(h, t)$  = Joint distribution of  $H_s$  and  $T_p$

$f_{H_s}(h)$  = Marginal distribution of  $H_s$

$f_{T_p|H_s}(t|h)$  = Conditional distribution of  $T_p$  given  $H_s$

$\mu$  = Mean of a population

$\mu_M$  = Mean of modified populations

$\sigma$  = Standard deviation of a population

$\sigma_M$  = Standard deviation of a modified population

$\sigma^2$  = Variance of a population

$\sigma_{\ln(t_p)}$  = Standard deviation for  $\ln(T_p)$

$\mu_{\ln(t_p)}$  = Mean of  $\ln(T_p)$

$a_1, a_2, a_3$  = Coefficients

$b_1, b_2, b_3$  = Coefficients

q = Probability of exceedance

$\Phi$  = Gaussian normal variable

$\Phi^{-1}$  = Inverse Gaussian normal variable

$\beta_{0.0001}$  = Radius in failure domain  
following probability of exceeding ALS  
value

$u_1$  = Variable for marginal  $H_s$  in standard  
Gaussian space

$u_2$  = Variable for conditional  $T_p$  in  
standard Gaussian space

$S_p$  = Average steepness criteria

m = Mass

$\ddot{x}$  = Second derivative of the response

c = Damping

$\dot{x}$  = Derivative of response

k = Stiffness

x = Response

$\lambda_D$  = Relative damping

$T_0$  = Eigenperiod

$\gamma$  = Peak enhancement factor

$F(t)$  = External load/force

$c_M$  = Coefficient of mass

$c_D$  = Coefficient of drag

A = cross-section

D = Diameter

$\rho$  = Density of sea water

u = Water particle velocity

$\dot{u}$  = Water particle acceleration

$\alpha_G$  = Gumbel distribution  $\alpha$  parameter for  
response

$\beta_G$  = Gumbel parameter  $\beta$  for response

a = Instantaneous airgap

$a_0$  = Still water air gap

$\eta$  = Wave elevation

$F_{C|H_s T_p}(c|h_s, t_p, d)$  = 2-Parameter Weibull distribution (Forristall's crest model)

$\alpha_F = \alpha$  parameter in Forristall's crest model

$\beta_F = \beta$  parameter in Forristall's crest model

$S_1$  = Steepness number

$U_r$  = Ursell number

$T_1$  = Mean wave period

$T_z$  = Zero-up crossing period

$g$  = Gravitational constant

$k_1$  = Wave number

$d$  = Water depth

$N_{3h}$  = Expected number during 3-hour

$F_{X_m|k}(x|k)$  = Gumbel distribution of a response  $X$  in storm step  $m$  in storm  $k$ .

$F_{X|\tilde{X}}(x|\tilde{X})$  = Distribution of the response given the most probable maximum response

$\tilde{X}$  = Storm's most probable maximum response

$\beta$  = Constant for a given threshold in the POT

$N_{storms}$  = The number of storms over the threshold limit

$\theta$  = Wave event direction

$F_{X|STORM}(x|storm)$  = Maximum response for a given storm

$E(X|\tilde{X})$  = Sample mean in the POT

$Var(X|\tilde{X})$  = Sample variance in the POT

$F_{\tilde{X}}(\tilde{x})$  = cdf of most probable maximum response

$\alpha$  = Distribution parameter in 3-parameter Weibull distribution

$\beta$  = Distribution parameter in 3-parameter Weibull distribution

$\lambda$  = Distribution parameter in 3-parameter Weibull distribution

$\mu_{\bar{x}}$  = Mean of most probable maximum response (first moment)

$F_{X|H_sT_p}(x|h, t)$  = Distribution of response given all sea states

$\sigma_{\bar{x}}^2$  = Variance of most probable maximum response (second moment)

$F_X(x)$  = Long term distribution of maximum response

$\nu_1$  = Skewness of most probable maximum response (third moment)

$F_{X_{3h}}(x)$  = Long term distribution of all sea states

$\hat{F}_k(k)$  = Empirical probability distribution

$Q_{X_{3h}}(x > x_q)$  = Relative contribution of sea states to the response.



# 1. INTRODUCTION

## 1.1 Background

The Norwegian Continental Shelf has a harsh environment due to the extended coastline and the large fetch. This leads to the propagation of large wind developed waves. Therefore, the elements such as wind, waves and currents around the NCS will create an environment in which structures operating in these seas need to be designed to handle the elements. This means be designed to achieve a robust design against extreme loads and responses, including fatigue.

Waves will govern the structural responses of most fixed structures. Therefore, the waves occurring in a storm and the responses associated with the structure need to be assessed to maintain a safe operating condition for the personnel, environment, and asset. Failing to address these extreme responses or loads, the outcome may lead to structural failure.

The design of offshore structures follows the method: Load and Resistance Factor Design (LRFD). The LRFD method provides a combination of safety and economic efficiency when designing structures. The method uses load and resistance factors when considering the uncertainty regarding the load and resistance. The structural safety is satisfied if the design load,  $S_d$  is less or equal to the design resistance,  $R_d$ [1], seen in Equation 1–1:

$$S_d \leq R_d \quad 1-1$$

The design load is categorized into several partial safety factors and characteristic responses, where the characteristic response is the q-probability exceedance response. The design resistance includes the characteristic resistance and a resistance factor, covering the material resistance in the structure[1]. From equation 1–2, the limit state design equation is introduced within different categories of loads:

$$\gamma_G x_G + \gamma_Q x_Q + \gamma_E x_E + \gamma_D x_D \leq \frac{R_k}{\gamma_M} \quad I-2$$

Where  $x_G, x_Q, x_E, x_D$  is denoted as the characteristic responses, and  $\gamma_G, \gamma_Q, \gamma_E, \gamma_D$  is the partial safety factors. The different categories are permanent load G, variable functional load Q, environmental load E, and deformation load D. From the design resistance,  $R_k$  is the characteristic resistance and  $\gamma_M$  the material factor[1]. However, since only environmental loads are considered, the other partial safety factor and characteristics are set to zero.

In this thesis, the focus will be on wave govern responses. Regarding characteristic responses, two criteria are implemented for design against overloads. The two criteria are ultimate limit state (ULS) and accident limit state (ALS)[2]. The target maximum exceedance probabilities associated with the limit states are  $10^{-2}$  for ULS and  $10^{-4}$  for ALS, respectively[2]. The target values are given as annual exceedance probabilities.

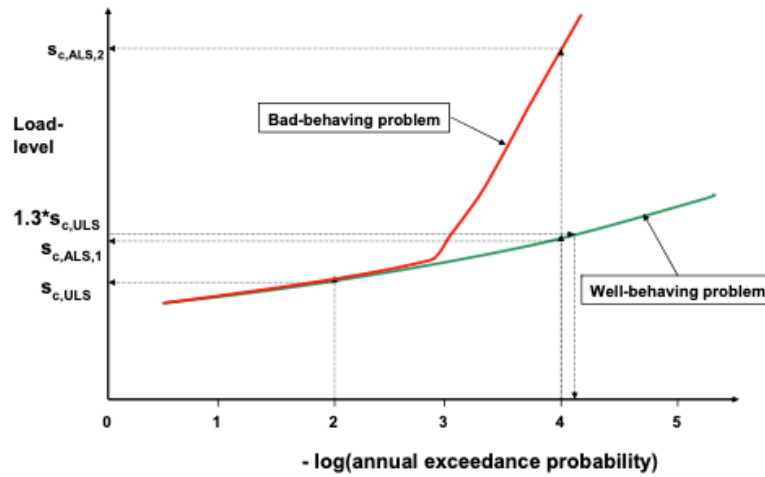


Figure 1: Load level for the same system undergoing an abrupt change for an annual exceedance probability lower than  $ALS(10^{-4})$ [3].

In a well-behaved system, seen in Figure 1, the partial safety factor for environmental loads will increase the characteristic value to correspond to the range of ALS, i.e., exceedance probability  $q = 10^{-4}$  [3]. However, for a badly behaved system, the ULS partial safety factor

may be insufficient to cause the necessary robust design. An example of badly behaved systems is a severe wave-in-deck impact on fixed structures and green water on floating vessels. In such cases, ALS may govern the design of the load[3]. The partial load and material safety factor in an ALS structure check is typically set to 1. This implies no margin of safety beyond the characteristic response ( $q = 10^{-4}$ ) [1]. In ALS, one may utilize non-elastic and system effects. In this thesis, the values corresponding to ULS and ALS will follow NORSOK[2] with the ULS value ( $q = 10^{-2}$ ) corresponding to a 100-year value and ALS ( $q = 10^{-4}$ ) corresponding to a 10.000-year value.

The characteristic loads described above are accurately predicted by a long term analysis with specified target annual exceedance probabilities. All inherent variability must be included in the analysis. The uncertainties regarding the unknowns are covered mainly by partial safety factors[4]. Haver[4] and DNV[5] gives some of the most used long term analysis methods in the NCS, the all sea state method and the POT method. Another used method for the initial design is the contour line approach, in this thesis, the contours will be constructed; however, no response will be calculated from the extreme sea stats obtained on the contours.

This thesis will focus on the POT. Analyses using POT will be thoroughly described. An all sea state approach will also be described, modified to only use the values over 8 m.

By utilizing the POT approach, the characteristic values are defined as the annual probability of exceedance for the most probable largest maximum response in a storm[6]. Important responses for a jacket structure are airgap, deck displacement, overturning moment, and base shear. All responses mentioned are covered in this thesis. The storms used in the POT analysis are storms obtained from Hindcast data. The data is produced from a finetuned and mathematical model to give wave and wind data where measurements are unavailable. The reference site for the hindcast data is located in the Norwegian Sea and is seen in Figure 3.

## 1.2 Objective

The motivation for utilizing the POT to predict q-probability extremes is that the approach is, to a large extent, not adopted in the NCS as a design method. The POT is mainly used in areas

where severe hurricane events occur since it is believed that the hurricanes will give the largest responses[4]. In the NCS, 3-hour hindcast measurements are utilized as the design basis since hurricanes are not a common weather phenomenon in Norway. The POT can be used with hindcast data after a storm has been introduced. Previous analyses and comparisons between the POT and all sea state show that the all sea state is more conservative in the q-probability estimates than the POT[4]. By adopting the POT as the long term analysis method, economic gains can be made without reducing the safety. This is the motivation for using the POT to predict the extreme responses of a jacket structure in this thesis.

The aim of the thesis is to predict q-probability responses for a jacket structure. The q-probability responses are obtained by a long term analysis utilizing the method POT and a modified version of the all sea state. The two methods will be compared for the q-probability responses. In addition to the all-sea state approach, relative contribution to extreme responses is found to investigate where more time-domain simulations are needed to better determine the long term distribution. The thesis will investigate the two long term analysis methods and evaluate if the all sea state is more conservative as seen in the literature[4].

The responses from the jacket structure are non-linear. This implies that time-domain simulations must be performed to obtain the correct short-term variability from the structure. Due to the structure's geometry, the waves are directed 270° on the structure to obtain most dynamics. No current is added in this thesis work. Usfos is the software used for the time-domain simulations, while MATLAB is used for post-processing the data.

### 1.3 Thesis outline

The outline of chapter 2 – 9 of the thesis is described in the following sub-chapter.

Chapter 2 starts with an introduction to the hindcast model and how the hindcast spectral peak period is corrected. From hindcast measurements, a joint model of the sea states  $H_s$  and  $T_p$  is obtained. Based on the joint model, contour lines are established. The hindcast is also used to obtain the joint distribution between significant wave height and spectral peak period for the long term analysis in chapter 7.

Chapter 3 gives the reader an introduction to the POT approach used in this thesis. A storm is defined based on the 3-hour measurements from hindcast data. The annual storms obtained over thresholds ranging from 7 m to 10 m are given. The storm data and annual storms are further used in the long term analysis using POT to predict extremes.

Chapter 4 gives the reader an introduction to the jacket model used in this thesis. To increase the dynamic behaviour of the jacket, the deck mass has been increased. This is observed in the prediction of q-probability extremes. A summary of properties regarding the structure is provided. The deck displacement node where the response is measured is also given. The jacket structure is further used when the short term variability of the structure is obtained by simulating various sea states in a 3-hour time-domain simulation.

Chapter 5 describes the simulation using the software Usfos. Background, useful functions, and settings to simulate the 3-hour time series are given. A comparison between two identical time series, where dynamic and static responses are described and compared, is also given. Further, the dynamic responses of the jacket structure when a linear crest and a second-order crest are compared are also seen. The chapter is included in order to help the reader understand the simulation of the responses using Usfos.

Chapter 6 is devoted to the jacket assessment. An airgap analysis is included to obtain knowledge about the clearance between a second-order wave crest and the underside of the deck on the jacket structure. A grid with simulation points is given, and the maximum response values for each 3-hour time-domain simulation are fitted to a Gumbel distribution. A response surface is constructed with a spline function based on the Gumbel parameters for each simulated sea state. The response surface for all relevant responses is further used in the long term analysis part in chapters 7 and 8.

Chapter 7 covers the long term analysis using a modified all sea state approach, where all sea states over 8 m are used. The example used is for the overturning moment. The relative contribution of sea states will be given for the. All responses are found in appendix C. The results obtained in this long term analysis will be compared with the POT.

Chapter 8 covers the long term analysis of the POT method. An example for calculating extremes is given for the overturning moment response. The thresholds used for defining storms are 8 – 10 m.

Chapter 9 compares the results obtained from the long term analyses methods POT and modified all sea state.

Chapter 10 gives insight into concluding remarks about the findings, with a section related to further improvements for future work.

## 2. WAVE DATA AND MODELLING

In the offshore environment, the main concern regarding structures is waves and, in particular, large waves. The regulation states that the waves or other environmental actions shall be determined by extrapolating exceedance probabilities to obtain a characteristic value[2]. Therefore, a substantial amount of environmental data must be available for the specific location to obtain a long term analysis of sea states[2]. This is often problematic for sites where previously no measurements have been obtained. As a result, the hindcast database was established. The hindcast database produces data by running a numerical model. The numerical model is based on historical weather data, and the database is thoroughly validated against actual measurements[4].

At NCS, hindcast data have been adapted as the primary design data since 2010[4]. NORA10 is a hindcast database covering the North Sea, the Norwegian Sea, the Barents Sea and the Eastern Atlantic with data over a 10 km spaced grid on x and y-direction over the total area covered. However, a hindcast database with a grid size of 3 km is now available; see NORA3[7]. The Nora10 database starts on the 1<sup>st</sup> of September, 1957, and continues to the present time, meaning nearly 65 years are presently available with data every 3-hours. In this thesis, data from 1957 to 2018 are used. The data output from the hindcast database is seen in Figure 2.

WAM WIND AND WAVES																
LATITUDE: 67.05, LONGITUDE: 7.00																
				WIND		TOTAL SEA				WIND SEA			SWELL			
YEAR	M	D	H	WSP	DIR	HS	TP	TM	DIRP	DIRM	HS	TP	DIRP	HS	TP	DIRP
1957	9	1	6	7.9	42.	1.2	5.2	4.3	36.	37.	1.0	5.2	36.	0.6	6.3	6.
1957	9	1	9	9.5	33.	1.3	5.2	4.3	36.	38.	1.2	5.2	36.	0.4	6.9	81.
1957	9	1	12	10.0	36.	1.5	5.7	4.5	36.	39.	1.5	5.7	36.	0.4	6.9	81.
1957	9	1	15	11.4	35.	1.8	6.3	4.8	51.	40.	1.8	6.3	51.	0.4	7.6	81.
1957	9	1	18	11.1	44.	2.1	6.3	5.2	51.	42.	2.0	6.3	51.	0.5	8.4	351.
1957	9	1	21	10.6	39.	2.1	6.9	5.3	51.	42.	2.0	6.9	51.	0.7	8.4	81.
1957	9	2	0	10.1	45.	2.1	6.9	5.4	51.	41.	1.9	6.9	51.	0.9	8.4	6.
1957	9	2	3	7.1	46.	1.8	6.9	5.4	51.	39.	0.8	5.2	51.	1.6	6.9	51.
1957	9	2	6	5.3	77.	1.5	6.9	5.5	36.	37.	0.4	3.9	81.	1.5	6.9	36.
1957	9	2	9	4.9	86.	1.3	6.9	5.4	36.	36.	0.3	3.6	81.	1.3	6.9	36.
1957	9	2	12	5.5	134.	1.1	6.9	5.1	36.	36.	0.3	3.2	126.	1.1	6.9	36.
1957	9	2	15	4.1	125.	1.1	6.9	4.9	36.	43.	0.2	2.9	126.	1.0	6.9	36.
1957	9	2	18	4.7	132.	1.0	6.3	4.8	36.	53.	0.3	3.2	126.	1.0	6.3	36.
1957	9	2	21	3.8	123.	0.9	6.3	4.7	36.	59.	0.2	2.7	126.	0.9	6.3	36.
1957	9	3	0	3.9	121.	0.8	6.3	4.7	36.	57.	0.1	2.4	126.	0.8	6.3	36.

Figure 2: Data contained in a hindcast database.

The data contained in the database for every 3-hours are:

- Mean wind speed at the height of 10 m over the sea level and the corresponding mean direction of the wind[4].
- Significant wave height, spectral peak period, mean wave periods, and the peak corresponding wave propagation direction for wind sea.
- Significant wave height, spectral peak period, mean wave period, and the peak corresponding wave propagation direction for swell.
- Total significant wave height, the spectral peak period of the combination of wind sea and swells. The peak and mean direction of propagation of the resulting waves.



## 2.1 Hindcast dataset

The hindcast data for the reference site used in the long term analysis is seen in Figure 3. The reference site is located at The Norwegian Sea with a Latitude of  $67.05^\circ$  and a Longitude of  $7.00^\circ$ . The dataset starts on the 1<sup>st</sup> of September, 1957, and ends on the 31<sup>st</sup> of October, 2018, and contains 178725 samples of  $H_s$  and corresponding  $T_p$  values with a data-sampling rate of 3-hour.

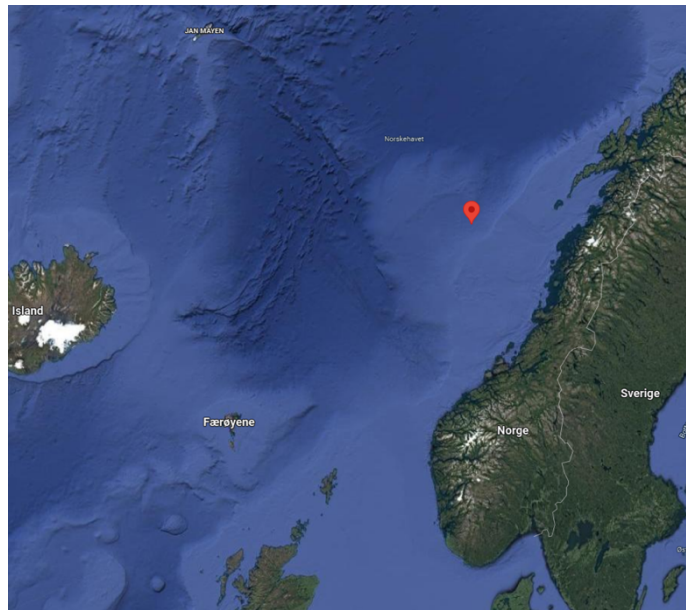


Figure 3: Map of hindcast location. Latitude  $67.05$ , Longitude  $7.00$  in the Norwegian Sea. Obtained from Google maps.

Simultaneous pairs of  $H_s$  and  $T_p$  are plotted by cyan circles in Figure 3. The resolution looks relatively poor for large  $T_p$ . This is due to the fixed resolution in terms of  $\ln(T_p)$  used by the hindcast model[4]. By inspecting the scatter plot in Figure 3, the lower values for  $T_p$  yields reasonably good resolution. However, due to the poor resolution for the high values of  $T_p$ , some sort of correction method must be adopted. Values of  $H_s$  has no recommended correction[4].

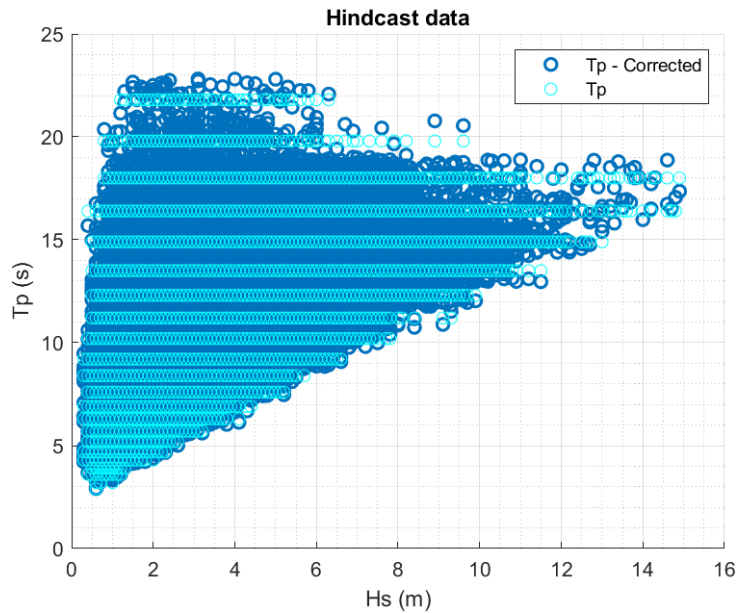


Figure 4: Scatter plot of hindcast data, with uncorrected and corrected data compared in the same plot (total sea).

Statoil (now Equinor) has made a correction method described by a Memo of Andresen and Mathiesen. The memo can be found in appendix D of Haver[4]. How to correct  $T_p$  will be given briefly below, but the scatter diagram with the corrected  $T_p$  is shown by blue circles in Figure 4. The resulting scatter diagram looks rather similar to what is obtained from measurements.

The equation for correcting  $T_p$  reads:

$$T_p^* = 3.224e^{0.09525(i-0.5-rnd)} \quad 2-1$$

$T_p^*$  is given as the value of the spectral peak period after correction. The variable “rnd” is a uniformly distributed random number between [0,1] for each real value of  $T_p$ . Variable “i” is given:

$$i = \text{round} \left( 1 + \frac{\ln \left( \frac{T_p}{3.244} \right)}{0.09525} \right) \quad 2-2$$

Where  $T_p$  is the actual values from hindcast data of the spectral peak period.

## 2.2 Site-specific hindcast analysis

The wave events in this thesis are “total sea”, and the total sea is a combination of wind sea and swells, given by the relation in equation 2–3.

$$\text{Total sea} = \sqrt{(H_{s,\text{wind sea}})^2 + (H_{s,\text{swell sea}})^2} \quad 2-3$$

Helpful information can be extracted from the hindcast dataset by minor data investigation to evaluate the location. Some overall patterns regarding wave propagation for the selected offshore site are seen in Figure 5 and Figure 6.

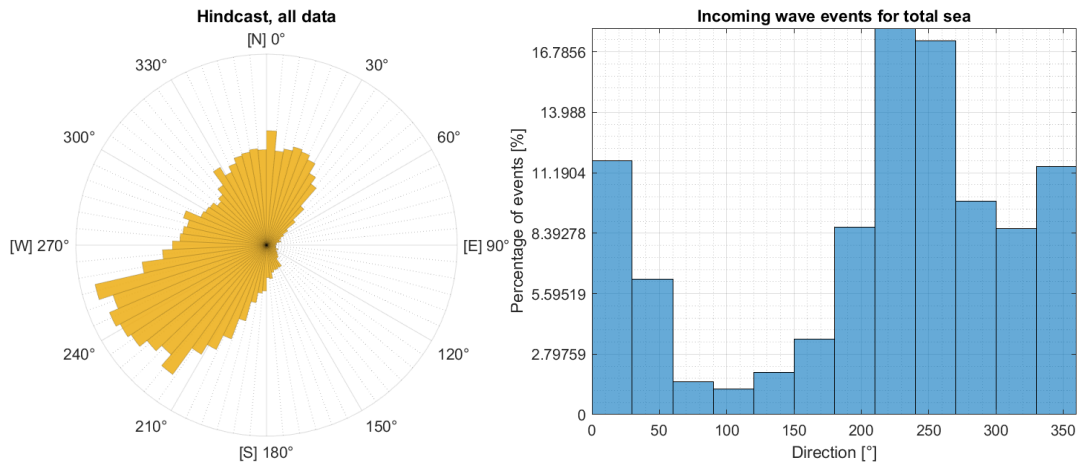


Figure 5: Wave propagation direction for all events in the hindcast dataset. Each bin is 30°.

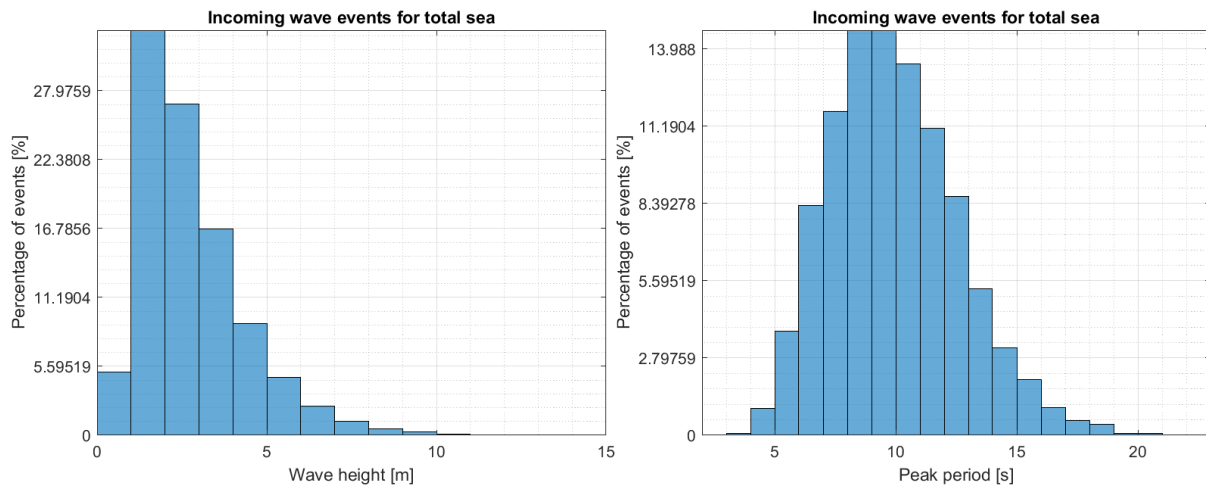


Figure 6: Histogram of wave height and wave period comparing the percentage of occurrences per bin. Each bin is of a length scale of 1 unit.

The wave directions of all events are seen in Figure 5 and include a rose diagram to obtain the direction relative to Figure 3. The bar diagram gives a more exact percentage of occurrences in each bin size. For example, from Figure 6, the dominant wave heights are between [1 m - 3 m] when taking all events in, while the dominant peak period is between [6 s – 13 s].

When estimating long term extremes, low sea states are often of little interest. For example, sea states lower than 6 m  $H_s$  will never affect extremes at the actual site, but they still cover 95 % of the data. More information can be extracted by adding a threshold to the data and inspecting the direction of the waves, the wave height and the peak period. The threshold applied to the data will help identify storms in this thesis. Based on wave data, the way to describe the sea state with reasonable accuracy is by a minimum two-parameter model.

### 2.3 Joint distribution of sea states

The two parameters used to describe a sea state are significant wave height ( $H_s$ ), and spectral peak period ( $T_p$ ). The two variables are described by a joint probability density function, which is obtained by the product of each probability density function of each variable. The joint distribution of all 3-hour sea states reads[3]:

$$f_{H_s T_p}(h, t) = f_{H_s}(h) f_{T_p|H_s}(t|h) \quad 2-4$$

$f_{H_s}(h)$  is the marginal distribution of  $H_s$  and  $f_{T_p|H_s}(t|h)$  is the conditional distribution of  $T_p$  given  $H_s$ . This represents the long term variability of the sea states. Both random variables will be obtained in this section for further use of the methodology in the modified all sea state approach.

A scatter diagram is constructed based on the observed sea states in the hindcast dataset. The diagram can be seen for all 3-hour sea states in appendix A, and will be further used in the distribution of conditional  $T_p$ .

### 2.3.1 Marginal distribution of $H_s$

In the marginal distribution of  $H_s$  the values obtained from the hindcast data are fitted to a probabilistic model. The 3-parameter model is a frequently used model for the marginal distribution of  $H_s$  [3], hence, a 3-parameter Weibull distribution will be used. The Weibull distribution reads with the parameters obtained by the method of moments and gives:

$$F_{H_s}(h) = 1 - \exp\left(-\left(\frac{h - 0.7797}{2.0884}\right)^{1.2450}\right); h \geq 0.7797 \text{ m} \quad 2-5$$

The method of moments estimation of a 3-parameter Weibull will be further explained in section 8. The empirical distribution and the fitted model are given in Figure 7 of the hindcast data at the reference site, and the data fitting is displayed in a Gumbel probability axis to keep a linear scale for  $H_s$  on x-axis.

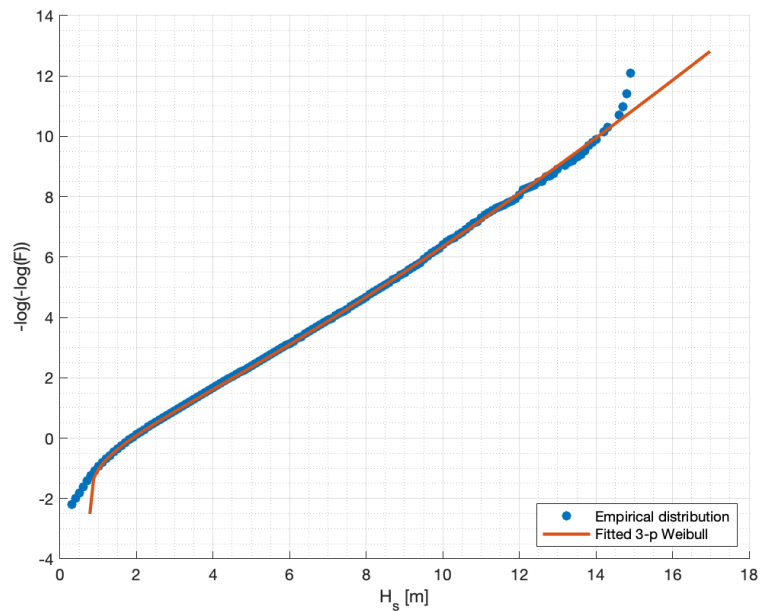


Figure 7: Marginal distribution of  $h_s$  fitted with a 3-parameter Weibull distribution.

The 3-parameter Weibull seems to fit the data reasonably well in the tail, until the last three  $H_s$  values. The model seems to be very conservative in the estimation of extremes. In the case of the sample being correlated, a further look into the three largest values deviating from the 3-parameter Weibull distribution is performed. From Table 1, it is seen that the three largest  $H_s$  values are not correlated. This raises a question about the conservatism of the 3-parameter Weibull distribution.

*Table 1: The three largest  $H_s$  values in the sample.*

<b>Significant wave height, <math>H_s</math> [m]</b>	<b>Spectral peak period, <math>T_p</math> [s]</b>	<b>Wave direction [°]</b>	<b>Date [dd-mm-yyyy]</b>
14.7	16.51	255	03-02-1992
14.8	17.06	239	28-01-1989
14.9	17.36	221	25-11-2011

For example, the 3-parameter Weibull distribution is used on data from the Ekofisk area. This area generally has lower sea states compared to the Norwegian sea. The fitting of  $H_s$  is seen in Figure 8. The tail of the sample distribution again indicates that the 3-parameter Weibull may be on the conservative side. The empirical distribution of both datasets gives the same increasing trend in the tail. This can again imply that the Weibull distribution is on the more conservative side of the marginal distribution of  $H_s$ .

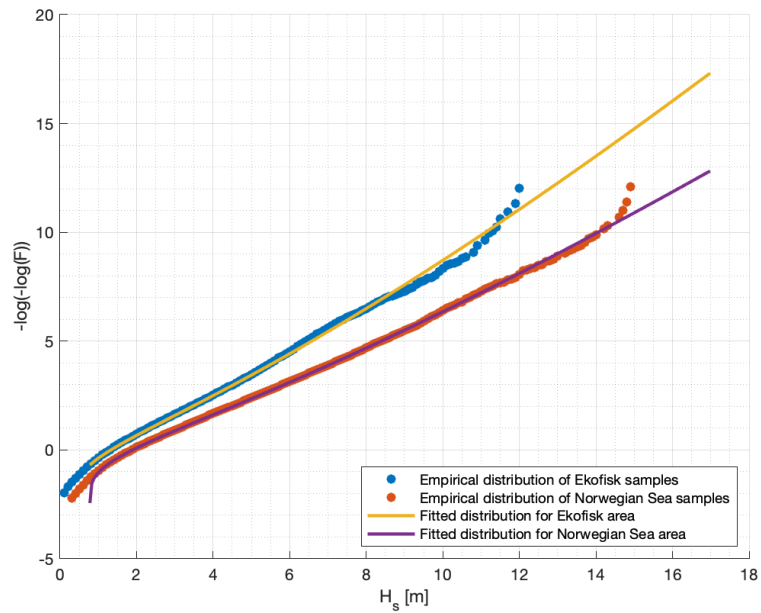


Figure 8:  $H_s$  values from the Ekofisk area fitted with 3-parameter Weibull distribution and compared to the original sample from the Norwegian Sea.

The extrapolated 100-year and 10.000-year return values for the marginal distribution, following a 3-parameter Weibull in the Norwegian Sea, are given in Table 2.

Table 2: Significant wave height values for the 3-parameter Weibull when extrapolated to the design criterion.

ULS [m]	ALS [m]
16.74	21.29



### 2.3.2 Conditional distribution of $T_p$ given $H_s$

The conditional distribution of  $T_p$  follows a log-normal distribution[8], and the log-normal distribution reads:

$$f_{T_p|H_s}(t|h) = \frac{1}{\sqrt{2\pi}t\sigma_{\ln(t_p)}(h)} \exp\left\{-\frac{1}{2}\left(\frac{\ln(t) - \mu_{\ln(t_p)}(h)}{\sigma_{\ln(t_p)}(h)}\right)^2\right\} \quad 2-6$$

From equation 2-6,  $\mu(h)$  and  $\sigma(h)$  are the expected value and the standard deviation of  $\ln(T_p)$ , given  $H_s$ . Since  $T_p$  is conditional on  $H_s$ , the parameters  $\mu$  and  $\sigma$  are calculated for all classes of  $H_s$  from the scatter diagram. Smooth functions are fitted to the point estimates in order to extrapolate the population beyond the observed range. The smooth function's parameters are obtained by applying curve fitting. Commonly adopted equations used to obtain a reasonable fit for mean and variance is presented in equation 2-7 and 2-8 [4]:

$$\mu = a_1 + a_2 \cdot h^{a_3} \quad 2-7$$

$$\sigma^2 = b_1 + b_2 \cdot \exp(-b_3 \cdot h) \quad 2-8$$

For this particular fitting, a fixed value for  $b_1$  was chosen. The reason is that the calculated value for  $b_1$  was negative. The best fit was obtained for  $b_1 = 0.001$ , and this value is further used. It should be emphasised that the variance can never become negative. The line estimate with the population is seen in Figure 9, and the resulting parameters for the estimated lines are seen in Table 3.

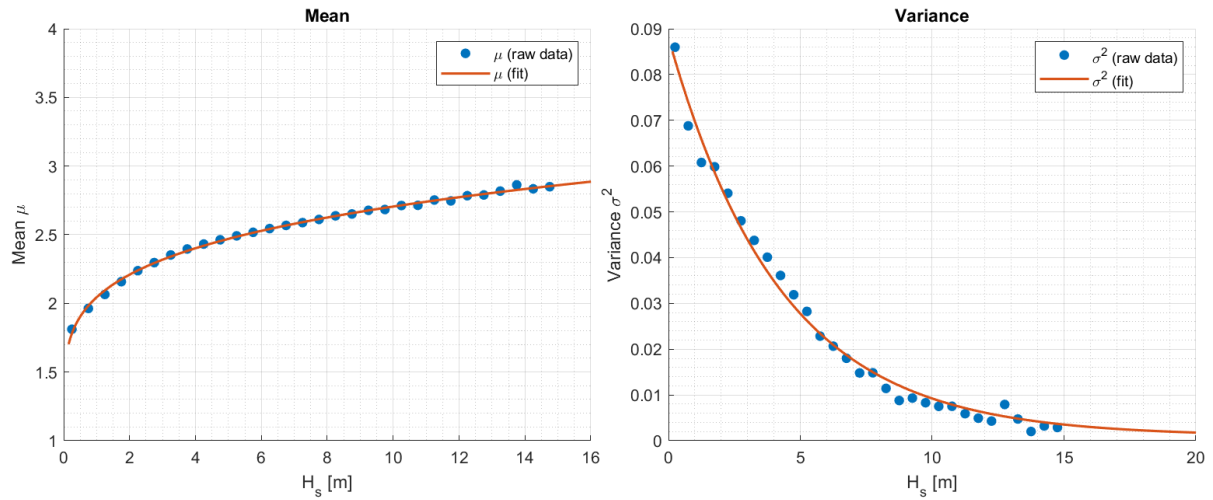


Figure 9: Obtaining line estimate for the point estimate. This is done for parameters  $\mu(h)$  and  $\sigma(h)$ .

Table 3: Parameters for the line estimate for  $\mu$  and  $\sigma^2$ .

$a_1$	$a_2$	$a_3$	$b_1$	$b_2$	$b_3$
1.0443	0	0.2203	0.0010	0.0871	0.2360

The conditional 90 % confidence interval for  $T_p$  with the mean period of the population, is shown in Figure 10. By implementing ULS and ALS values for  $H_s$  it is possible to find the  $T_p$  value corresponding to the same probability of exceedance. The extreme values for  $T_p$  are presented in Table 4.

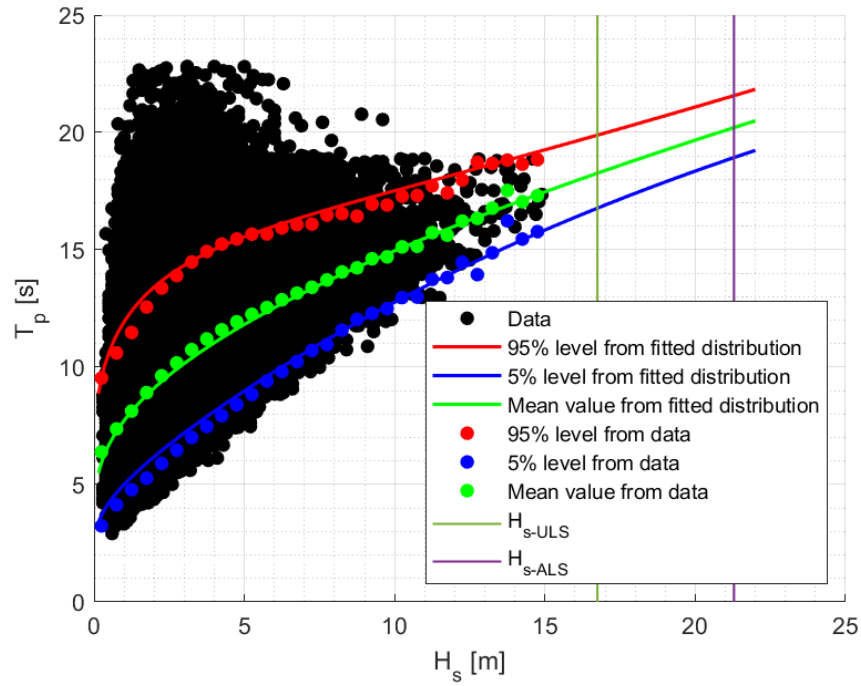


Figure 10: The 90 % band for  $T_p$  and the conditional mean from hindcast data from the reference site.

Table 4: Extreme sea states obtained from all sea states.

	$H_s$ [m]	$T_p$ 5 % [s]	$T_p$ mean [s]	$T_p$ 95 % [s]
<b>ULS (<math>10^{-2}</math>)</b>	16.74	16.77	18.26	19.88
<b>ALS (<math>10^{-4}</math>)</b>	21.29	18.93	20.21	21.57

Based on the joint distribution  $f_{H_s T_p}(h, t)$  of  $H_s$  and  $T_p$ , and of a known annual  $q$ -probability, contour lines can be constructed based on the IFORM method.

### 2.3.3 Contour lines

The motivation behind utilizing the contour line approach is to obtain an approximation for the long term analysis by using only short term sea states[3]. Therefore, the contour lines can be a convenient tool to utilize when the short term response is rather complicated and must be performed for an extensive range of sea states [9]. Contour lines are an approach where the aim is to obtain a closed curve in  $H_s$ - $T_p$  plane. All combinations along the closed curve will correspond to a given annual exceedance probability[4]. The method utilized in this thesis is based on IFORM methods obtained from the study field of structural reliability [10]. The approach uses short-term statics to obtain a relatively accurate estimate for the full long-term extremes[9]. This method is rather convenient when the structural response is complicated, i.e. time-consuming, in order to establish the short term conditional distribution for a 3-hour maximum response. The contour lines presented in this section are determined from the conditional density function,  $f_{H_s T_p}(h_s, t_p)$ .

The first step in constructing the contour lines is transforming the distribution of  $H_s$  and  $T_p$  to the standard Gaussian space by utilizing a Rosenblatt transformation[11]. The joint distribution is given by a 3-parameter Weibull for  $H_s$  and a log-normal distribution for  $T_p$  is then transformed into standard Gaussian variables  $u_1 = N(0,1)$  and  $u_2 = N(0,1)$ :

$$\Phi(u_1) = F_{H_s}(h_s) \Leftrightarrow u_1 = \Phi^{-1}\left(F_{H_s}(h_s)\right) \quad 2-9$$

$$\Phi(u_2) = F_{T_p|H_s}(t_p|h_s) \Leftrightarrow u_2 = \Phi^{-1}\left(F_{T_p|H_s}(t_p|h_s)\right)$$

It should be noted that the transformation results for  $u_1$  and  $u_2$  are uncorrelated. Since they are both Gaussian distributed, they are statistically independent[4].

The Rosenblatt transformation[11] of the variables  $H_s$  and  $T_p$  will for a given probability of exceedance, ULS and ALS, give circles in standard Gaussian space. The radius associated with the circles in standard Gaussian space is given with the constant  $\beta$ . The radius of the circle given by  $\beta$  is in terms of annual exceedance probability, which means all 3-hour sea

states. In this case, the annual number is 2920 3-hour sea states in a year. If POT is used, the annual exceedance value is the number of mean storms per year.

$$\beta_{0.0001} = -\Phi^{-1}\left(\frac{10^{-4}}{2920}\right) = 5.3951 \quad 2-10$$

The radius in standard Gaussian space is obtained from  $\beta_{0.0001}$  for ALS, as seen in equation 2-10. This radius has a return period of 10,000-years, respectively. However, this is only a radius line, which has to be closed. The circle is formed by multiplying a vector, which has points making up a circle,  $[0 - 2\pi]$ . In standard Gaussian space, the circle will be in a closed form, with the radius corresponding to the target annual exceedance probability. The equations for the circle when ALS is the target exceedance probability is given in equation 2-11 for  $u_1$  and  $u_2$  respectively:

$$u_1 = \beta_{0.0001} \cos \theta \quad 2-11$$

$$u_2 = \beta_{0.0001} \sin \theta$$

The circle obtained from equation 2-11 in standard Gaussian space is seen in Figure 11.

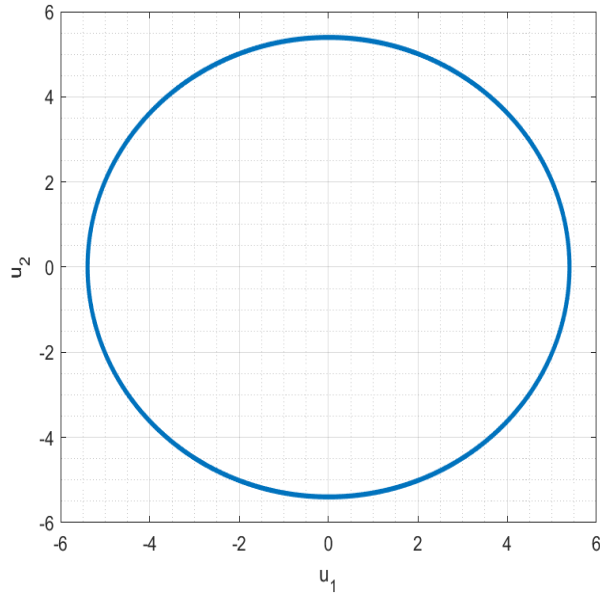


Figure 11: Obtained circle in standard Gaussian space for the variables  $u_1$  and  $u_2$ .

The pairs of  $u_1$  and  $u_2$  denoting points along the circle with radius  $\beta$  can further be transformed back into the physical  $H_s$ - $T_p$  space. This is done by reversing the Rosenblatt transformation. For  $H_s$  the 3-parameter Weibull the transformation will be:

$$h = \lambda + \alpha \left( -\ln(1 - \Phi(u_1)) \right)^{\frac{1}{\beta}} \quad 2-12$$

The Rosenblatt transformation for  $T_p$  will become:

$$t = \exp(\mu_{\ln(T_p)} + \sigma_{\ln(T_p)} u_2) \quad 2-13$$

The result of the transformation into the physical  $H_s$ - $T_p$  space is a continuously shaped figure, corresponding to all values of the annual exceedance probability chosen.

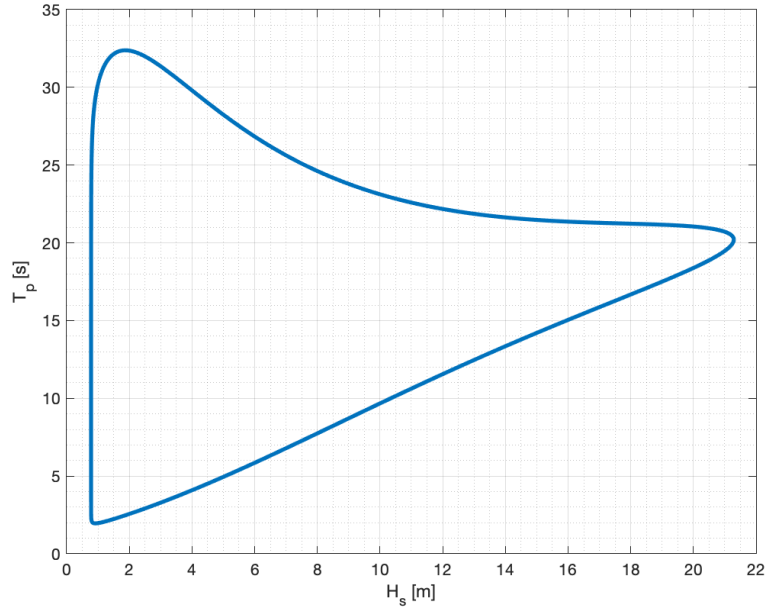


Figure 12: Transformation from standard Gaussian space to physical space with contour line corresponding to an annual exceedance probability of  $10^{-4}$ .

Three return periods are chosen to be displayed with the observed sample with  $H_s$  and  $T_p$ . A DNV significant wave height limitation conditional on  $T_p$  is also implemented[5]. The limit model is obtained from empirical measurements on the Norwegian Continental Shelf. The DNV average wave steepness criteria are given as[5]:

$$S_p = \frac{2\pi H_s}{g T_p} \quad 2-14$$

Where  $S_p$  is chosen based on whether  $T_p$  is over or under the given boundary, otherwise the value for  $S_p$  is interpolated between the boundaries.

$$S_p = \frac{1}{15} \text{ for } T_p \leq 8 \text{ s}$$

$$S_p = \frac{1}{25} \text{ for } T_p \geq 15 \text{ s}$$

The limit is thought by DNV to correspond to a 100-year return. This lets us expect the 10.000-year return contour to be slightly outside the limit. The steepness is a limiting situation for  $T_p \leq 8$  s, for larger  $T_p$  values, the waves will not reach breaking dominated sea states. However, this can occur with sufficiently strong wind, resulting in waves outside the limit.

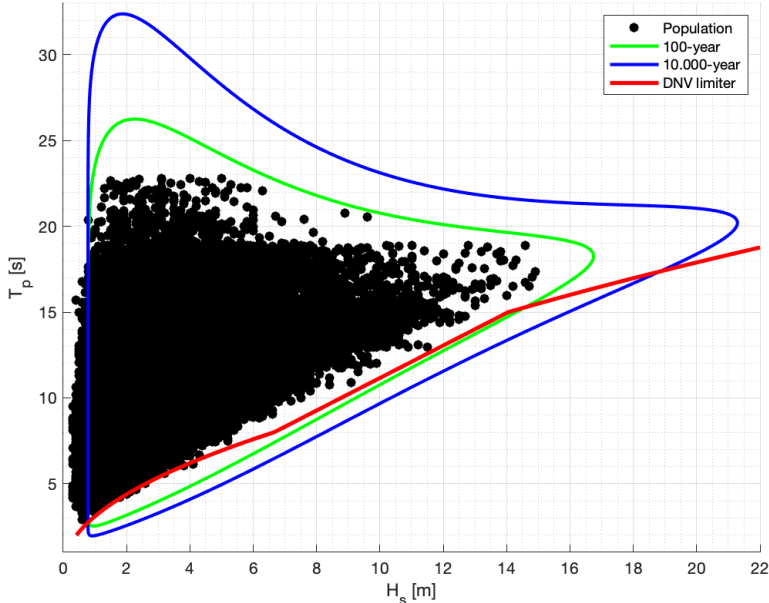


Figure 13: Contour lines based on the joint distribution of  $H_s$  and  $T_p$ . The contour lines have an annual exceedance probability corresponding to a 100-year and 10.000-year return period. There are added DNV wave height limit to the contour plot.



### 3. Peak over threshold approach

This chapter will introduce the long term method POT to the reader. It will start with some background theory in this chapter before proceeding to an example in chapter 8. Next, a storm will be defined based on the hindcast data for various thresholds, which will be used further for the example of using POT for extreme jacket responses.

POT is a long term analysis method used to predict extreme responses. The method was initially applied to areas where severe sea states occur, such as hurricanes[4]. Hurricanes are the worst storms that will yield the most extreme responses that the structure will encounter. For this reason, the sea states between the hurricanes are not engaging in an extreme response analysis[4].

As a basis for extreme analysis, all data must be independent. In a POT analysis, this is achieved by implementing a threshold. Several ways to reduce the storm data correlation have been implemented based on previous work. Tromans and Vanderschuren[6] describe two methods. The first method involves disregarding significant wave height data if the height is less than 30 – 40 % of the storm's largest significant wave height[6]. The second method involves breaking a storm into two separate parts if the trough between the two storm peaks is less than 80 % of the lowest storm peak height[6]. Using a minimum time between each storm, i.e., 24 – 48-hours, is also a way to reduce the correlation[12]. Any storms within this time will be disregarded. A sensitivity study on both threshold and time between two consecutive storms should always be done to find the optimal threshold and time between storms.

At the Norwegian Continental Shelf, a general threshold limit is used but is not limited to values between 7 - 9 m[13].

In the POT, the storm should be treated as a random event[6]. This is different from previous response analysis methods, i.e., the all sea state approach where 3-hour sea states are treated as a random event and characterised by a significant wave height and a spectral peak period. In the POT, the target variable is storm maximum response. One extreme response per storm will make the involved observations less correlated[13]. This is very different from the all sea

state approach, and the trade-off of adopting the POT approach is fewer data. The summary of storms by increasing the threshold is seen in Table 5.

The response problem analysed follows a Gumbel distribution, and the response is denoted X. However, this is not limited to one distribution.

A storm sample is further established from hindcast data at the reference site. The data sampling rate in NCS is 3-hour. The threshold is selected based on sensitivity study or extensive knowledge about the area. The storms are modelled as a sequence of 3-hour stationary steps where environmental data is known for each step. In this example, it is assumed that the response is following a Gumbel distribution, calculated for each storm step m, in storm number k. with known parameters  $\alpha_T$  and  $\beta_T$ .

$$F_{X_m|k}(x|k) = \exp \left\{ -\exp \left\{ -\frac{x - \alpha_{T_{m,k}}}{\beta_{T_{m,k}}} \right\} \right\} \quad 3-1$$

Assuming statistically independent data for each storm maximum step, this leads to the exact storm distribution of the response:

$$F_{X_k|k}(x|k) = \prod_{m=1}^{m_k} \left\{ \exp \left\{ -\exp \left\{ -\frac{x - \alpha_{T_{m,k}}}{\beta_{T_{m,k}}} \right\} \right\} \right\} \quad 3-2$$

The storm maximum distribution is obtained from each storm (3-2), and then the most probable maximum response  $\tilde{X}$ , can be calculated as the pdf reaches maximum  $\frac{dF_{X_k|k}(x|k)}{dx_k} = 0$ . As long as the exact distribution (3-4) is closely following a Gumbel distribution, the most probable maximum  $\tilde{X}$  is given as the storm's most probable maximum response and is estimated for each storm when the distribution is equal to the quantile  $e^{-1}$ .

The conditional distribution of storm maximum response  $X$ , given the most probable maximum  $\tilde{X}$ , is the short term variability and is here approximated by the Gumbel distribution:

$$F_{X|\tilde{x}}(x|\tilde{x}) = \exp\left\{-\exp\left[-\frac{x - \tilde{x}}{\beta\tilde{x}}\right]\right\} \quad 3-3$$

The  $\beta$  value is estimated for each storm as long as the variance for the exact storm is known. The value will fluctuate as the storms are different from the previous. A value of  $\beta$  is calculated for the selected threshold, and this mean- $\beta$  is assumed to be equal for all storms in the selected threshold[13].

$\tilde{X}$  (mpm), is described by fitting a probabilistic model to the sample obtained of  $\tilde{X}$ . This is the long term distribution of  $\tilde{X}$  and is given by  $f_{\tilde{x}}(\tilde{x})$ . The long term distribution of the response is obtained when the integral in equation 3-4 is solved. The long term distribution of the response reads:

$$F_X(x) = \int_0^{\infty} F_{X|\tilde{x}}(x|\tilde{x})f_{\tilde{x}}(\tilde{x})d\tilde{x} \quad 3-4$$

Based on the long term distribution of response, q-probability values can be calculated by solving equation 3-5:

$$1 - F_X(x) = \frac{q}{N_{storms}} \quad 3-5$$

Where  $q$  is the probability of exceedance and  $N_{storms}$  is the annual number of storms over the threshold.

### 3.1 Storms

A storm is defined by Tromans & Vanderchuren[6] as a continuous period where the sea states will increase beyond a threshold of say  $H_s = 9\text{ m}$  to a maximum during the development phase. Then, from the maximum, the storm  $H_s$  will decay until it goes under the selected threshold limit. An example of this is a storm taken from the dataset with a threshold that starts its development phase at 9 m. This is seen in Figure 14. Each event is assumed to be stationary for 3-hours, and the step function has environmental data for each 3-hour step.

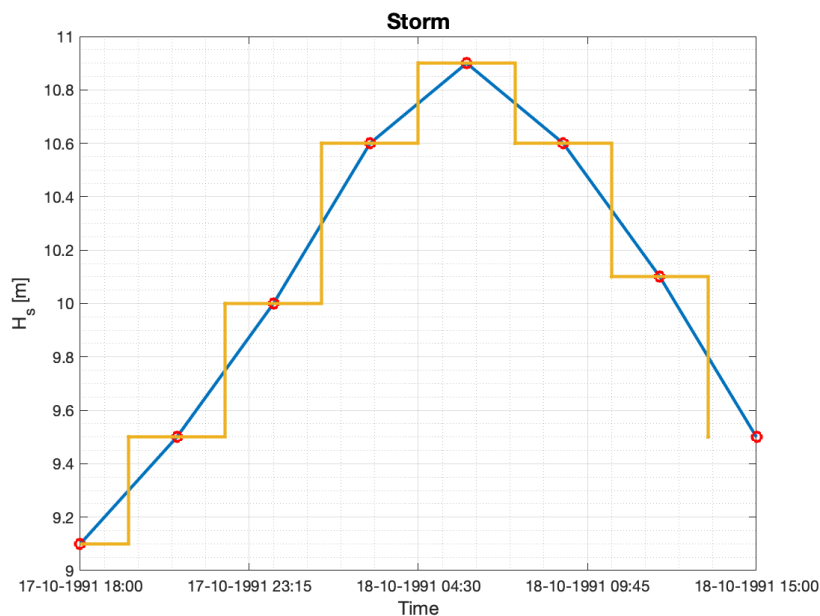


Figure 14: A random storm extracted over a threshold of 9 m.

From the hindcast dataset, storms have been extracted for the various thresholds. Table 5 displays how many events of 3-hour storms and mean storms per year occur in the dataset over the pre-defined threshold limit at the specific location.

Table 5: Storms and storm events extracted over various thresholds.

Threshold	7 [m]	8 [m]	9 [m]	10 [m]	11 [m]
All 3-hour events	3841	1774	803	328	136
All storms events	770	436	224	110	49
Storm events per year	12.61	7.14	3.67	1.80	0.80

By selecting a threshold, the main incoming direction of waves over the threshold will be slightly different for all 3-hour wave events. This is also true for the significant wave height and the peak period. For example, the direction for the wave events with wave heights between 8-10 m, 10-12 m and >12 m are given in the polar plots in Figure 15. It is seen that the larger waves from Figure 15 do come from the same direction.

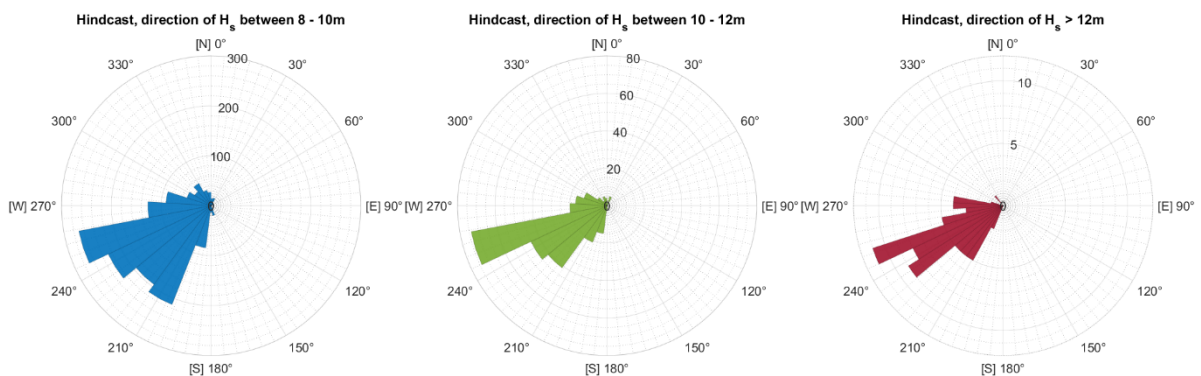


Figure 15: Polarhistogram of wave direction with different wave heights as the input parameter.

If a threshold of 8 m is defined, the corresponding wave height at this threshold will count for 50 % of the wave height, as shown in Figure 16. Lastly, the peak period of the events over the threshold of 8 m has mainly a period of [13 s – 15 s] for over 50 % of the events.

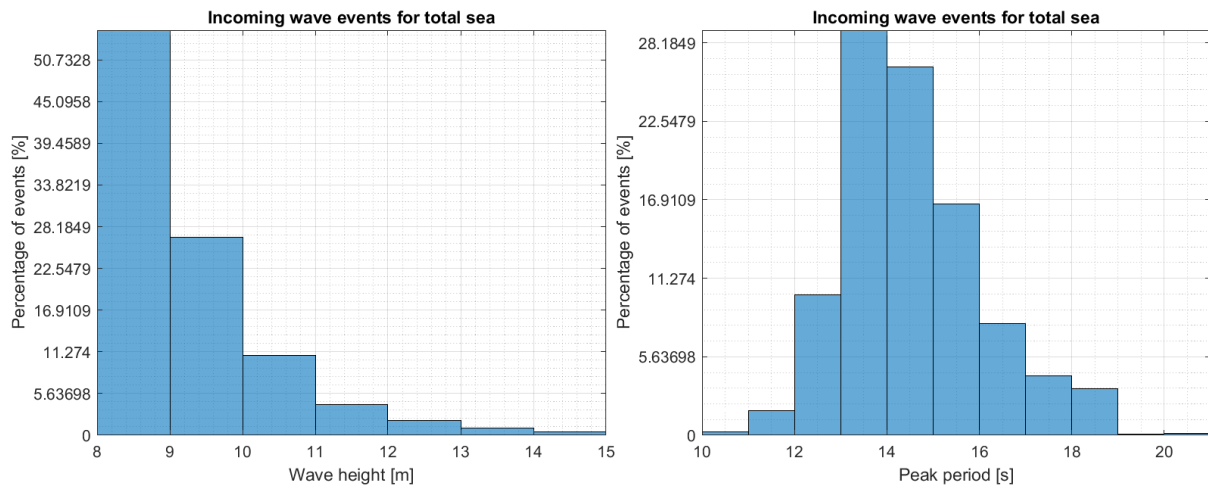


Figure 16: Histogram of wave height and wave period comparing the percentage of occurrences per bin. Each bin is of length scale 1 unit, with an 8 m threshold.

## 4. JACKET STRUCTURE

There are different offshore structures, both floating and fixed, used worldwide. In this thesis, the jacket is the structure of interest. The jacket is a fixed structure with a welded tubular frame. It is fixed into the sea bed by driven piles through the substructure into the seabed. These piles are permanent solutions to hold the jacket structure into its original placement on the seabed. The deck is often installed after the structure has been installed[14]. The jacket structure is mainly used in areas where the water depth is  $< 150$  m. However, this is not always the case. For example, the jacket structure Bullwinkle in the Gulf of Mexico, owned by Shell, is seated at a depth of 529 m[15]. On the NCS, jackets are among the most frequently used fixed structures. Due to its relatively large dynamics, the most known jacket structure in these waters is probably the Kvitbjørn jacket structure[16], which is operated by Equinor and installed at a water depth of about 190 m.

This thesis examines an example jacket used in about 110 m water depth to wave conditions in deep water found in the Norwegian Sea. The depth is somewhat inconsistent. The thesis aims to determine the adequacy of response analysis by the POT method. This chapter will mainly cover the structure and the structural properties. The structure described in this chapter will be used in all analyses in later chapters.

### 4.1 Model

The jacket structure in Figure 17 and Figure 18 is a realistic structure from the North Sea[17]. The information about this structure is obtained from Usfos[17]. The jacket structure consists of eight legs, with the leg arrangement being two by four, making it a rectangular shape. The jacket's bottom foundation has four clusters in each corner, consisting of eight skirt piles in each cluster. The dimensions at the mudline of the structure are 56 x 70 m, while the top has the dimensions of 27 x 54 m. The structure's height is 142 m, with five horizontal bracings levels. The support used for this jacket is a mix of X and K bracings. This particular structure is considered fit to operate in water depths of around 110 m[17]. Therefore the water depth in this thesis is chosen to be 110 m.

On top of the jacket structure, there is a support frame consisting of trusswork beams. The arrangement of the beams is two longitudinal trusses and four transverse trusses. The overall dimensions of this module are 27 x 68 m with a height of 9.75 m. For the thesis, the deck weight has been increased. This is in order to increase the eigenperiod of the structure and the dynamics for the example jacket, given that the structure itself is a quasi-static structure. The “top side” has been modelled with extra weight on the support frame. The extra weight has been added in a uniform “x” shape to not disturb the balance of the structure in waves. A summary of the jacket structure information is given in Table 6, while a more detailed side and front view of the structure is seen in Figure 18.

Table 6: Summary of information regarding the jacket structure used in this thesis[17].

	<b>Jacket structure</b>	<b>Modified jacket structure</b>
<b>Total height</b>	142 m	142 m
<b>Total mass</b>	9720.5 Tons	15230.7 Tons
<b>Water depth</b>	110 m	110 m
<b>Number of legs</b>	8	8
<b>Leg diameters</b>	1.6 – 3.0 m (Top – bottom)	1.6 – 3.0 m (Top – bottom)
<b>Overall dimentions top</b>	27 m x 54 m	27 m x 54 m
<b>Overall dimentions bottom (mudline)</b>	56 m x 70 m	56 m x 70 m
<b>CoG z-dir</b>	-53.218 m	-21.393 m



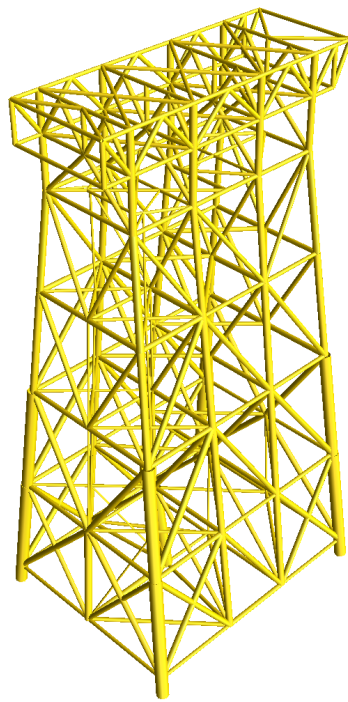


*Figure 17: Jacket structure replica from the North Sea. The structure is in the Urfos software.*

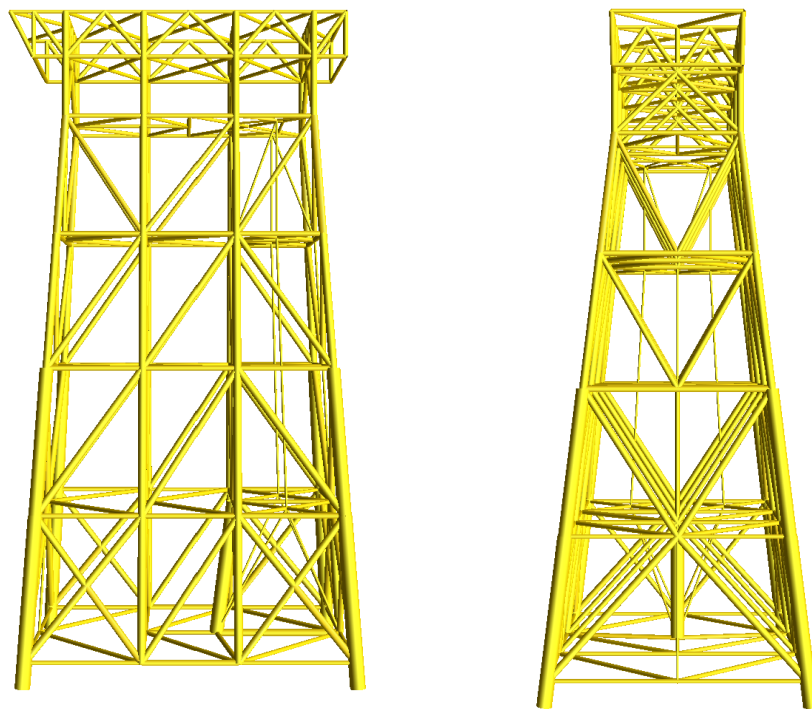


*Figure 18: Front and side view of the jacket structure.*

Damping is the structure's way of reducing oscillations after a response has been implemented. If the system is under-damped, the oscillations will decrease with time [18]. According to Ove T. Gudmestad[18], offshore structures are under-damped by nature.

The damping of the structure is obtained from solving the equation of motion for a free damped system. For a linear system, it is relatively easy to perform free vibration analysis, and this can be done by solving free the damped vibration. The jacket structure is analysed by a non-linear load. If the jacket structure is undergoing extreme conditions, i.e., large waves, drag load may dominate. This is best solved by a time-domain analysis.

The general damping of fixed systems will be around 2-3 % of critical damping[18]. However, this is a general value and may not suit every structure. In this thesis, the structural damping of the jacket structure is set to 1 % of the critical damping. There is also implemented hydrodynamic damping in terms of relative velocity.

The water depth will highly influence the stiffness of a jacket structure. This will again affect the eigenperiod of the system by the relation of  $\omega_0$ . The mass tends to increase as more equipment is loaded onto the topside. Hence the period may deviate from the original prospect.

*Table 7: The two first eigenmodes of the jacket structure. The periods are obtained from USFOS with added gravity.*

<b>Eigenmode</b>	<b>Model [s]</b>	<b>Model (added weight) [s]</b>
Mode 1 (bending in x-dir)	0.5601	1.2369
Mode 2 (bending in y-dir)	0.5391	1.1126

To increase the structure's dynamic, weight was added to the top support frame. The weight was added centred. By increasing the deck mass, the eigenperiod increased as expected, and this can be seen in Table 7. However, due to the realism in the model, it was chosen not to further increase the loads on the support frame.

## 4.2 Deck displacement node

The deck displacement response in a jacket structure is vital to understanding the behaviour. The jacket structure is slender and stiff, meaning wave-in-deck phenomena can cause dangerously large deck displacement if this is not counted for. Therefore, the deck displacement measurement point is taken at the centre node of the support frame on the jacket structure. The node 145 where the displacement is measured is marked as a red ring, as seen in Figure 19.

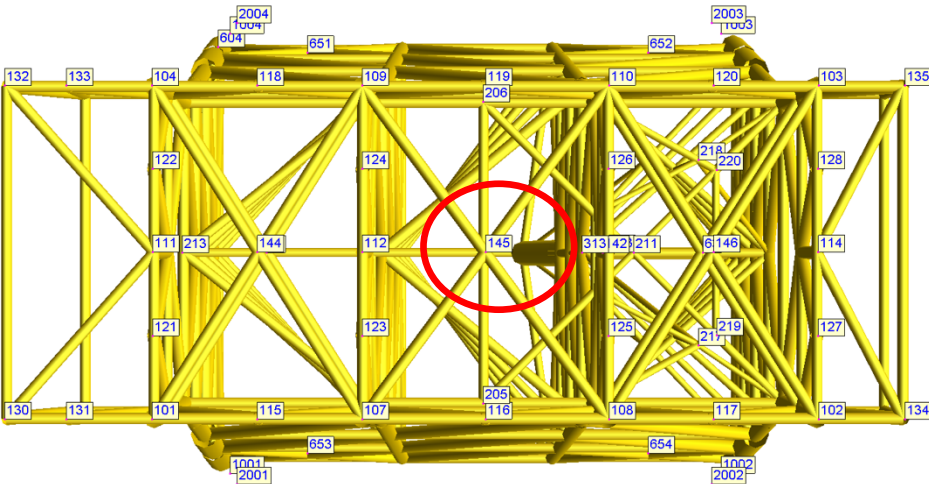


Figure 19: Deck displacement measurement on node 145.

## 5. USFOS SIMULATION

Before simulating sea states, some sort of non-linear simulation software must be introduced. The software used to obtain the responses from structures in simulated sea states is named Usfos and is from the company DNV. This chapter will introduce time-domain simulations with the relevant wave theory, which will be used to simulate the surface elevation to obtain the non-linear responses of the jacket.

Usfos is a software for assessing non-linear static and dynamic analyses of structures[19]. The software analyses integrity assessment, collapse analysis, extreme load analysis, and more. Usfos can do fast time-domain simulations due to smart functions implemented in the software. This thesis uses the software to obtain dynamic responses from the jacket by collecting the maximum response obtained in many different sea states for each 3-hour realization.

### 5.1 Time-domain simulations

To obtain a dynamic response, the equation of motion has to be solved in time. The equation reads from equation 4-1[2] for a system with one degree of freedom (DOF). However, more DOFs are usually solved, and the parameter for mass, damping, and stiffness will be in a matrix format.

$$m\ddot{x}(t) + c(x, \dot{x})\dot{x}(t) + k(x, \dot{x})x(t) = F(t) \quad 5-1$$

Where:

$m$  is the system's mass, including added mass if relevant.

$c(x, \dot{x})$  is the system damping for the given DOF.

$k(x, \dot{x})$  is the system stiffness for the given DOF.

$F$  is the external force contributing to the response. For a slender structure, this force is the Morison equation.

$x$  is the response with its derivatives  $\ddot{x}$  and  $\dot{x}$ .

As seen from equation 4-1, on the left-hand side, is the response from the jacket structure, and on the right-hand side, is the external forces. The Morison equation is usually adopted as a loading formula for a jacket. The response considered in this thesis is deck displacement, overturning moment and base shear[20].

The equation of motion can be solved with various solvers to obtain a solution. Some numerical integration techniques that can be chosen in Usfos are Newmark- $\beta$ , direct and predictor-corrector [21].

From Haver[4], the direct approach is solved. From equation 4-1, the assumption is that the system is of linear nature. To solve this directly, one assumes the known position of the response  $x_i = x(t_i)$  simultaneously with  $\dot{x}_i$  and  $\ddot{x}_i$  and  $f_{i+1} = f(t_{i+1})$ . Utilizing this knowledge, it is possible to obtain the response  $x(t_{i+1})$  for  $t_{i+1}$ . The equation for the dynamic equilibrium of motion at  $t = t_{i+1}$  reads[4]:

$$m\ddot{x}_{i+1} + c\dot{x}_{i+1} + kx_{i+1} = f_{i+1} \quad 5-2$$

The equation is solved directly with initial conditions. In this case, the initial condition is  $t = t_i$  for solving the response at time  $t = t_{i+1}$ . Furthermore, some assumptions need to be included to obtain the solution to the response. The timestep ( $\Delta t$ ) between  $t_i$  and  $t_{i+1}$  must be small for the acceleration between the points to be constant and averaged, and in order to yield a reasonable accuracy of the solution[4].

A step-by-step guide for solving responses for a jacket structure follows[4]:

1. Construct irregular linear waves with various  $H_s$  and  $T_p$  from a JONSWAP spectrum with  $\gamma = 2$ . The simulation duration is 10800 s, 3-hours, which is the standard measurement in The NCS for waves. It may be necessary to add a start-up time.
2. Calculate the wave kinematics from the generated waves exposed to the structure. To obtain the best accuracy, the kinematics should be calculated at the actual surface

elevation of the wave.

3. Calculate the loads for each timestep of the simulated sea surface process. For example, the load vector is obtained from the Morison equation.
4. Solve the equation of motion based on the load vector obtained in step 3. The time solving the equation of motion is based on the requirement of solving the damping and stiffness for each iteration.

## 5.2 Wave generation

Waves are generated and sent towards the structure to obtain a structural response according to the interaction between the waves and the structure. The waves will increase the structural response based on the significant wave height and the spectral peak period. A wave is described by different mathematical expressions, where a linear wave is the most basic way to describe a wave. Other wave theories, more often applied in engineering, is a second-order wave or Stokes 5<sup>th</sup>.

Different wave theories can describe the surface elevation in Usfos[22]. For example, first-order and second-order waves can be chosen to describe the irregular wave elevation in a dynamic time-domain simulation. For a regular wave, the Stokes 5<sup>th</sup> wave can be selected.

The linear wave will not be the correct choice of theory to imitate the natural waves. A wave found in nature will never have the exact distance between the troughs and crests as linear waves do. By selecting a second-order theory for the waves, the waves will have a higher crest than the trough. A second-order wave is typically accepted as accurate for engineering design purposes, say, obtaining the short term response of a structure[20].

This thesis chose simple linear waves to describe the surface elevation. An argument is that this will reduce the computational time for the time-domain simulations. The trade-off is the accuracy that a second-order wave gives. However, as an improvement of the standard linear theory, which will not display any wave kinematics over the still water line ( $z = 0$ ), Usfos has

built-in wave extrapolation. The extrapolation is a stretched Airy theory, also named Wheeler stretching. The wave kinematics calculated at the still water-line is extended to be calculated at the true surface elevation. The kinematic profile down to the seabed is stretched as needed. A graphic display of how Wheeler stretching works is seen in Figure 20.

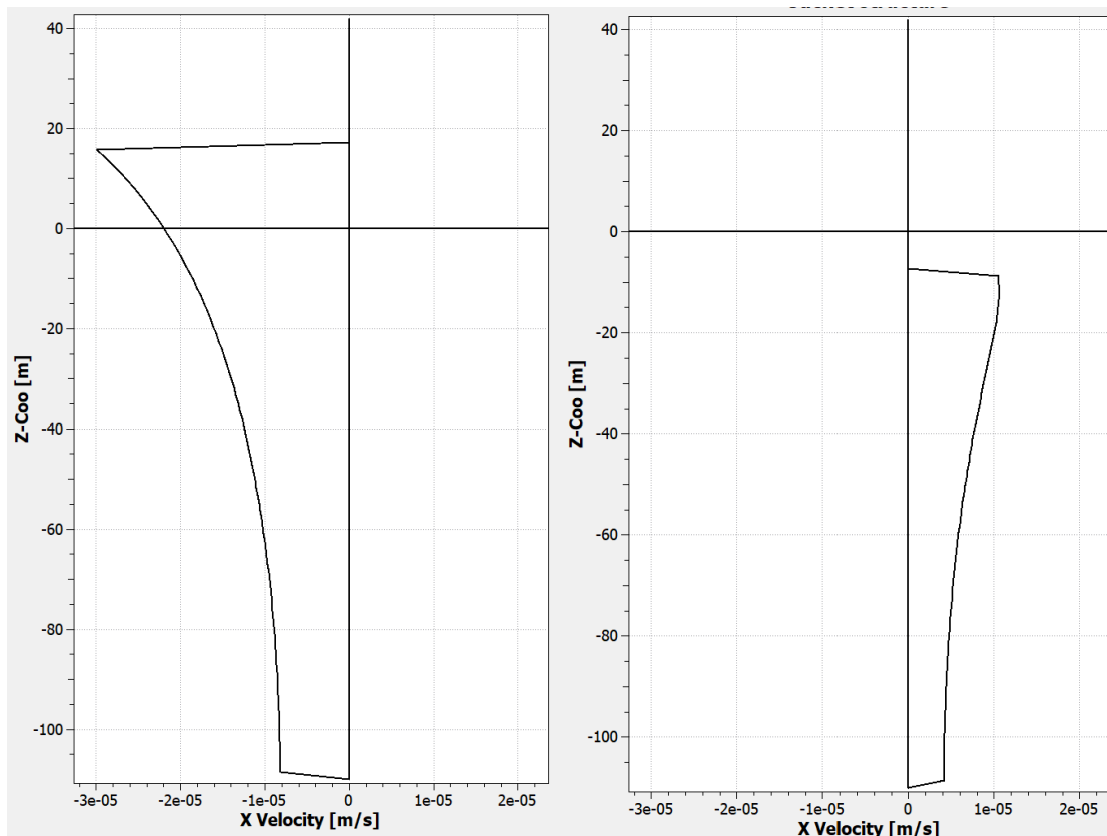


Figure 20: True Wheeler stretching on a linear wave. The two graphs are from the same time-domain simulation of different waves. The waves are negative due to the orientation of the coordinate system.

The linear waves with Wheeler stretching are under estimating the maximum crest, hence, the structural response will be underestimated for a jacket structure. The under-estimation of the crest height between a Rayleigh 3-hour maximum crest model fitted from the population and a Forristall second-order crest is seen in Figure 21.

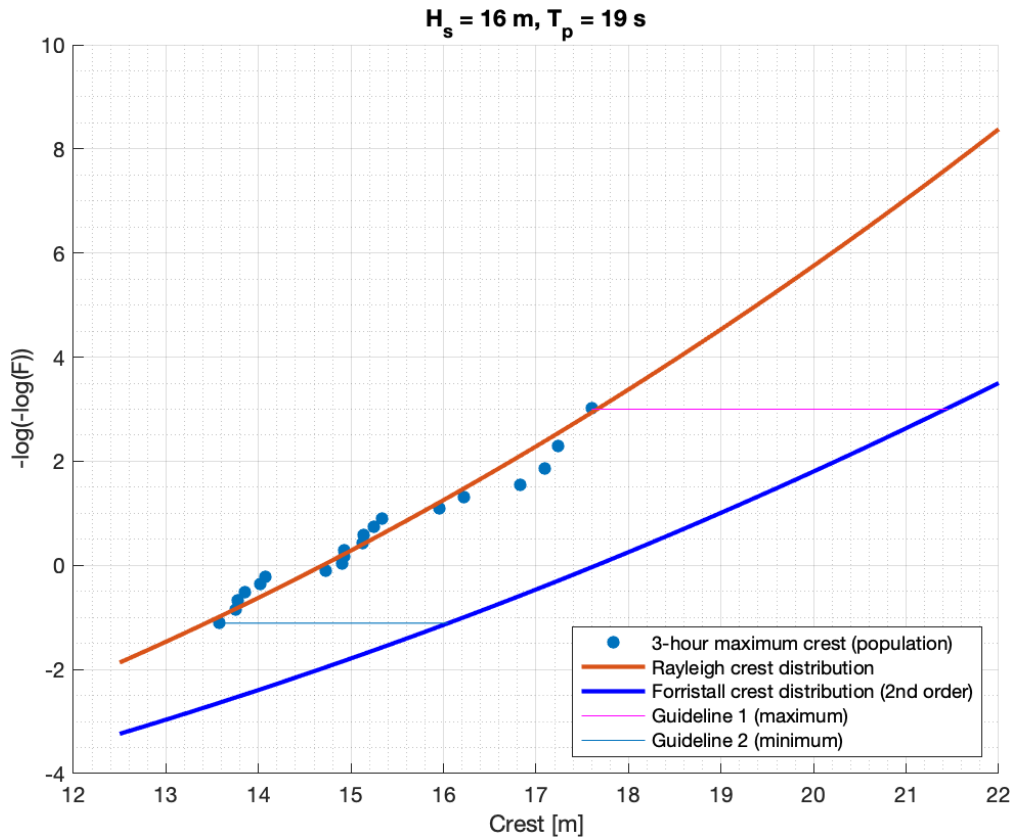


Figure 21: Rayleigh linear crest versus Forristall second-order crest model. The simulated seeds from the time-domain simulation are added using the same sea state.

The observed 3-hour maximum crest height from simulations fit the Rayleigh crest model reasonably well, as expected since the 3-hour maximum crest heights are simulated with linear wave theory. However, the difference between the Rayleigh and the Forristall models is relatively significant. This emphasizes that the linear waves will underestimate the response by a rather large quantity. By inspecting the maximum observed crest height, it is seen that the value for a Forristall second-order crest would be roughly 21.45 m. This means an increase over the linear crest by as much as 21.87 %. Similarly, for the smallest observed value, equal to the Forristall model, the crest will be 16.05 m. The increase in percentage between the smallest observed value and Forristall is 18.19 %. A Summary of the largest and the smallest observed population and the corresponding value for the Forristall crest model is given in Table 8:



Table 8: Summary of the observed population (linear crest) versus a Forristall second-order crest model. The sea state is  $H_s = 16$  m and  $T_p = 19$  s.

	<b>Observed population, linear model</b>	<b>Forristall second-order crest model</b>	<b>Difference</b>
<b>Minimum crest</b>	13.58 m	16.05 m	18.19 %
<b>Maximum crest</b>	17.60 m	21.45 m	21.87 %

It should be mentioned that second-order wave kinematics would be preferred over any extrapolation methods. In the later versions of Norsok N-003 (2017), it is recommended not to use the Wheeler stretching in combination with linear waves[4].

Usfos can choose irregular waves based on spectrum and linear wave theory or alternatively second-order wave theory to obtain more realistic waves. In Norway, a generalized version of the Pierson-Moskowitz spectrum, called JONSWAP, is the preferred wave spectrum for the short term variability of the sea states[5]. The JONSWAP spectrum was the recommendation of the Joint North Sea Wave Project (JONSWAP)[23]. Although the spectrum is obtained from observing the growing wind sea in the south of the North sea, the spectrum does not account for swells. The equation for calculating the JONSWAP spectrum in a simplified format reads:

$$s_{EE}(f) = 0.3125h_s^2t_p^{-4}f^{-5} \exp\{-1.25t_p^{-4}f^{-4}\} (1) \quad 5-3$$

$$- 0.287 \ln(\gamma))\gamma \exp\left\{-0.5\left[\frac{f-f_p}{\sigma f_p}\right]^2\right\}$$

Where  $f_p = \frac{1}{t_p}$  and  $\sigma = 0.07$  if  $f \leq f_p$ , otherwise 0.09.

The peak enhancement factor  $\gamma$  is often calculated as[24]:

$$\gamma = 42.2 \left( \frac{2\pi h_s}{gt_p^2} \right)^{\frac{6}{7}}$$

From the equation,  $g = 9.81 \frac{m}{s^2}$  is the gravitational constant,  $H_s$  is the significant wave height, and  $T_p$  is the spectral peak period.

An example of a JONSWAP spectrum can be seen in Figure 22, where  $\gamma$  has been decided based on equation 5-4.

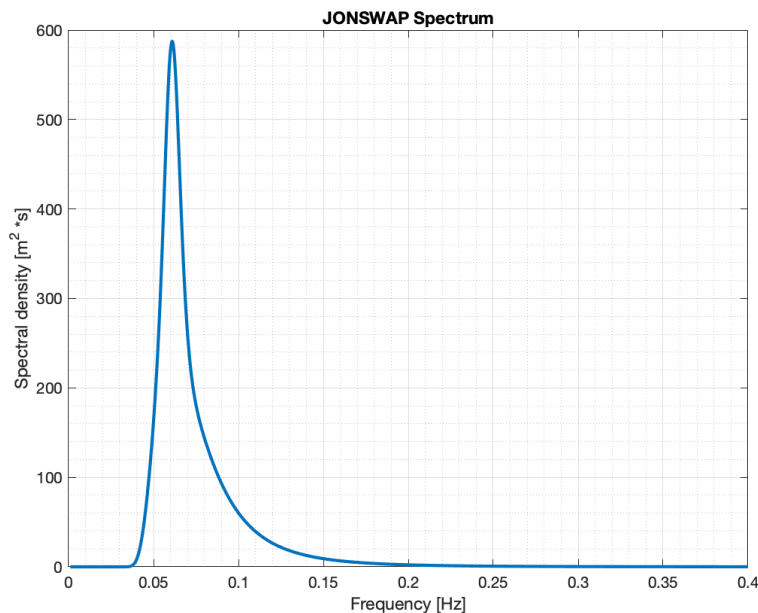


Figure 22: JONSWAP spectrum for  $H_s = 14.9$  m,  $T_p = 16.4$  s and  $\gamma = 2.4$

Irregular linear waves are used for the time simulation in Ufso. The JONSWAP spectrum used to generate the waves have a  $\gamma = 2$ . The equal areal method has been used to distribute the different frequencies in the spectrum. A total of 300 frequencies have been selected between the period  $T = 2$  s and  $T = 25$  s.

### 5.3 Load govern response

The wave kinematic obtained from the generated waves in a time domain simulation is used to determine the load on the structure. The jacket structure is classified as a slender structure[4]. Therefore, the drag term is essential for slender structures interacting with waves as part of the hydrodynamic loading[4]. Slender structures are categorized into sub-classes regarding predicting extreme responses, namely quasi-static and dynamic behaviour. The quasi-static behaviour occurs for a jacket structure in water depths of roughly  $< 150$  m[4]. For a structure with a low eigenperiod, say  $< 2$  s, the mass and damping term can be neglected while solving the equation of motion. As a result, the equation of motion will reduce to the following:

$$x(t) = \frac{F(t)}{k} \quad 5-5$$

The structure's dynamic effects may be important for increased water depth and consequently increased eigenperiod. However, when the structure goes from quasi-static to dynamic is rather vague[4].

For a jacket structure in more considerable water depths and a higher eigenperiod, say 4-5 s[16], the mass and damping term can no longer be neglected. This results in the equation of motion having to be fully solved in the time domain with the proper drag load[4]. In this thesis, the jacket behaves quasi-static due to the low eigenperiod even with the increased deck mass. Regardless of the quasi-static behaviour, it is still chosen to use time-domain simulations to illustrate the method.

Due to the slender construction, the classes described will have the hydrodynamic loads applied from Morrison's equation. The load will act per unit length on the structural members. The equation reads:

$$F(z, t) = c_M \rho A(z) \dot{u}(z, t) + \frac{1}{2} c_D \rho D(z) u(z, t) |u(z, t)| \quad 5-6$$

Where  $c_M$  is coefficient of mass,  $c_D$  is coefficient of drag,  $\rho$  is the density of sea water,  $A(z)$  is the cross-section of the member,  $D(z)$  is the diameter of the member,  $u(z, t)$  is the water particle velocity, and  $\dot{u}(z, t)$  is the water particle acceleration.

However, the Morison equation will only be valid if the wave length is larger than the member's diameter. This is such that the water is not disturbed by the refraction of the wave as it flows through the member[4]. For the response problem of the jacket structure in this thesis, the following values for the coefficients have been used.

*Table 9: Overview of the chosen coefficients in the Morrisons equation for  $C_D$  and  $C_M$*

<b>Drag coefficient <math>C_D</math></b>	<b>Intertia coefficient <math>C_M</math></b>
1.20	1.20

## 5.4 Spool to a peak elevation

A long term response analysis requires a significant amount of time-domain simulations for various sea states of a non-linear load on a structure. This means that the time it will take to generate all those time series will often take too long. In Usfos, however, a built-in function called spool wave is implemented. The user put in the simulation duration, 10800 s, which is 3-hour. During this duration, the peak or the most significant wave is unknown. However, Usfos searches for the largest surface elevation in the entire period instead of simulating the beginning obtaining responses of no interest regarding extreme responses. The simulation is spooled to a time before the largest peak, set by the user. This is described graphically in Figure 23. The time-domain simulation is executed through the most significant peak, and the structural response captures. This function can be performed for the five most significant wave realizations in the time series. If the fifth largest peak is desired, then the spool to wave function will be re-executed five times, where each iteration will reduce the wave until the fifth largest is obtained.

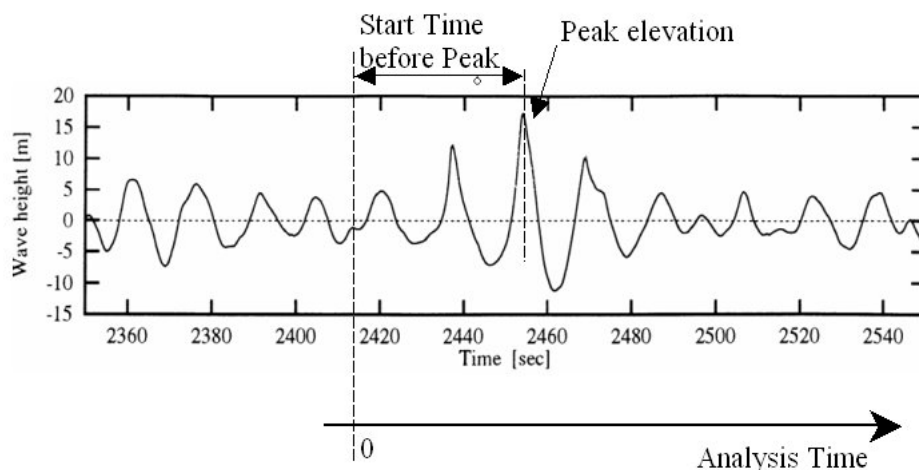


Figure 23: Spool wave function found in Usfos software. A graphic description of how the function works[25].

The spool wave function must have an extensive time before the peak, in order for the structure to have all its dynamics accounted for. This will become very important for structures with a large eigenperiod, and the time before the peak must therefore be increased. On the other hand, the dynamics will settle fast for a jacket structure with a low eigenperiod;

thus, the time before the most significant peak can be reduced. For the jacket response problem in this thesis, the time before the peak was set to 80 s. This time should be more than enough regarding the low eigenperiod of roughly 1.24 s. This statement has not been further investigated, but no evidence from the time domain simulations showed that this number was too low for this particular structure.

It must be said that this function has added uncertainties regarding obtaining the maximum response from the maximum wave elevation. We say that the largest response is obtained given the largest elevation with this function. However, this is not always the case. For example, it might be that the second-largest wave gives the largest response due to the difference in wave period. As a result, the largest wave elevation might underestimate the result. To increase the reliability of obtaining the largest response, run the simulation for the five largest wave elevations and find where the largest response occurs.

## 5.5 Dynamic and static behaviour of responses

A test has been performed in order to check the responses obtained by the time domain simulations by Usfos. Due to the low eigenperiod of the jacket structure, the dynamic and static responses should be close in value. Usually, the dynamic responses are the largest among the time-domain simulations. Therefore, an investigation has been made to verify the responses with dynamic effects active and disabled. When the dynamics are disabled, only static responses are obtained. The differences between the dynamic and static time series are seen in Table 10 and are graphically displayed in Figure 24.

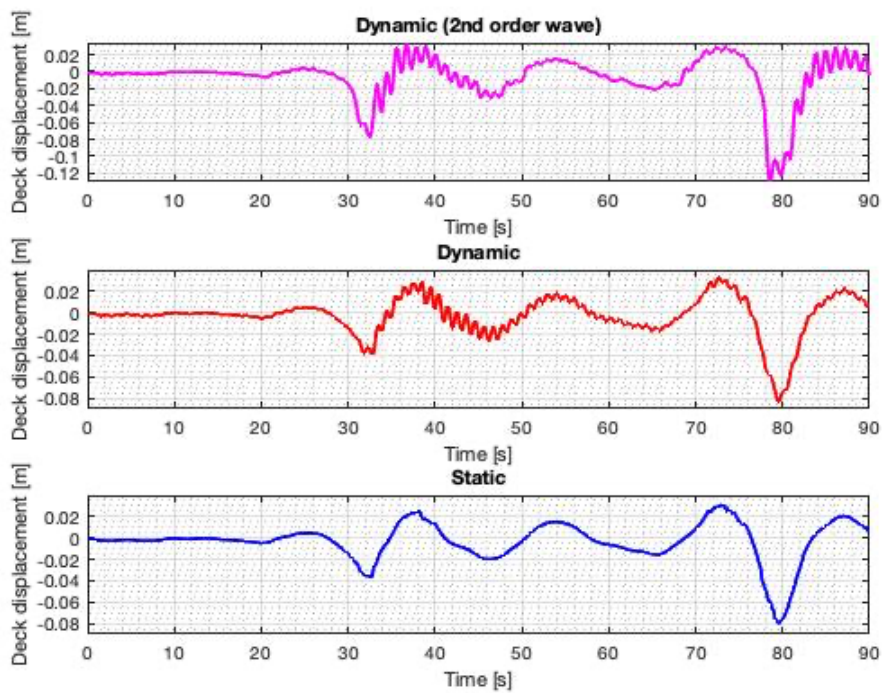


Figure 24: Comparison of dynamic and static deck displacement. The three figures display a dynamic second-order response, dynamic linear response and static linear response. The linear responses have also Wheeler stretching.

Table 10: Differences between dynamic and static simulations of the same sea state and seed.

	<b>Dynamic</b>	<b>Static</b>	<b>Difference [%]</b>
<b>Deck displacement [m]</b>	0.0838	0.0791	5.94
<b>Overturning moment [Nm]</b>	6.7077e+09	6.4809e+09	3.49
<b>Base shear [N]</b>	4.5607e+07	4.4336e+07	5.18

A simulated dynamic time series where the waves were of the second-order was also performed, which is seen in Table 11. This was done to obtain a more realistic crest than the linear wave with Wheeler stretching. The differences can be seen in this particular sea state. However, the difference may change for other sea states.

Table 11: Differences between dynamic responses simulated with a second-order wave theory and simulation performed with linear waves + Wheeler stretching. The sea state and seed are the same for both.

	<b>Dynamic (2nd order)</b>	<b>Dynamic (linear + stretching)</b>	<b>Difference [%]</b>
<b>Deck displacement [m]</b>	0.1299	0.0838	55.01
<b>Overturning moment [Nm]</b>	9.3232e+09	6.7077e+09	38.99
<b>Base shear [N]</b>	6.0042e+07	4.5607e+07	31.65

The time series of surface elevation for linear and second-order for this simulation sea state is seen in Figure 25. The crest of a second-order wave has a higher peak and is sharper in shape than a linear wave with Wheeler stretching.



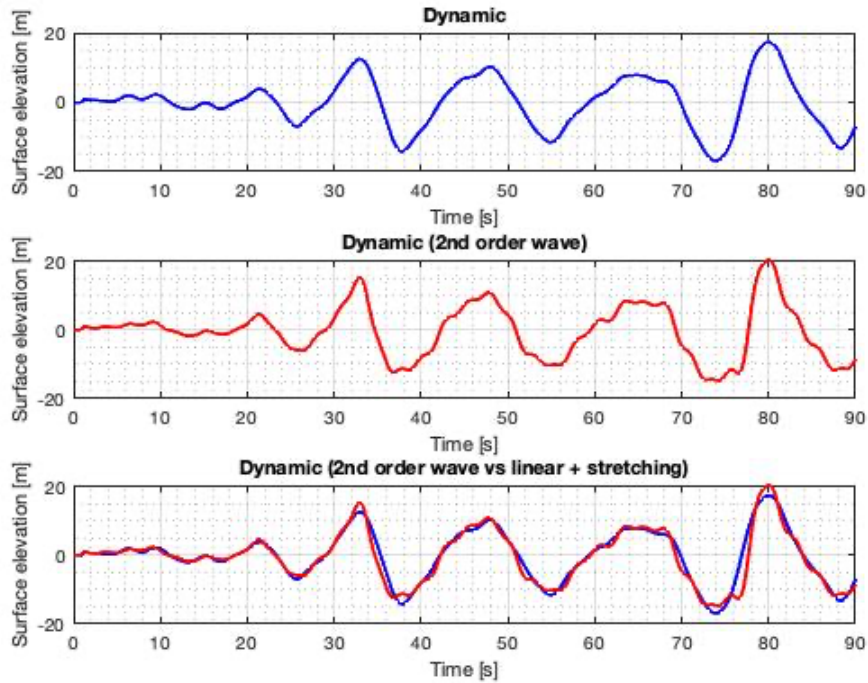


Figure 25: Surface elevation for second-order wave and linear wave + Wheeler stretching.

The difference between dynamic and static responses for the same wave elevation is on par with reasonability. The highest response values were obtained with dynamic activated on the structure. However, the static responses were underperforming the response values by 3-6 %, given in Table 10.

Based on Table 11 and Figure 25, the linear wave + Wheeler stretching is underestimating the values for the short term variability of the responses. The responses obtained for second-order wave elevation are 30-55 % higher than linear waves + wheeler stretching. As a result, the approaches to estimate the long term responses with the target exceedance probability will underestimate the extreme responses. Simulating all responses with the second-order wave will give a more reasonable short term response surface than linear waves + Wheeler stretching.

## 6. JACKET ASSESSMENT

This chapter describes how the 3-hour maximum deck displacement, overturning moment and base shear responses obtained from the jacket structure are fitted to a Gumbel distribution. Based on the response fitting, the Gumbel distribution is adequate to be used. The Gumbel parameters, location and shape are constructed into a response surface to be further used in the long term analysis sections. The main objective of this chapter is to obtain the short term variability for airgap and the response surfaces from the short term variability of 3-hour extremes.

The time-domain simulations have been performed with Usfos, with the structure introduced in chapter 4. Due to the jacket structure's rectangular shape, the waves were sent at an angle of 270° to obtain the most dynamics possible.

### 6.1 Airgap analysis

Airgap assessment is an important topic for a jacket structure. The jacket deck should go clear a 10.000-year crest height. A long term analysis of crest height is therefore needed. The short term crest model used in this assessment is a Forristall second-order wave crest[26], meaning it is more realistic than the linear model used to obtain responses from the jacket structure.

In an offshore environment, the still water air gap  $a_o$  is given as the distance between the still water line and the underside of the structure's deck. The waves will contribute to an instantaneous airgap  $a(x, y, t)$ , which is affected by the wave motions where the airgap will change with the wave elevation  $\eta(x, y, t)$ , hence, being different from  $a_o$  [27]. A fixed structure has no heave direction response due to the seabed's fixed position. There will not be any relative wave elevation for bottom fixed structures. The equation for instantaneous airgap reads:

$$a(x, y) = a_o(x, y) - \eta(x, y, t) \quad 6-1$$

The instantaneous airgap must be positive, which indicates that the wave crest is not hitting the deck. By a negative instantaneous airgap, the wave crest is higher than  $a_o$ , and leads to a wave-in-deck event.

The wave crest heights follow Forristall's second-order wave crest model[26]. A long term analysis is performed using a POT approach and a modified all sea state approach. The air gap is investigated against the crest height of design characteristics and is defined by annual exceedance probabilities of  $10^{-2}$  and  $10^{-4}$  [2]. The return period of these probabilities equals 100-year and 10.000-year wave crest heights.

Based on the second-order wave theory and many time-domain simulations of waves in various depths and steepnesses, Forristall[26] proposes a probabilistic model for the crest heights based on his findings. The model is proposed as a two-parameter Weibull. The model reads from equation 6-2:

$$F_C(c) = 1 - \exp \left[ - \left( \frac{c}{\alpha_F h_s} \right)^{\beta_F} \right] \quad 6-2$$

The parameters  $\alpha_F$  and  $\beta_F$  in the Forristall wave crest height distribution[26] are functions of steepness  $S_1$  and the Ursell number  $U_r$ . The functions for steepness and the Ursell number relate to how the water depth influences the non-linearity of the waves[4].

From DNV[5], the steepness number is given:

$$S_1 = \frac{2\pi h_s}{g T_1^2} \quad 6-3$$

Where  $g$  is the gravitational constant,  $T_1$  is the mean wave period, and  $H_s$  is the significant wave height. Further,  $T_1$  reads:

$$T_1 = \frac{m_0}{m_1} \quad 6-4$$

The value of  $T_1$  will change depending on which wave spectrum is followed. This is due to the definition of  $m_0$ , and  $m_1$  which is given in equation 6-5:

$$M_n = \int_0^{\infty} f^n S(f) df \text{ for } n = 0,1,2, \dots \quad 6-5$$

If the data follows a JONSWAP spectrum[23],  $T_1$  and  $T_z$  can be related to the peak period by using the approximations given in equations 6-6 and 6-7 from DNV[5]:

$$\frac{T_1}{T_p} = 0.7303 + 0.04936\gamma - 0.006556\gamma^2 + 0.0003610\gamma^3 \quad 6-6$$

$$\frac{T_z}{T_p} = 0.6673 + 0.05037\gamma - 0.006230\gamma^2 + 0.0003341\gamma^3 \quad 6-7$$

However, this is only valid if  $\gamma$  is in the interval  $[1 \leq \gamma < 7]$  [5].

The  $\gamma$  value represents the peak shape factor in the JONSWAP spectrum. With a  $\gamma = 2$  into equation 6-6 and 6-7,  $T_1$  and  $T_z$  is found numerically:

$$T_1 = 0.805684T_p \approx 0.806T_p$$

$$T_z = 0.7457928T_p \approx 0.746T_p$$

The Ursell number is defined in DNV[5], from equation 6–8 as:

$$U_r = \frac{h_s}{k_1^2 d^3} \quad 6-8$$

Variables included in the Ursell number are the significant wave height  $H_s$ , water depth  $d$ , and wavenumber  $k_1$ . The wave dispersion relation must be solved to find  $k_1$ . The linear dispersion relation is valid for 2<sup>nd</sup> order nonlinear waves. This is because the wave celerity in a second-order wave theory is equal to small-amplitude wave celerity, e.g., linear wave.

The dispersion relation to solving for the wavenumber is given in equation 6–9 and in DNV[5]:

$$\frac{2\pi}{t_1} = g k_1 \tanh(k_1 d) \quad 6-9$$

Where,  $T_1$  is the mean wave period given in equation 6–6,  $g$  is the gravitational constant,  $k_1$  is the wave number and will be solved by iterating several numbers to find  $k_1$  which will make both sides equal, and water depth  $d$ .

When numbers are obtained for Steepness number  $S_1$  and the Ursell number  $U_r$ , parameters  $\alpha_F$  and  $\beta_F$  in Forristall's proposed model[26] can be solved by equation 6–10 and 6–11:

$$\alpha_F = 0.3536 + 0.2892S_1 + 0.1060U_r \quad 6-10$$

$$\beta_F = 2 - 2.1597S_1 + 0.0968U_r^2 \quad 6-11$$

The distribution function for the 3-hour extreme crest height following second-order theory is obtainable with equation 3-11:

$$F_{C|H_s T_p}(c|h_s, t_p, d) = \left[ 1 - \exp\left(-\left(\frac{c}{\alpha_F h_s}\right)^{\beta_F}\right) \right]^{N_{3h}} \quad 6-12$$

Where  $N_{3h}$  is the expected number of crest heights during 3-hour (10800s = 3-hour) with given  $T_p$ .  $T_z$  is the zero-up crossing wave period and is given by equation 6-7. Thus,  $N_{3h}$  reads:

$$N_{3h} = \frac{10800}{0.746t_p}$$

The distribution function in equation 6-12 is further used to obtain q-probability values of the air gap through the long term analysis methods POT and modified all-sea states. Although the weather data are from a deep water location (~1100 m), the weather characteristics will be applied for the jacket positioned at 110 m water depth.

## 6.2 Time-domain simulations

For a non-linear response of a jacket structure, a reasonable amount of time-domain simulations must be performed to obtain an accurate short term behaviour of extremes. The response accuracy will increase with an increased number of sea states simulated. Therefore, many seeds should be used for each sea state to reduce the statistical uncertainty of the obtained response. The result then becomes an accurate short term variability of 3-hour extremes.

The asymptotic short term variability of 3-hour extremes follows a Gumbel distribution[20][3]. The two parameters, location and scale, of the Gumbel distribution are estimated from the obtained 3-hour extremes of simulations and found by the method of moments[28]. The obtained Gumbel parameters for each response are plotted for the selected sea state simulated. A continuous function is applied (spline function) with a biharmonic (v4) surface between the selected sea states to obtain a function which will make it possible to obtain the short term variability of sea state, which has not been simulated. The response surface obtained by the spline function is further used in the long term analysis. By implementing the POT and the all-sea state approach, q-probability extreme responses can be estimated.

### 6.2.1 Simulations

The most accurate way to present the short term response from the structure would be to do an thousands of 3-hour time-domain simulations for all  $H_s$  and  $T_p$ . However, this is not always realistic. Instead, several 3-hour simulations are performed to capture the weather domain of interest through a grid pattern. The sea states must be reasonably spaced out within the area. One possible way to evaluate which sea states to simulate, is by inspecting the contours of the worst sea states in the hindcast dataset. The simulated sea states for this thesis are given in Figure 26. In practice, the sea states outside the DNV limit[5] will be hard to see due to the high wind speed needed to obtain these sea states. However, those points act as outer boundaries for the points on the right-hand side of the limit.

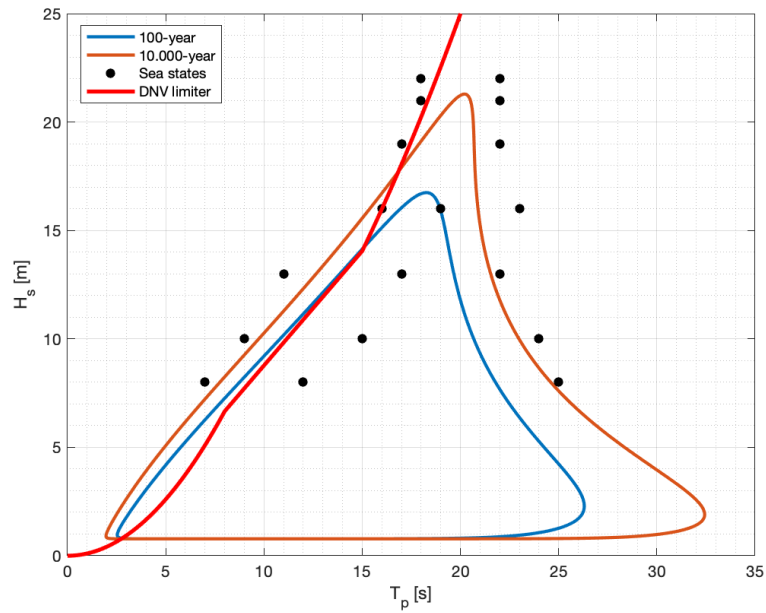


Figure 26: Simulated sea states for time-domain simulation of the jacket structure.

A total of 18 sea states have been chosen to simulate, with ten seeds per sea state. The total number of simulated 3-hour extremes is 180, however, it was later added three more simulations with 20 seeds. Due to the low seed number per sea state, the statistical uncertainty will be high. NORSOK N-003[2] requires a minimum of 20 - 40 seeds per sea state in a long term analysis. However, the number of sea states used to obtain the response in this thesis will give an approximate accuracy of the responses. The simulated sea states are given in Table 12.

Table 12: Selected sea states to simulate responses in the time domain.

Sea state	$H_s$ [m]	$T_p$ [s]		
<b>1 – 3</b>	8	7	12	25
<b>4 – 6</b>	10	9	15	24
<b>7 – 9</b>	13	11	17	22
<b>10 – 12</b>	16	16	19	22
<b>13 – 14</b>	19	17	22	-
<b>15 – 16</b>	21	18	22	-
<b>17 – 18</b>	22	18	22	-



### 6.2.2 Distribution of 3-hour extremes

The response maximum is considered following a Gumbel distribution[20]. The distribution function is seen in equation 6–13:

$$F_{X|H_s, T_p}(x|h, t) = \exp \left\{ - \exp \left[ - \frac{x - \alpha_G(h, t)}{\beta_G(h, t)} \right] \right\} \quad 6-13$$

Gumbel parameters  $\alpha_G$  and  $\beta_G$  are estimated for each sea state. The parameters are obtained by the method of moments[28]. From equation 6–14, this implies finding the mean  $\mu$ , and standard deviation  $\sigma$ , of the sample, which in this case is responses obtained from different seeds for one sea state. Gumbel parameters are estimated by[4][28]:

$$\alpha_G = \mu - 0.5772\beta_G \quad 6-14$$

$$\beta_G = \frac{\sigma\sqrt{6}}{\pi}$$

To obtain the adequacy of the Gumbel distribution for the 3-hour maximum response. A Gumbel probability plot has plotted one sea state for three responses. The sea state has  $H_s = 16 \text{ m}$  and  $T_p = 19 \text{ s}$ . The plot has a fitted line based on the parameters obtained from the method of moments and the 3-hour maximum response obtained from the simulations. Figure 27 displays the Gumbel probability plots, where figure (a) is base shear, (b) is deck displacement and (c) is overturning moment.

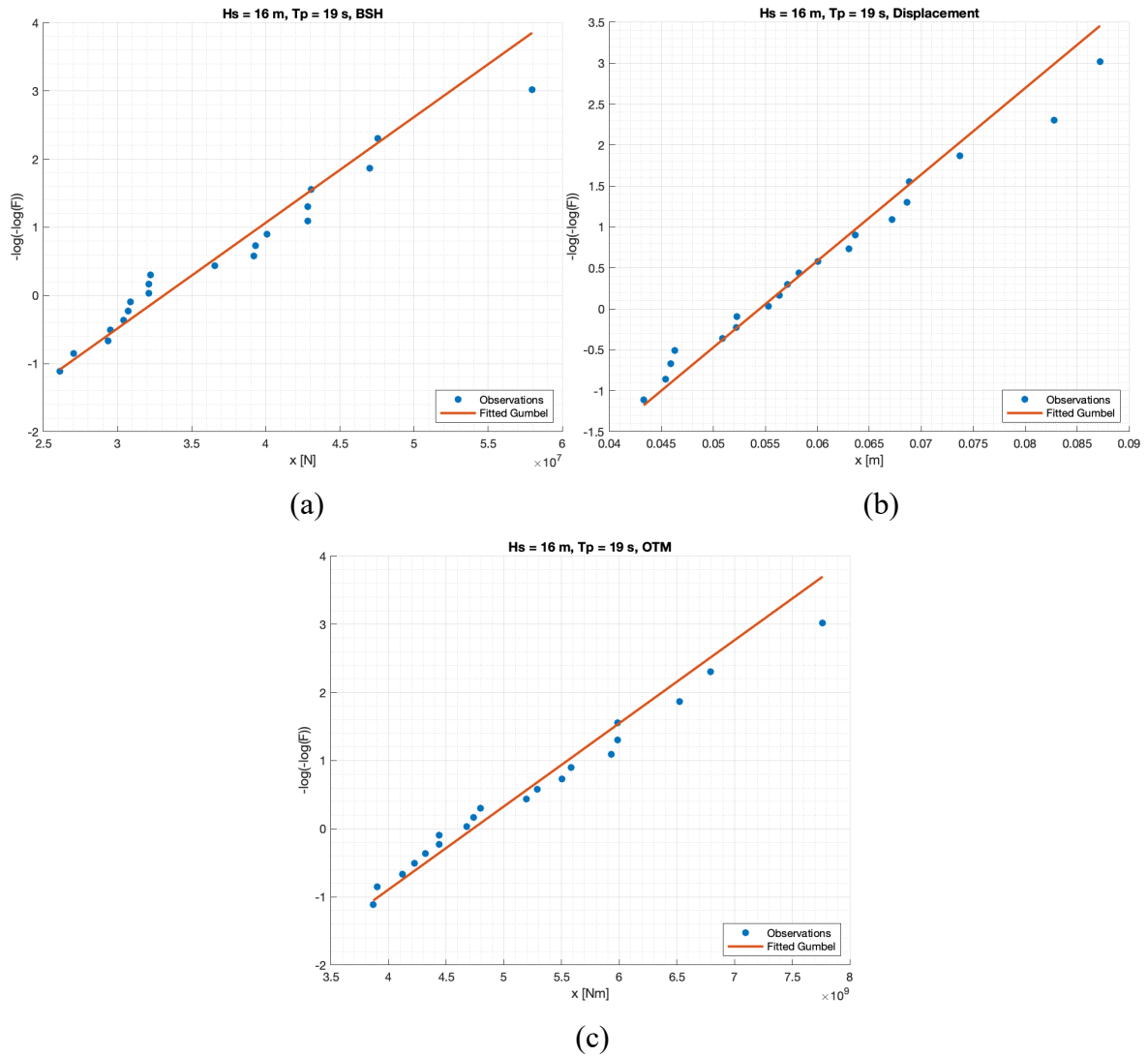


Figure 27: Gumbel distribution of 3-hour maximum responses. The selected sea state is  $H_s = 16$  m,  $T_p = 19$  s. Figure (a) response is base shear, (b) is deck displacement and (c) is overturning moment.

From Figure 27, it is clear that the underlying distribution has reached an asymptotic limit. This shows that the Gumbel distribution is suitable for modelling the responses of a jacket structure.

From all the 18 sea states, one  $\alpha_G$  and one  $\beta_G$  have been calculated. To obtain the response for the values not accounted for in the simulation, some sort of interpolation has to be implemented for the Gumbel parameters.

### 6.2.3 Response surface for Gumbel parameters

A surface where the Gumbel parameters  $\alpha_G$  and  $\beta_G$  are functions of  $H_s$  and  $T_p$  has to be obtained. This is done utilizing MATLAB's spline function, with the method biharmonic (v4) four gridded method[20]. The Gumbel parameters will change depending on the  $H_s$  and  $T_p$  input, e.g.,  $\alpha_G(h_s, t_p)$  and  $\beta_G(h_s, t_p)$ . The response surfaces for  $\alpha_G$  and  $\beta_G$  is seen in Figure 28, Figure 29, and Figure 30.

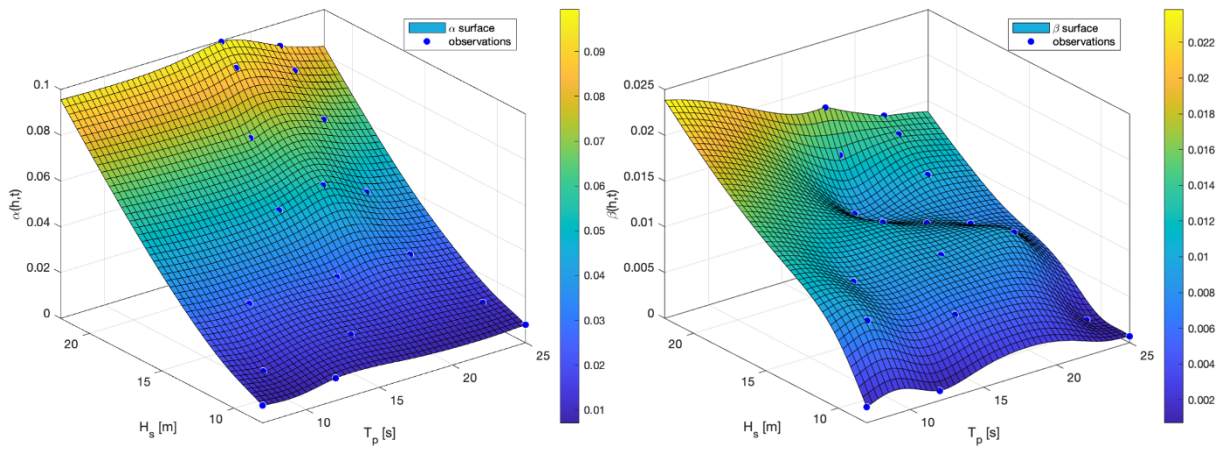


Figure 28: Deck displacement response surface for  $\alpha_G$  and  $\beta_G$

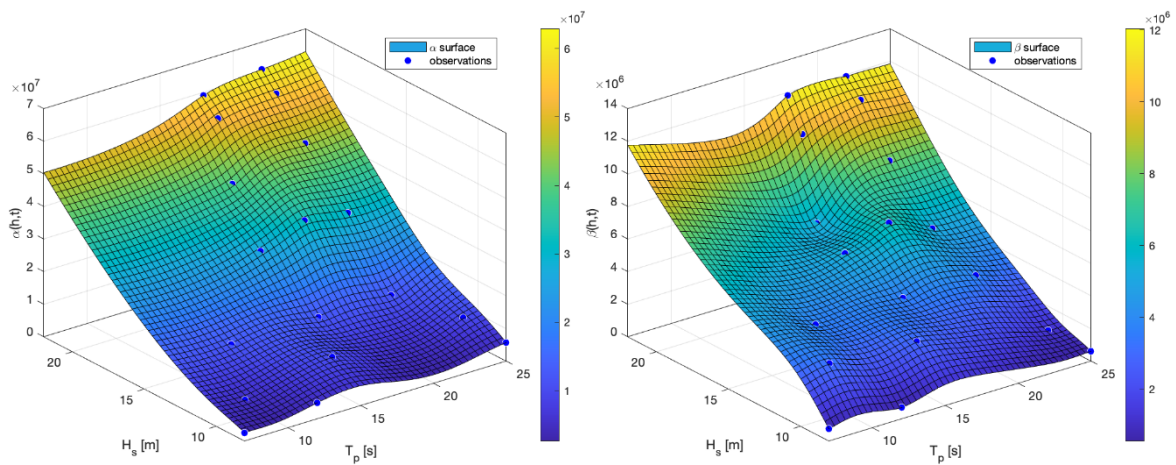


Figure 29: Base shear response surface for  $\alpha_G$  and  $\beta_G$

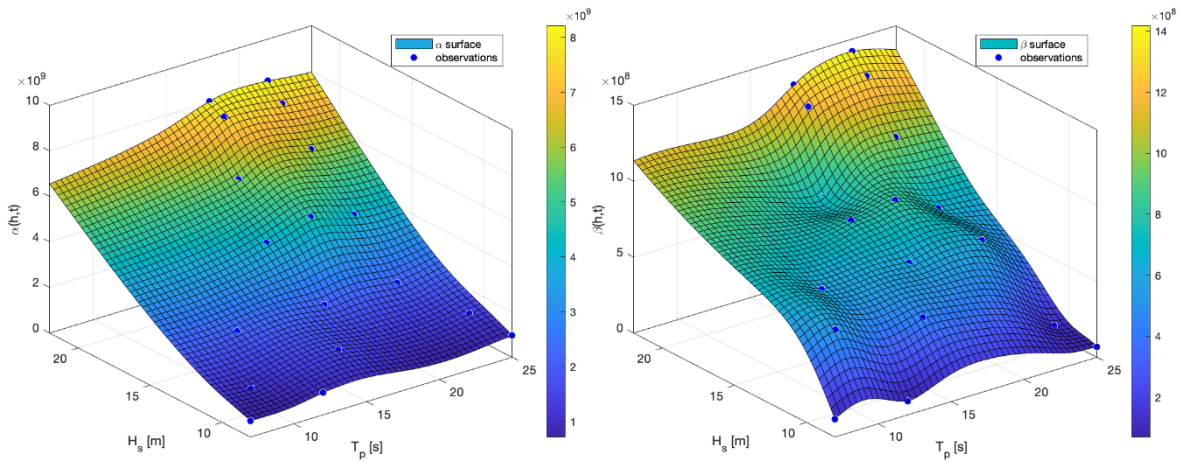


Figure 30: Overturning moment response surface for  $\alpha_G$  and  $\beta_G$

From the response surfaces, a cut-out is presented in Figure 31. The evolution of  $\alpha$  and  $\beta$  - response parameters in the Gumbel distribution is given for an increased  $H_s$  and a fixed  $T_p$ .

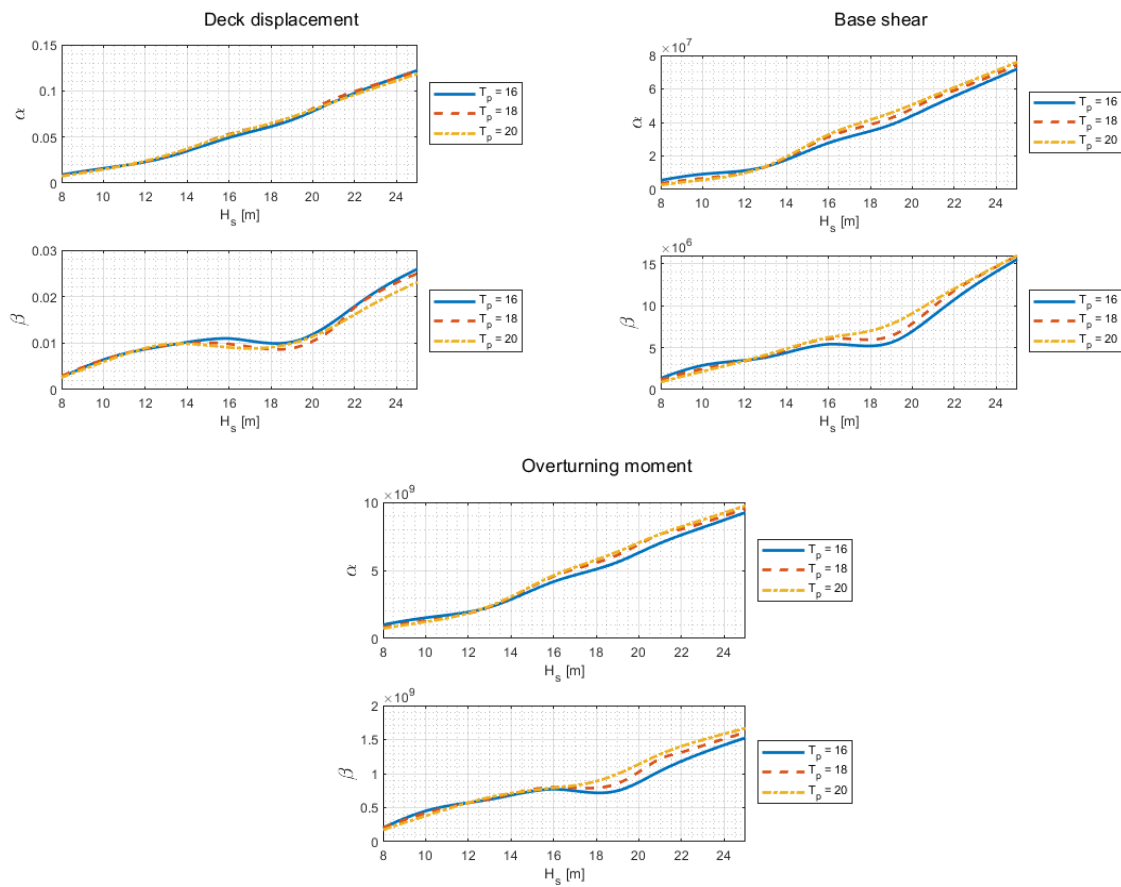


Figure 31: The evolution of Gumbel response parameters  $\alpha$  and  $\beta$  for the responses deck displacement, base shear and overturning moment. The evolution is considering an increasing  $H_s$  range and fixed  $T_p$ .

In addition, the evolution of  $\alpha$  and  $\beta$  -response parameters are also given for  $T_p$  when  $H_s$  is fixed, as seen in Figure 32.

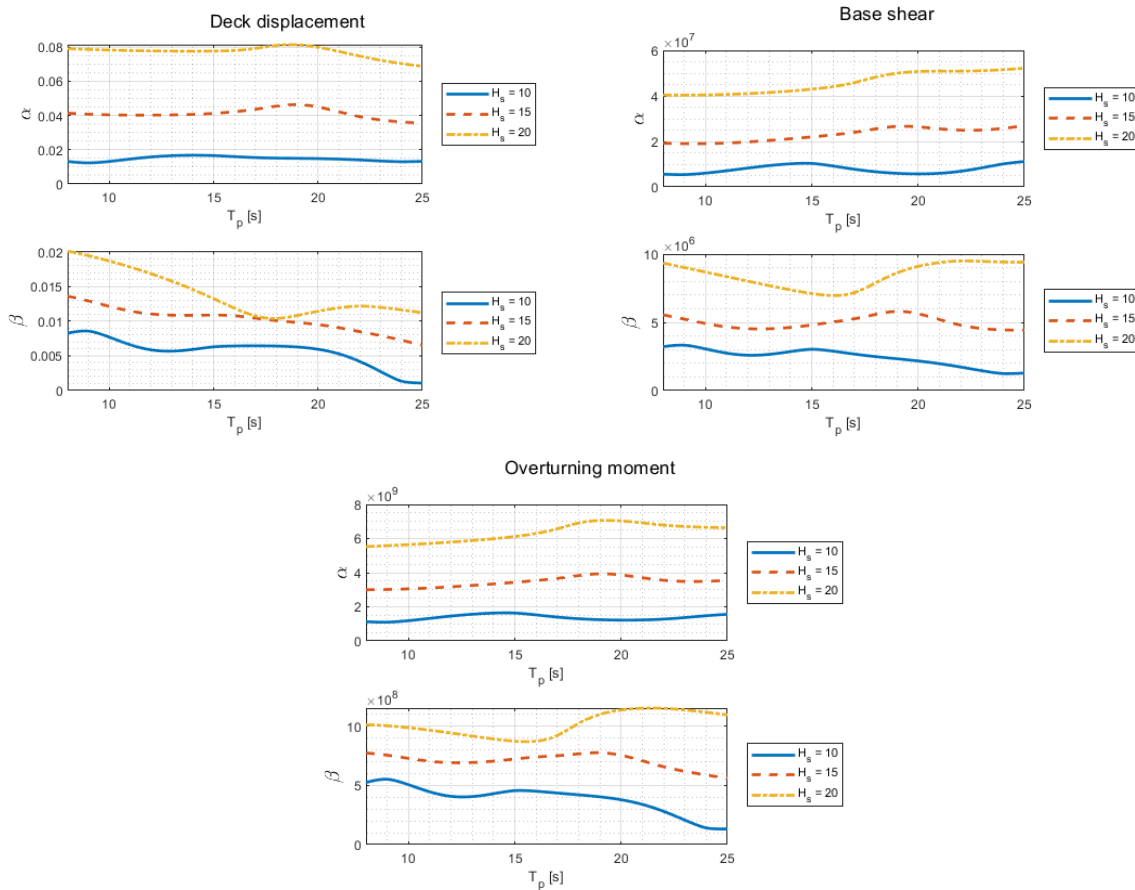


Figure 32: The evolution of Gumbel response parameters  $\alpha$  and  $\beta$  for the responses deck displacement, base shear and overturning moment. The evolution is considering an increasing  $T_p$  range and fixed  $H_s$ .

As seen in Figure 31 and Figure 32, the outcome is that the parameters in the response surfaces are increasing, as one would expect, since the response itself will increase for increased sea states. However, the spline function can behave in an unfavourable way if the spacing between each node and the difference between the interpolated values are large. In this case, this happens since the seed count for each simulated sea state is low and the node points are far spaced, due to the low simulated  $T_p$  values.

The reduction in  $\beta$  for the responses for  $H_s$  the range between 16 - 18 m and the fixed value  $T_p = 16$  s is probably occurring due to the low resolution of simulated sea states. Therefore,

the simulated sea states should be increased, and as a result, the spacing between the node points will be reduced, making the spline function behave better. The outcome of using spline on an increased sea state grid will be less unexpected shapes, such as a sudden decrease between two sea states when the response parameters should have increased.

The Gumbel parameter functions  $\alpha_G(h_s, t_p)$  and  $\beta_G(h_s, t_p)$  are further used in this thesis to describe the short term variability for the different responses[20].

## 7. LONG TERM ANALYSIS MODIFIED ALL SEA STATE

The long term analysis method used for the selected responses, second-order crest, deck displacement, overturning moment and base shear is a modified all sea state where only 8 m and above sea states are selected.

### 7.1 Modified all sea state approach

The most used long term method in the Norwegian Continental Shelf to estimate extreme values is the all sea state approach DNV[5]. This method uses all 3-hour events to predict extreme responses, which can be very time consuming since, in theory, all the sea states need to be simulated to obtain a reasonable estimate for extreme responses. The sea states are modelled as a joint distribution between the significant wave height and spectral peak period. The joint distribution of sea states can be seen in section 2.3. The long term response distribution is found by solving the integral:

$$F_{X_{3h}}(x) = \int_0^{\infty} \int_0^{\infty} F_{X_{3h}|H_s T_p}(x|h, t) f_{H_s T_p}(h, t) dt dh \quad 7-1$$

Where  $F_{X_{3h}|H_s T_p}(x|h, t)$  is the response given as a Gumbel distribution, where the parameters are obtained from the response spectrum for the given response.  $f_{H_s T_p}(h, t)$  is the joint modelling of sea states from hindcast data.

Due to time limitations and the fact that this is a master thesis and not design work, it was decided to remove the sea states below the threshold of 8 m. This was done to save time in the time domain simulations needed to obtain a proper response at the low sea states. As a fact, this thesis is more about utilizing the POT approach to predict extreme responses.

The reader is referred to section 2.3 to review how each distribution is obtained. The process will not be covered step by step in this section. However, some additional information will be provided.

### 7.1.1 Modified marginal distribution of $H_s$

The marginal distribution of the modified sea states for all events equal and over 8 m follows a 3-parameter Weibull distribution reasonably well. The distribution for  $H_s$  with the Weibull parameters reads:

$$F_{H_s}(h) = 1 - \exp\left(-\left(\frac{h - 7.899}{1.296}\right)^{1.098}\right) \quad 7-2$$

Where the parameters  $\alpha$ ,  $\beta$  and  $\lambda$  are obtained from the method of moments. The procedure for the method of moments for 3-parameter Weibull is described further in section 8.2.1. The fitting of marginal  $H_s$  for all values equal and over 8 m is seen in Figure 33 in a linear scale, e.g., Gumbel scale.



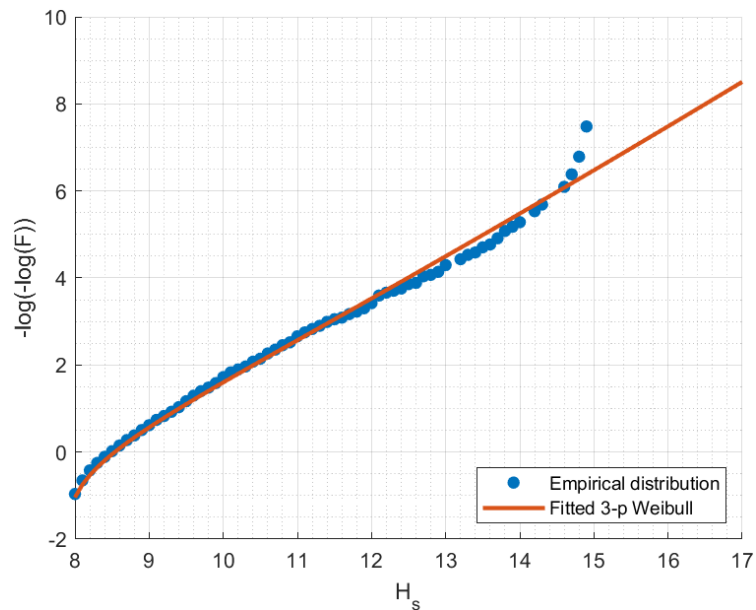


Figure 33: Fitted marginal distribution for  $H_s$  equal and over 8 m to a 3-parameter Weibull distribution. The distribution is seen in the Gumbel scale.

Comparing the all sea state 3-parameter Weibull from Figure 7 and the modified version found in Figure 33. It is clear to see how well the 3-parameter Weibull works for the larger values of  $H_s$  at the base of the distribution, i.e., at 8 m – 13 m. Both the base and almost the entire tail look like a very reasonable fit except for the outer end. As described before in section 2.3.1, the 3-parameter Weibull distribution seems to be more on the conservative side for areas where larger waves are present.

The order of magnitude of  $H_s$  based on the 3-parameter Weibull distribution using ALS and ULS design criterion is given in Table 13.

Table 13: Long term extrapolation of  $H_s$  to target probability.

ULS (100-year) [m]	ALS (10.000-year) [m]
16.48	20.90

### 7.1.2 Conditional distribution of $T_p$ given modified $H_s$

The conditional distribution of  $T_p$  follows the same log-normal distribution found in equation 2–6. The log-normal distribution parameters are fitted to each  $H_s$  group from the scatter diagram seen in appendix B. Based on this, fitting parameters for the non-linear fit are obtained. The equations for the non-linear fit with the corresponding coefficient values are seen in 7–3 and 7–4.

$$\mu_M = 1.0125 + h^{0.2276} \quad 7-3$$

$$\sigma_M^2 = 0.001 + 0.0631 \cdot \exp(-0.2231 \cdot h) \quad 7-4$$

Further, the fitting is seen in Figure 34 for  $\mu$  and Figure 35 for  $\sigma^2$ .

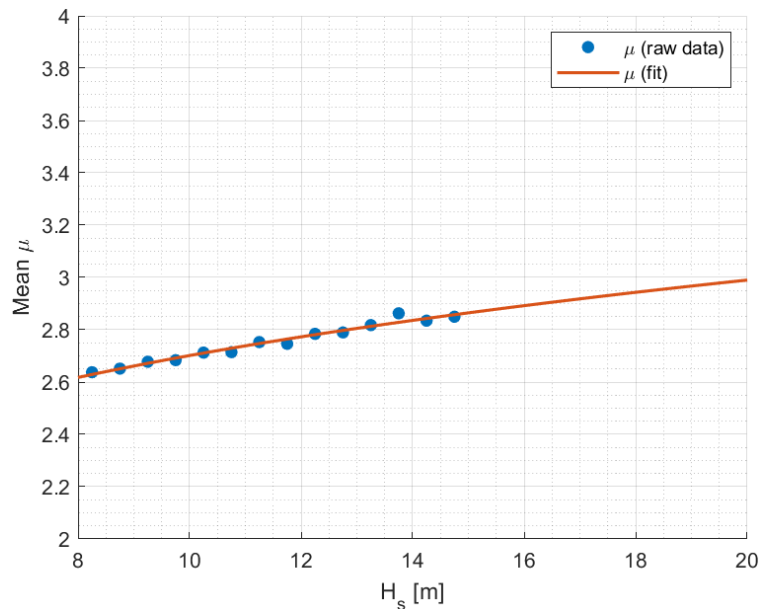


Figure 34: Non-linear fitting of log-normal parameter  $\mu$  for modified  $H_s$  values.

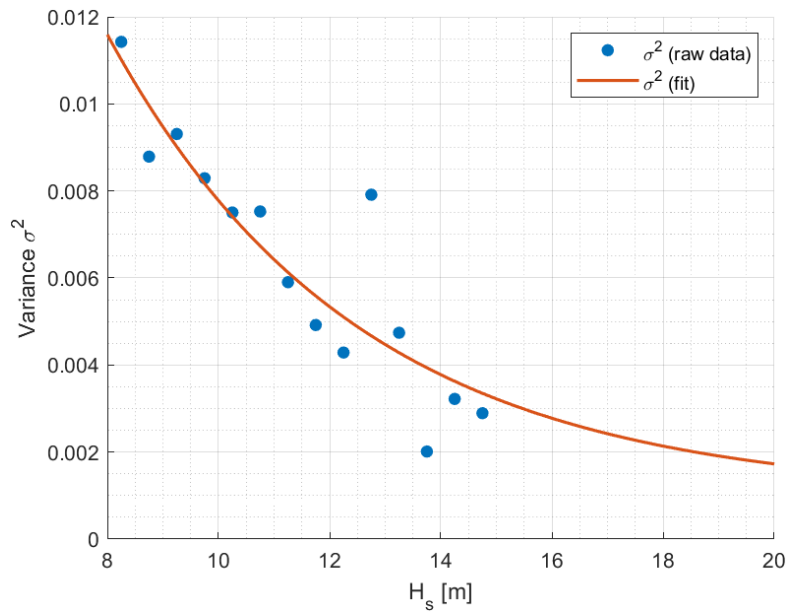


Figure 35: Non-linear fitting of log-normal parameter  $\sigma^2$  for modified  $H_s$  values.

A 90 % band for  $T_p$  can be found based on the fitted parameters. A low, mean and high value of  $T_p$  is found in Figure 36, and the values are given in Table 14.

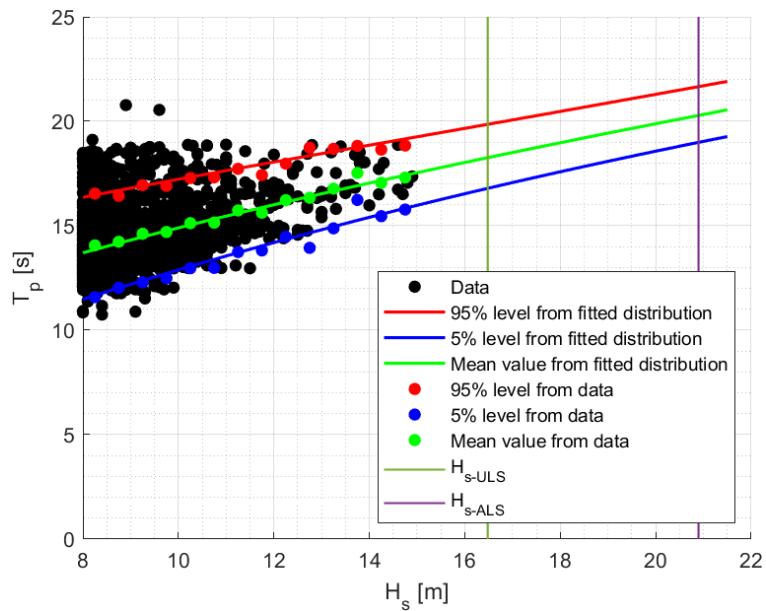


Figure 36: A 90 percentile of  $T_p$ , based on fitted  $T_p$  data.

Table 14: Values from the 90% band of ULS and ALS values.

	<b>H<sub>s</sub> [m]</b>	<b>T<sub>p</sub> 5 % [s]</b>	<b>T<sub>p</sub> mean [s]</b>	<b>T<sub>p</sub> 95 % [s]</b>
<b>ULS (10<sup>-2</sup>)</b>	16.48	16.79	18.26	19.85
<b>ALS (10<sup>-4</sup>)</b>	20.90	18.99	20.28	21.66

### 7.1.3 Contour lines based on modified H<sub>s</sub> values

The contour lines are constructed following the procedure in section 2.3.3. A new annual q-probability value is introduced since the number of sea states is equal to and over 8 m. The way to obtain the new annual exceedance probability is to divide the number of values over and equal to 8 m with the collection time in years. Here the data set consists of 61 years of data. The new q-probability for the ULS design criterion will be:

$$q = \frac{0.01}{29.0631} \quad 7-5$$

The contour lines based on the joint distribution of modified sea states with the q probability values of design levels of ULS and ALS are seen in Figure 37. The DNV limiter is added to the contour lines.

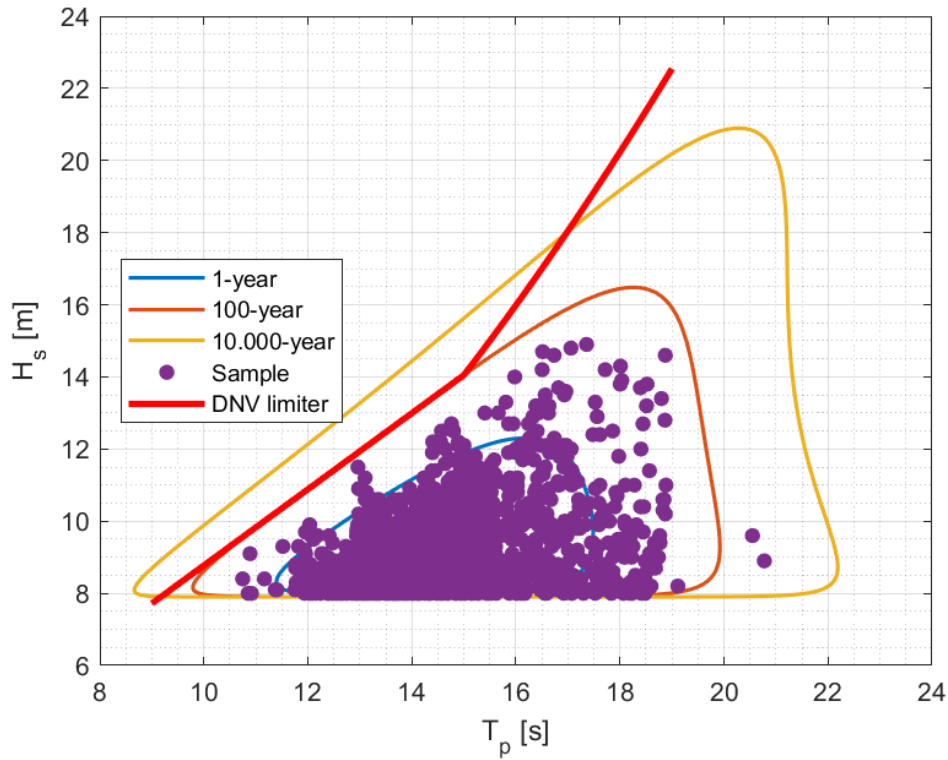


Figure 37: Contour lines based on the joint distribution of modified sea states.

#### 7.1.4 Long term analysis

The response distribution of the 3-hour maximum is obtained when solving the integral, and when the equation is set equal to the value desired to exceed every year. The q-probability for design regarding NORSOK[2] is given beforehand, and this leads to the long term analysis as the following[20]:

$$F_{X_{3h}}(x_q) = \iint_0^{\infty} F_{X_{3h}|H_s T_p}(x_q|h, t) f_{H_s T_p}(h, t) dt dh \quad 7-6$$

The following equation finds the probability of exceeding the target concerning the modified sea states[20]:

$$Q_{x_{3h}}(x_q) = 1 - F_{x_{3h}}(x_q) = \frac{q}{29.0631} \quad 7-7$$

Where  $q$  is the target probability, according to NORSOK[2], ULS value  $q = 10^{-2}$  and ALS value  $q = 10^{-4}$ . The value 29.0631 is described in section 7.1.4. All  $q$ -probability response values are given in appendix C.

Another available and rather interesting evaluation can be assessed from the all sea state approach. The relative contribution to the target response given the different sea states of  $H_s$  and  $T_p$ . The equation of relative contribution to the response reads:

$$Q_{x_{3h}}(x > x_q) = \iint_0^{\infty} (1 - F_{x_{3h}|H_sT_p}(x_q|h, t)) f_{H_sT_p}(h, t) dt dh \quad 7-8$$

Based on the response probability being larger than  $x_q$ , a colour map has been constructed to better show relative contributions from each sea state. As a result, the map will have a more intense red colour where the contributions of the sea state are highest. Furthermore, based on the map of relative contributions, more time-domain simulations can be performed to enhance the response in the area of the highest probability of extreme response occurring. This will give a more accurate long term analysis. Since this thesis deals with four responses, the relative contributions for each response regarding target probability will be shown in appendix C.

## 8. LONG TERM ANALYSIS POT

The long term analysis method POT is used for the selected responses, second-order crest, deck displacement, overturning moment and base shear.

The POT method for the overturning moment response will be thoroughly described in this chapter. The other responses are given in appendix D.

### 8.1 Short term modelling

The exact distribution of a storm is described by Haver[9], and it considers the storm as a step function. Each step of 3-hours is assumed to be stationary. The number of storm steps for a random storm can be described as a variable  $M$ . Hence, the storm will contain  $M$  storm steps of 3-hours with information about  $H_s$ ,  $T_p$ ,  $\theta$ [*direction*] and the occurring date. These are some of the measurements included in the hindcast database within the NCS. Each step extreme within the storm is assumed to be statically independent.

The distribution function for storm maximum response can be obtained and reads as follows:

$$F_{X|STORM}(x|storm) = \prod_{i=1}^M \left\{ \exp \left( -\exp \left( -\frac{x - \alpha_G}{\beta_G} \right) \right) \right\} \quad 8-1$$

In the case of a second-order crest height, the Gumbel model is replaced by the Forristall crest height model. The Gumbel parameters  $\alpha_G$  and  $\beta_G$  are the through response parameters obtained from the response surface. The cumulative density function (CDF) for the exact storm maximum response distribution from equation 8-1 is obtained by multiplying each consecutive storm step together to a storm maximum. For example, the CDF for each storm step response and the storm maximum response can be seen in Figure 38. The effect of the

storm's 2-3 largest steps contributes mainly to the storm's maximum crest height. This will be the case for most storms.

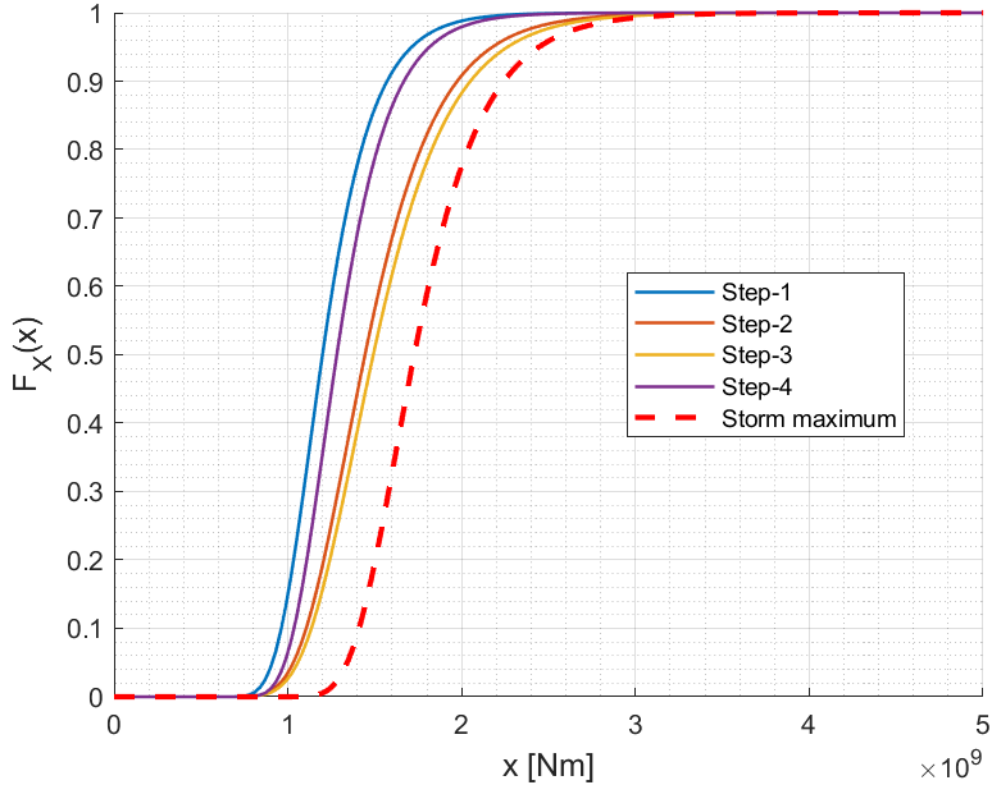


Figure 38: Cumulative density function for each storm step in a given storm. The functions for each step are multiplied to a storm maximum, seen as a dashed line in the figure.

Based on the work of Tromans & Vanderschuren[6], it is found that the exact distribution of storm maximum approaches asymptotic shapes. The exact storm response distribution  $F_{X|STORM}(x|storm)$  is further approximated by a Gumbel distribution[4]:

$$F_{x|\tilde{x}}(x|\tilde{x}) = \exp \left\{ - \exp \left[ - \frac{x - \tilde{x}}{\beta \tilde{x}} \right] \right\} \quad 8-2$$



The Gumbel parameter  $\tilde{x}$  is the location parameter and  $\beta$  is the scale parameter in the distribution. The distribution parameters for scale and location are solved by using the method of moments. The sample mean and variance are needed to obtain Gumbel parameters[4]:

$$E(X|\tilde{X}) = \tilde{x} + 0.5772\beta$$

$$Var(X|\tilde{X}) = \frac{\pi^2}{6}(\tilde{x}\beta)^2$$

Two requirements must be met for the Gumbel distribution to work as an approximation of the exact distribution.

- 1) Each storm's most probable maximum (mpm) must be the same for the approximated (8-2), and the exact distribution (8-1)[4].
- 2) The exact storm distribution's standard deviation must be equal to the standard deviation of the approximated Gumbel distribution[4].

The most probable maximum response  $\tilde{X}$ , is from Tromans & Vanderschuren[6] obtained when the exact distribution of the storm response  $F_{X|STORM}(x|storm)$  is equal to  $\frac{1}{e}$  read from equation 8-3.

$$F_{X|STORM} \approx e^{-1} \tag{8-3}$$

The calculation in equation 8-3 is performed for all acquired storms within the data giving a range of different most probable maximum response values. The most probable maximum response for a given storm can be assessed in Figure 39.

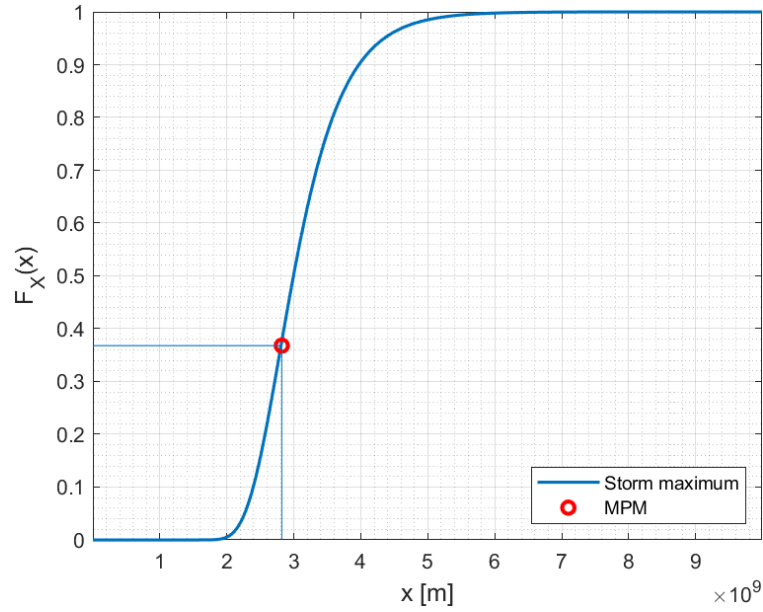


Figure 39: Cumulative density function of the exact storm, displaying its most probable maximum.

To obtain the standard deviation of the exact distribution, both the expected value and the variance have to be calculated first. This is done by the theoretical definition of expected value and variance following equations 8-4 and 8-5 [4]. However, since the cdf for all storms has already been calculated, the following integral will be solved numerically using the following relation between cumulative density function and probability density function,  $dF_X(x)_i = F_X(x)_{i+1} - F_X(x)_i$ .

$$E(X) = \int_0^{\infty} x \cdot f_X(x) dx = \sum_{i=1}^{k-1} x_i \cdot dF_X(x)_i \quad 8-4$$

$$Var(X) = \int_0^{\infty} [x - E(X)]^2 \cdot f_X(x) dx = \sum_{i=1}^{k-1} [x_i - E(X)]^2 \cdot dF_X(x)_i \quad 8-5$$

The variance of the storms is now obtained from the exact distribution. Combining the standard deviation  $\sigma = \sqrt{Var(x)}$  of a given storm with the corresponding  $\tilde{X}$  (mpm) storm value, the storm's  $\beta$  value can be calculated and read from equation 8-6.

$$\beta = \frac{\sigma\sqrt{6}}{\pi \tilde{x}} \quad 8-6$$

The  $\beta$  values obtained from each storm's maximum response are plotted in Figure 40. Each storm will have a slightly different value due to the storm's maximum response difference. Due to the fact that this is a short term variability, one can take the mean value of all the  $\beta$  values. This value will become the constant  $\beta$  value for the selected threshold for all storms. It is shown that the  $\beta$  value for deck displacement for a threshold of 8 m is 0.1758.

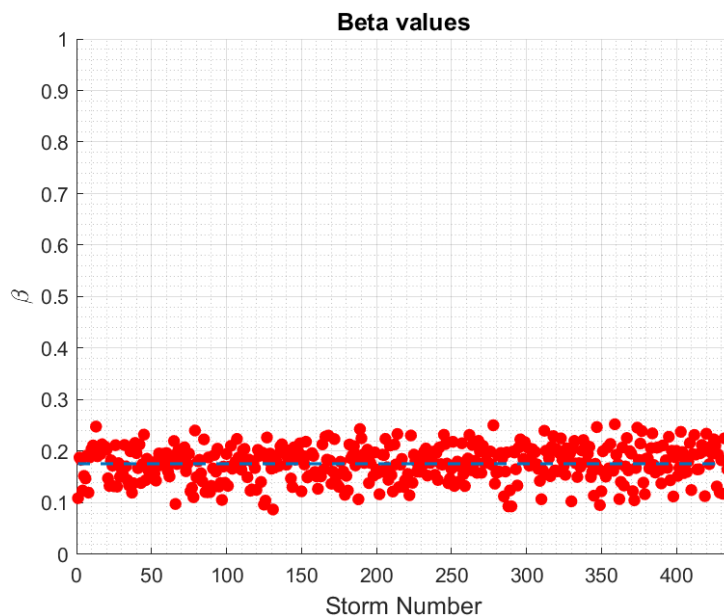


Figure 40:  $\beta$  values for all the storms over the threshold of 8 m.

After the  $\beta$ -constant is adopted to all storms, plots comparing the approximated Gumbel distribution  $F_{X|\tilde{x}}(x|\tilde{x})$  and the exact distribution  $F_{X|STORM}(x|storm)$  for a given storm in the

data series can be produced. Figure 41 shows the exact and approximated distributions plotted in a Gumbel probability paper. Based on Figure 41, it can be concluded that the asymptotic behaviour is met. This means that the approximated distribution is very close to the exact distribution.

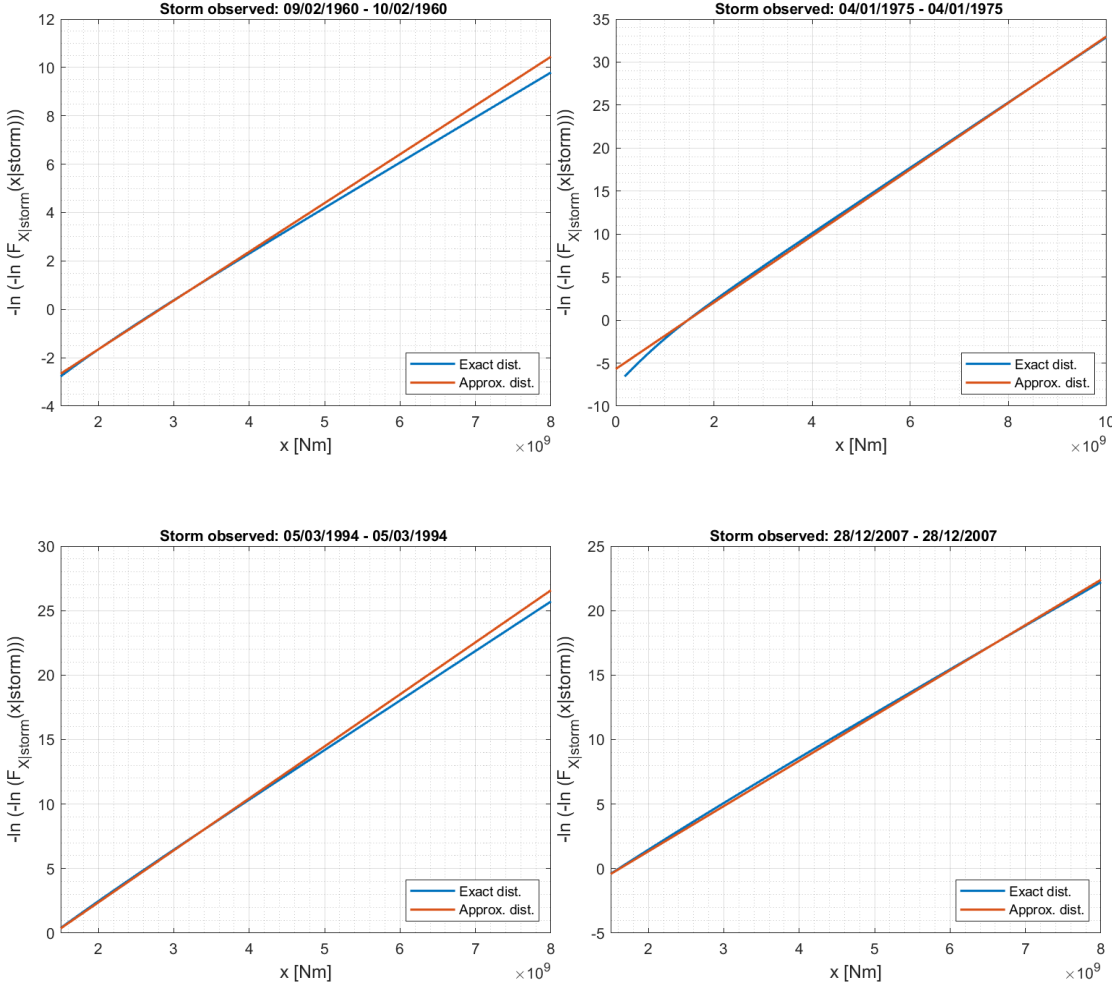


Figure 41: Compares the exact and approximated storm distribution in a Gumbel probability paper for random storms in the dataset. The exact distribution is from the overturning moment response.

## 8.2 Long term analysis

The long term analysis consists of the long term analysis of the most probable maximum response  $\tilde{X}$ , and the long term analysis of  $X$ .

### 8.2.1 Long term analysis of mpm storm max, $\tilde{X}$

For each given threshold, a corresponding  $\tilde{X}$  (mpm) is obtained for every storm. These most probable maximum response values can be fitted to a probabilistic model to obtain the long term distribution of the most probable maximum response  $\tilde{X}$ . The reasonable fit for  $\tilde{X}$  was obtained with a 3-parameter Weibull distribution given in equation 8-7[28].

$$F_{\tilde{X}}(\tilde{x}) = 1 - \exp \left[ - \left( \frac{\tilde{x} - \lambda}{\alpha} \right)^\beta \right] \quad 8-7$$

In this distribution, the three unknown parameters  $\alpha$ ,  $\beta$  and  $\lambda$  are the scale, shape and location parameters of the distribution. A requirement of using this equation is  $\tilde{x} \geq \lambda$ [28].

The unknown parameters are obtained using the method of moments (MoM) [4]. The moments used in a 3-parameter Weibull distribution are read from equations 8-8 to 8-10:

$$\mu_{\tilde{X}} = \lambda + \alpha \Gamma \left( 1 + \frac{1}{\beta} \right) \quad 8-8$$

$$\sigma_{\tilde{X}}^2 = \alpha^2 \left[ \Gamma \left( 1 + \frac{2}{\beta} \right) - \Gamma^2 \left( 1 + \frac{1}{\beta} \right) \right] \quad 8-9$$

$$v_1 = \frac{\Gamma\left(1 + \frac{3}{\beta}\right) - 3\Gamma\left(1 + \frac{1}{\beta}\right)\Gamma\left(1 + \frac{2}{\beta}\right) + 2\Gamma^3\left(1 + \frac{1}{\beta}\right)}{\left[\Gamma\left(1 + \frac{2}{\beta}\right) - \Gamma^2\left(1 + \frac{1}{\beta}\right)\right]^{\frac{3}{2}}} \quad 8-10$$

The values from the sample are the sample mean, sample variance and sample skewness. By obtaining these quantities from the sample and inserting them into the given equations above, the unknown parameters in the 3-parameter Weibull distribution will be known[4].

In order to fit the data in a probability paper, the correct interpretation of the data is needed. This means sorting the data by increasing values and removing duplicated values from the total sample size  $n$ . Finally, the empirical probability distribution function 8-11 is calculated as:

$$\hat{F}_k(k) = \frac{k}{n+1} \quad 8-11$$

The empirical distribution can be plotted in a probability paper to determine if the fit is reasonable, and the following fitted distribution is to be used further in estimating extreme values.

Since the sample data is fitted using a 3-parameter Weibull distribution, two probability plots can be constructed based on the 3-parameter Weibull distribution, one in logarithmic and one in linear scale. A Weibull probability paper, which reads:

$$\ln\left(-\ln\left(1 - F_{\tilde{x}}(\tilde{x})\right)\right) = \beta \ln(\tilde{x} - \lambda) - \beta \ln \alpha \quad 8-12$$

Furthermore, a Gumbel probability paper should be used to obtain a non-scaled extrapolation towards extremes. Due to the logarithm scale on the x-axis, the Weibull probability paper will not give. The Gumbel probability paper equation is given as:

$$-\ln\left(-\ln\left(F_{\tilde{X}}(\tilde{x})\right)\right) = \frac{\tilde{x} - \alpha}{\beta} \tag{8-13}$$

The results of plotting  $\tilde{X}$  both probability papers described above are found in Figure 42 and Figure 43. The plots give the sample as dots, while a fitted line represents the 3-parameter Weibull distribution with parameters described in Table 29. In both plots, the threshold has been set to 8 m, yielding a 3-parameter distribution as:

$$F_{\tilde{X}}(\tilde{x}) = 1 - \exp\left[-\left(\frac{\tilde{x} - 9.29e08}{8.05e08}\right)^{1.33}\right]$$

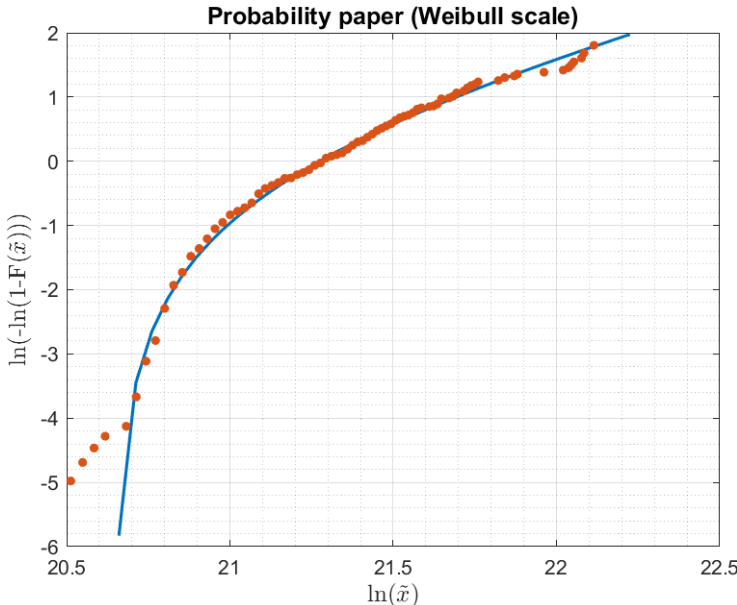


Figure 42: Probability plot in Weibull scale, where a fitted 3-parameter Weibull distribution is compared to an empirical sample of  $\tilde{X}$  values.

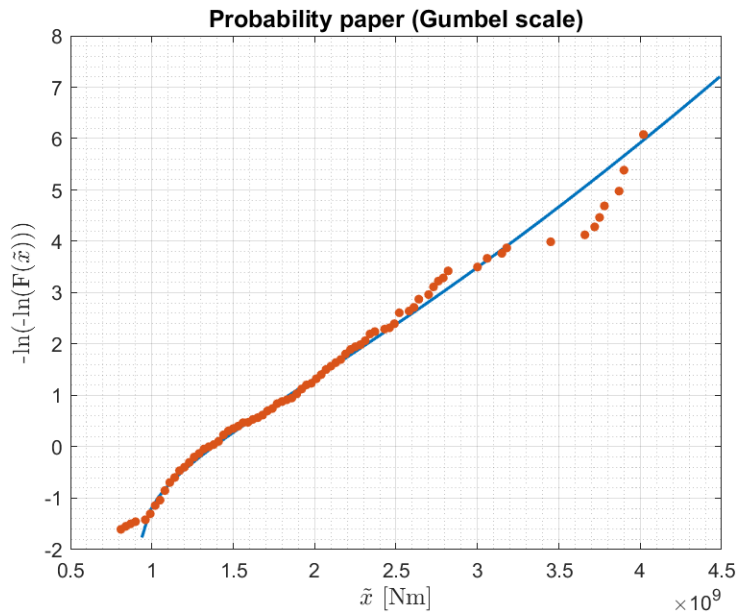


Figure 43: Probability plot in Gumbel scale, where a fitted 3-parameter Weibull distribution is compared to an empirical sample of  $\tilde{X}$  values.

The 3-parameter Weibull seems to fit the data reasonably well. However, there are some uncertainties regarding the furthest tail, the most extreme values. From Figure 42, the fit seems exceptionally good, which means that the extrapolation to a design mpm response value would seem accurate. However, plotting it in a true scale, i.e. without logarithm, more uncertainty will immerse in the tail regarding extrapolated values to the wanted values. The distribution's base (opposite the tail) yields an inaccuracy. For this thesis, we are neglecting this since these mpm values are of lower responses and ultimately will not change the outcome of the distribution fitted line.

Table 15: Most probable maximum overturning moment corresponding to ULS and ALS values at threshold 8 m.

ULS (100-year) [m]	ALS (10.000-year) [m]
4.2509e+09	5.8838e+09

To better understand the magnitudes of the most probable maximum response in the long term distribution of most probable maximums, calculations regarding ULS and ALS-mpm responses are computed, and given in Table 15. This will, however, indicate the response



level since this is only a short-term analysis. The long-term analysis will likely yield larger values for the given response.

### 8.2.2 Long term analysis of X

The long term distribution of deck displacement response is given in equation 8–14:

$$F_X(x) = \int_0^{\infty} F_{X|\tilde{x}}(x|\tilde{x})f_{\tilde{x}}(\tilde{x})d\tilde{x} \tag{8-14}$$

Where the conditional distribution function of the most probable maximum overturning moment in a storm  $F_{X|\tilde{x}}(x|\tilde{x})$  is multiplied with the long term distribution function of the most probable overturning moment maximum  $f_{\tilde{x}}(\tilde{x})$ . The distribution function of  $F_X(x)$  can be seen in Figure 44 and is given in a Gumbel probability paper in Figure 45.

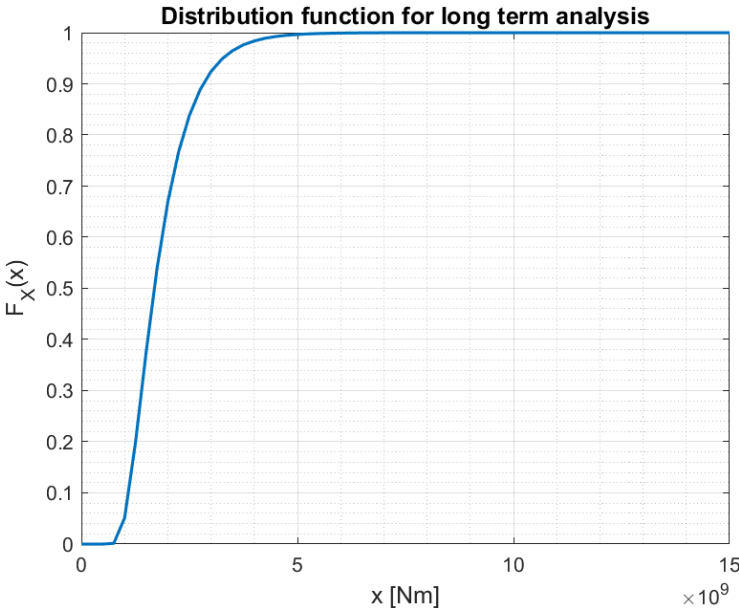


Figure 44: Distribution function for the long term analysis of overturning moment. The threshold is 8 m.

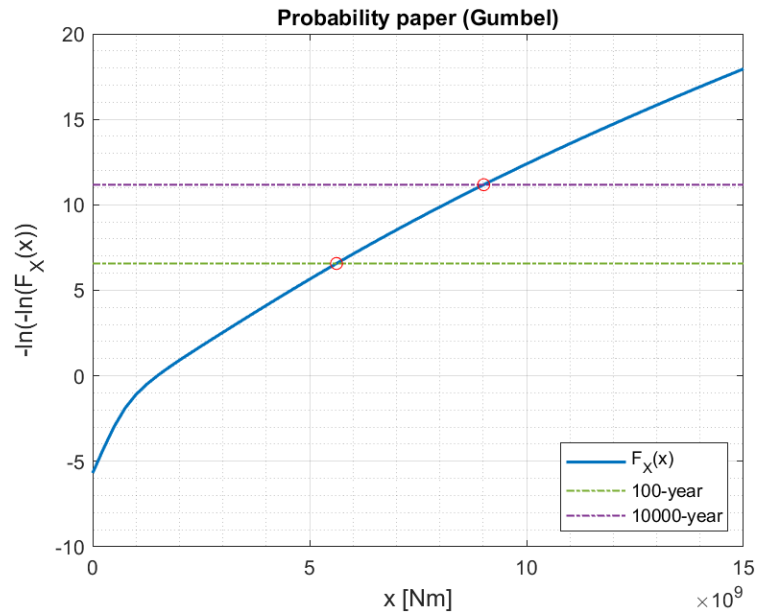


Figure 45: Distribution function for the long term analysis of an overturning moment in a Gumbel probability paper. The threshold is 8 m.

From a design perspective, a characteristic value of the overturning moment is needed. The exceedance probability used in NORSOK[2] and in general in the NCS is the probability of exceedance  $q = 10^{-2}$  (ULS) and  $q = 10^{-4}$  (ALS). This is calculated by the following equation 8–15:

$$1 - F_X(x) = \frac{q}{N_{storms}} \quad 8-15$$

Where the  $q$  is equal to the exceedance probability,  $F_X(x)$  is the long term analysis of overturning moment distribution and  $N_{storms}$  is the number of a storm occurring each year. This quantity is found by dividing all storms over the threshold limit by the number of years of data. This number will change for each threshold selected. The characteristic most significant values are given in Table 16 for both ALS and ULS.

Table 16: Characteristic most significant values for the overturning moment given ULS and ALS for different thresholds.

ULS (100-year) [m]	ALS (10.000-year) [m]
5.6023e+09	9.0127e+09

As expected, the long term overturning moment is larger than the magnitude of the  $\tilde{X}$  values obtained in the long term distribution of the most probable response maximum. However, this implies that it is not possible to use the long term  $\tilde{X}$  values as the design parameter. Instead, a full long term analysis of the overturning moment is needed.

### 8.3 Threshold sensitivity study

A selected threshold is used to filtrate the lower sea states to obtain the storm data. By increasing this threshold, a reduction in the number of storms can be seen, as displayed in Table 17. However, this will eventually lead to insufficient data if the threshold is raised too high, impacting the q-probability values. The aim is to obtain the highest threshold possible but still obtain a reasonable accuracy on the predicted extremes. If this is not possible and a lower threshold is needed, then the point of using a storm based approach goes away. However, the trade-off in a POT approach will always be less available data.

Table 17: Sensitivity study of the storms by threshold.

Threshold	8 m	9 m	10 m
Storms	436	224	110
Storms per year	7.14	3.67	1.80

There is no clear way to obtain the most accurate threshold level. The general way is to find a preferred area between the threshold levels where the values are relatively stable with little

increase. However, this is hard to find since the response will increase in most cases. However, it might be best to find the smallest increase in response or other relevant values between two threshold levels.

In this thesis, two values will be evaluated for threshold selection,  $\beta_v$  which is the parameter in the short term variability in the POT. The second is the ALS values for all the responses considered in the POT analysis.

Table 18:  $\beta_v$  values for all responses given different thresholds.

Threshold [m]	Crest	Displacement	Overturning moment	Base shear
8	0.0636	0.2201	0.1758	0.2000
9	0.0639	0.2638	0.2104	0.2258
10	0.0654	0.2900	0.2334	0.2456

Table 19: Comparison for threshold analysis of ALS responses of the jacket structure.

ALS	8 m	9 m	10 m	Step 8 - 9 m	Step 9 – 10 m
Crest [m]	23.91	23.58	23.42	-1.40 %	-0.68 %
Deck displacement [m]	0.1351	0.1459	0.1553	8.73 %	6.44 %
Overturning moment [Nm]	9.0127e+09	9.7211e+09	1.0506e+10	7.86 %	8.07 %
Base shear [N]	6.0347e+07	6.3423e+07	6.9012e+07	5.09 %	8.81 %

The storms observed over threshold level 10 m are four times less than 8 m. In practice, this means that the amount of available data is limited, and there is a high uncertainty using the estimated q-probability numbers at this time. This will, however, change in the future, when more storm data is available. At threshold level 10 m,  $\beta_v$ , as seen in Table 18, is at the highest value. This supports that the threshold at 10 m should not be recommended for further use in this thesis.

Based on the ALS responses between 8 – 9 m for the jacket, the response values increased by 5 – 8.73 %. It could be reasonable to use 9 m since it is desired to use the largest possible

threshold in the POT, without increasing the response values too much. However, there are more storm data at 8 m, and therefore the q-probability values are more accurate. Therefore, a range between 8 – 9 m is reasonable in this thesis.

It would be optimal to select the threshold that yields roughly the same characteristic values. For example, the percentage increase from Table 19 for the responses of threshold 8 m – 9 m is almost the same as for 9 m – 10 m, although there are almost four times the amount of storms for 8 m compared to 10 m. Other usages of POT in the NCS[13][12] have suggested 8 - 9 m to be a reasonable choice of threshold.

## 9. COMPARISON BETWEEN LONG TERM ANALYSES METHODS POT AND MODIFIED ALL SEA STATE

The characteristic responses obtained by the predictions from the long term analysis methods POT and modified all sea states, are given in Table 20 for threshold 8 m and in Table 21 for threshold 9 m.

*Table 20: Comparison table of responses predicted by POT and modified all sea state. The threshold is 8 m.*

Threshold = 8 m for POT	POT	Modified all sea state	POT	Modified all sea state
	100-year	100-year	10.000-year	10.000-year
Crest height [m]	18.30	18.61	23.91	24.33
Deck displacement [m]	0.0781	0.0792	0.1351	0.1272
Base shear [N]	3.7136e+07	4.2389e+07	6.0348e+07	7.7881e+07
Overturning moment [Nm]	5.6203e+09	6.2214e+09	9.0127e+09	1.0530e+10

*Table 21: Comparison table of responses predicted by POT and modified all sea state. The threshold is 9 m.*

Threshold = 9 m for POT	POT	Modified all sea state	POT	Modified all sea state
	100-year	100-year	10.000-year	10.000-year
Crest height [m]	18.23	18.61	23.58	24.33
Deck displacement [m]	0.0838	0.0792	0.1459	0.1272
Base shear [N]	3.8829e+07	4.2389e+07	6.3423e+07	7.7881e+07
Overturning moment [Nm]	5.9846e+09	6.2214e+09	9.7211e+09	1.0530e+10

Based on the ULS and ALS values chosen, the q-probability responses are compared. The jacket responses overturning moment and base shear will be in focus. As seen in Table 20 and Table 21, the deck displacement does not give a consistent value. From the relative contribution of the sea states in Figure 47 for deck displacement, it is seen that the responses in ULS and ALS are incorrect. The response surface was slightly changed as an investigation towards finding the error. By doing this, the relative contribution changes for the worse, indicating that the deck displacement response surface is source of error. The deck displacement must be sensitive, since both responses for overturning moment and base shear were relatively good. All the responses are obtained from the same time-domain simulations.

The base shear has the largest difference between the long term analysis methods. The ULS level is 14.14 % when POT has a threshold of 8 m. Similarly, for the overturning moment, the difference is 10.70 %. When the threshold is increased to 9 m for the POT, the difference for ULS for base shear reduces to 9.17 % and, similarly for overturning moment, to 3.94 %. Since the responses increases with an increased threshold for POT, the differences in ULS predictions are less for 9 m than for 8 m.

By investigating the ALS predicted values for both long term analysis methods with a threshold for POT at 8 m, it is seen that the difference in base shear is 29.0 %. Similarly, for overturning moment, the difference is 16.80 %. The large difference between POT and modified all sea state must again be the response surface. By increasing the threshold to 9 m for the POT, the base shear difference in ALS reduces to 22.78 %, and, similarly for the overturning moment, to 8.31 %.

Based on the ULS and ALS results when using the two methods, it is clear that the POT underestimates the predicted q-probability responses compared to the modified all sea state. In general, the modified all sea state approach will yield more conservative estimates due to the correlation between the successive sea states, which is neglected in the POT.

## 10. CONCLUSION

The thesis aimed to obtain a short term variability of a jacket structure and then compare the characteristic response values from the POT with the more known conservative method, the all sea state. However, in this thesis, the all sea state approach was modified to only include waves equal to and larger than 8 m significant wave height.

The characteristic values obtained from the POT showed a less conservative estimate for the q-probabilities compared to the all sea state. A slight deviation was obtained from the deck displacement. This can be seen regarding the response surface, and would not have been an issue if more time-domain simulations had been performed. The relative contribution of sea states shows that an issue is occurring for this response only. The conservatism of the all sea state approach can be seen by neglecting the correlation between the successive sea states, which in reality is highly correlated. The assumption of neglecting the sea states under 8 m will, in this case, reduce the conservative estimates in the all sea state. The POT approach has less observed data than the all sea state. However, the data quality is significantly higher due to the uncorrelated data observed from a storm maximum between storms.

The challenge for the POT is the amount of storm data, which the chosen threshold will highly influence. From Table 5, it is seen that the amount of storms is reduced by almost half for a 1 m increased threshold. This is seen for every threshold increase from 7 - 10 m. Therefore, by the number of storms available and the change in q-probability response, it would be assumed that the thresholds between 8 m and 9 m will be the optimal threshold selection. This is also considered by Haver & Bratland[13] to be a reasonable choice for assessing airgap on the NCS.

As a closing remark, the less conservative values obtained by the q-probability responses in a POT analysis. Compared to the all sea state, this will give a more optimized design regarding economy without any compromise on the safety aspect of the structural design.



## 10.1 Future work

As a closing remark to this thesis, I would like to address future work based on the knowledge gained while working on the subject.

### **Storms**

The storms in the POT analysis are obtained without any specified time between each storm. This ensures that the statistical uncertainty is larger than if a time was specified between each storm. For practical meaning, if a storm drops below the threshold limit and then increases to a new maximum within the same storm, it will be counted as two uncorrelated storms. In reality, it will be the same storm but counted as two. Therefore, a sensitivity study should be performed to find the optimal time between each consecutive storm. From past studies, the time between two storms can be in the range of 24-hours to 48-hours should be sufficient[12]. Tromans & Vanderscuren[6] have proposed two methods to identify storms, the first disregards the time of the sea states below 30 – 40 % of the largest significant wave height in the storm. The second method purposes that if the trough between two storm peaks is less than 80 % of the lowest significant wave peak of the two, then the storms should be broken from the trough into two storms.

### **Simulated wave elevation**

The simulated waves in Usfos utilized linear wave theory with Wheeler stretching. This is not representative of the real ocean and is not recommended by NORSOK N-003[2]. Future simulations should follow second-order wave theory to obtain the responses. It shows that the larger crests increase the responses from 30 - 55 % for the jacket structure in this thesis for one sea state. The long term distribution of q-probability responses will also be more in the range of what can be expected in the ocean.

## Response surface

There were 18 simulated sea states in total, with 10 seeds per sea state. Due to the low seeds per sea state, there are large statistical uncertainties. This means that if two responses are very large in the ten seeds, the mean and standard deviation will be statistically higher than if there were, for example, 40 seeds. The simulated sea states in the grid should also include more points and focus on areas where POT sea states are dominant. By increasing the simulated sea states and seeds, the accuracy in the spline function would increase hence a better long term analysis. The optimal simulation location of sea states could be obtained from the relative contribution of sea states to the relevant response.

## Current

In this thesis, the current was not included as a part of the calculation of extremes. The current speed is relatively low, compared to the horizontal particle speed of the wave. The current velocity is very important for drag load-dominated structures in obtaining extremes. This is shown by extracting the wave-particle and current velocity out by considering the drag load per unit length[4]:

$$(u_w + u_c)^2 = u_w^2 + 2u_w u_c + u_c^2 \quad 10-1$$

The term where the current velocity is multiplied by the wave velocity and 2 is very important and will increase the drag load by as much as 25 % in some extreme cases[4]. This implies that current must be added for a better prediction of extremes regarding structures of load govern responses.

## REFERENCES

- [1] “Design of offshore steel structures, general - LRFD method.” DNV GL AS, Jul. 2015.
- [2] “NORSOK standard N-003 - Actions and effects.” NORSOK standard, Sep. 2007.
- [3] Sverre Haver and Steven R. Winterstein, “Environmental Contour Lines: A Method for Estimating Long Term Extremes by a Short Term Analysis,” *Society of Naval Architects and Marine Engineers*, Jan. 2008.
- [4] Sverre Haver, *METOCEAN MODELLING AND PREDICTION OF EXTREMES*. Stavanger, 2018.
- [5] “Environmental Conditions and Environmental Loads - DNV-RP-C205.” Det Norske Veritas AS, Apr. 2014.
- [6] Peter S. Tromans and Luc Vanderschuren, “Response Based Design Conditions in the North Sea: Application of a new Method,” Houston, Texas, 1995.
- [7] I. M. Solbrekke, A. Sorteberg, and H. Haakenstad, “Norwegian hindcast archive (NORA3) - A validation of offshore wind resources in the North Sea and Norwegian Sea,” Apr. 2021. doi: 10.5194/wes-2021-22.
- [8] Sverre Haver and K. A. Nyhus, “A Wave Climate Model for Long Term Response Calculations,” presented at the Proceedings of OMAE 1986, Tokyo, Apr. 1986.
- [9] Sverre Haver, Gro Sagli Baarholm, and Kjersti Bruserud, “Environmental contour method: An approximate method for obtaining characteristic response extremes for design purposes,” Stavanger.
- [10] S. R. Winterstein, T. C. Ude, C. A. Cornell, P. Bjerager, and S. Haver, “ENVIRONMENTAL PARAMETERS FOR EXTREME RESPONSE: INVERSE FORM WITH OMISSION FACTOR,” presented at the Proceedings ICOSSAR-93, Innsbruck, Austria, Aug. 1993.
- [11] H. O. Madsen, S. Krenk, and N. C. Lind, *Methods of Structural Safety*. Mineola, New York: Dover Publications, inc., 2006.
- [12] J. Wang, L. Li, J. B. Jakobsen, and S. K. Haver, “Metocean Conditions in a Norwegian Fjord in Relation to the Floating Bridge Design,” *Journal of Offshore Mechanics and Arctic Engineering*, vol. 141, Oct. 2018, doi: 10.1115/1.4041534.
- [13] S. K. Haver and B. Anne Katrine, “Joint Probabilistic Model for Wind Sea and Swell: Results for Cases with Wind Sea South - Southeast Field.” Jan. 2018.

- [14] Srinivasan Chandrasekaran, *Dynamic Analysis and Design of Offshore Structures*, vol. 5. India: Springer, 2015.
- [15] Zafarullah Nizamani, *Environmental Load Factors and System Strength Evaluation of Offshore Jacket Platforms*, vol. 4. Malaysia: Springer.
- [16] Daniel Karunakaran and Sverre Haver, “Dynamic behaviour of Kvitebjørn jacket structure - Numerical predictions versus full-scale measurements,” EUROODYN, Paris, 2005.
- [17] Structural Engineering, Marintek, “USFOS Getting Started.” SINTEF GROUP, 10 2001.
- [18] O. T. Gudmestad, *Marine Technology and Operations - Theory & Practice*. Stavanger: WITpress, 2015.
- [19] USFOS, “USFOS.no,” Apr. 30, 2022. [Online]. Available: <https://www.usfos.no/>
- [20] Gro Sagli Baarholm, Sverre Haver, and Ole David Økland, “Combining contours of significant wave height and peak period with platform response distributions for predicting design response,” *Marine Structures*, vol. 23, Apr. 2010.
- [21] MARINETEK, “USFOS User’s Manual Chapter 3,” pp. 25–28, Feb. 17, 1999.
- [22] “USFOS Hydrodynamics - Theory Description of use Verification,” Feb. 10, 2010.
- [23] Klaus Hasselmann, “Measurements of Wind-wave growth and swell decay during the Joint North Sea Wave Project (JONSWAP),” Deutches Hydrographisches Institut, Hamburg, Jan. 1973.
- [24] Knut Torsethaugen and Sverre Haver, “Simplified double peak spectral model for ocean waves.” 2004.
- [25] “Irregular Wave, ULS. Spool to peak Elevation.” Accessed: Apr. 30, 2022. [Online]. Available: <https://www.usfos.no/examples/usfos/hydrodynamics/spoolwav1/index.html>
- [26] George Forristall, “Wave Crest Distributions: Observations and Second-Order Theory,” *Journal of Physical Oceanography*, Aug. 2000, doi: 10.1175/1520-0485(2000)030<1931:WCDOAS>2.0.CO;2.
- [27] “Prediction of air gap for column stabilised units - DNVGL-OTG-13.” Jun. 2019.
- [28] K. Bury, *Statistical Models in applied Science*. New York: John Wiley & Sons, 1975.

## APPENDICES

## A Scatter diagram

Table 22: Scatter diagram for all  $H_s$  and  $T_p$  values. Data is obtained from hindcast.

Hs [m] Tp[s]	2-3	3-4	4-5	5-6	6-7	7-8	8-9	9-10	10-11	11-12	12-13	13-14	14-15	15-16	16-17	17-18	18-19	19-20	20-21	21-22	22-23	Sum
0-5	0	1	33	20	18	17	15	5	2	0	0	0	0	1	0	0	0	0	0	0	0	112
0.5-1	1	84	577	1562	2217	1725	1215	776	379	230	129	50	28	18	9	4	1	2	1	0	0	9008
1-1.5	0	23	925	2728	4596	6158	5616	3503	2059	1079	584	251	144	100	65	32	17	4	2	2	1	27889
1.5-2	0	0	211	1920	4058	4728	6223	5419	3582	2139	1240	605	302	190	121	62	44	13	18	3	9	30887
2-2.5	0	0	13	442	2608	3801	4160	4844	4093	2718	1831	864	487	277	148	74	43	19	12	4	9	26447
2.5-3	0	0	0	76	1065	2722	3359	3559	3700	2932	1974	1081	583	292	158	60	63	18	18	5	3	21668
3-3.5	0	0	0	3	262	1295	2720	2608	2856	2648	1962	1150	620	401	184	93	64	15	13	7	4	16905
3.5-4	0	0	0	0	47	393	1732	2242	2271	2108	1737	967	679	443	188	107	70	19	15	9	1	13028
4-4.5	0	0	0	0	7	104	777	1610	1789	1592	1332	861	604	406	162	94	66	14	17	2	2	9439
4.5-5	0	0	0	0	0	12	272	953	1383	1300	1089	737	419	311	166	73	65	17	11	2	4	6814
5-5.5	0	0	0	0	0	5	85	468	931	1101	872	607	353	253	136	86	53	8	3	3	3	4967
5.5-6	0	0	0	0	0	0	17	162	526	827	793	449	265	221	92	48	42	3	3	1	2	3451
6-6.5	0	0	0	0	0	0	3	45	277	593	645	391	231	144	96	48	36	3	3	0	1	2516
6.5-7	0	0	0	0	0	0	0	10	118	325	522	342	179	117	60	44	32	2	2	0	0	1753
7-7.5	0	0	0	0	0	0	0	1	41	164	349	307	143	87	33	34	23	1	0	0	0	1183
7.5-8	0	0	0	0	0	0	0	1	17	92	200	283	143	65	22	32	27	1	1	0	0	884
8-8.5	0	0	0	0	0	0	0	0	3	18	105	213	110	64	31	22	14	1	0	0	0	581
8.5-9	0	0	0	0	0	0	0	0	0	8	46	145	98	56	21	10	5	0	1	0	0	390
9-9.5	0	0	0	0	0	0	0	0	1	4	14	84	77	58	12	11	11	0	0	0	0	272
9.5-10	0	0	0	0	0	0	0	0	0	1	11	43	82	40	13	5	7	0	1	0	0	203
10-10.5	0	0	0	0	0	0	0	0	0	0	1	19	47	25	15	8	5	0	0	0	0	120
10.5-11	0	0	0	0	0	0	0	0	0	0	1	11	25	20	7	6	2	0	0	0	0	72
11-11.5	0	0	0	0	0	0	0	0	0	0	1	14	18	9	4	4	0	0	0	0	0	50
11.5-12	0	0	0	0	0	0	0	0	0	0	1	0	7	6	8	1	0	0	0	0	0	23
12-12.5	0	0	0	0	0	0	0	0	0	0	0	0	5	2	12	3	1	0	0	0	0	23
12.5-13	0	0	0	0	0	0	0	0	0	0	0	0	4	2	3	2	2	0	0	0	0	13
13-13.5	0	0	0	0	0	0	0	0	0	0	0	0	0	3	4	1	2	0	0	0	0	10
13.5-14	0	0	0	0	0	0	0	0	0	0	0	0	0	0	4	0	4	0	0	0	0	8
14-14.5	0	0	0	0	0	0	0	0	0	0	0	0	0	1	1	1	1	0	0	0	0	4
14.5-15	0	0	0	0	0	0	0	0	0	0	0	0	0	0	2	2	1	0	0	0	0	5
<b>Sum</b>	<b>1</b>	<b>108</b>	<b>1759</b>	<b>6751</b>	<b>14878</b>	<b>20960</b>	<b>26194</b>	<b>26206</b>	<b>24028</b>	<b>19879</b>	<b>15438</b>	<b>9461</b>	<b>5649</b>	<b>3621</b>	<b>1782</b>	<b>967</b>	<b>705</b>	<b>140</b>	<b>121</b>	<b>38</b>	<b>39</b>	<b>178725</b>

## B Modified scatter diagram

Table 23: Modified scatter diagram for all  $H_s$  and  $T_p$  values over the threshold of 8 m. Data is obtained from hindcast.

Hs [m]   Tp[s]	10-11	11-12	12-13	13-14	14-15	15-16	16-17	17-18	18-19	19-20	20-21	Sum
8-8.5	3	18	105	213	110	64	31	22	14	1	0	581
8.5-9	0	8	46	145	98	56	21	10	5	0	1	390
9-9.5	1	4	14	84	77	58	12	11	11	0	0	272
9.5-10	0	1	11	43	82	40	13	5	7	0	1	203
10-10.5	0	0	1	19	47	25	15	8	5	0	0	120
10.5-11	0	0	1	11	25	20	7	6	2	0	0	72
11-11.5	0	0	0	1	14	18	9	4	4	0	0	50
11.5-12	0	0	1	0	7	6	8	1	0	0	0	23
12-12.5	0	0	0	0	5	2	12	3	1	0	0	23
12.5-13	0	0	0	0	4	2	3	2	2	0	0	13
13-13.5	0	0	0	0	0	3	4	1	2	0	0	10
13.5-14	0	0	0	0	0	0	4	0	4	0	0	8
14-14.5	0	0	0	0	0	1	1	1	1	0	0	4
14-5.15	0	0	0	0	0	0	2	2	1	0	0	5
<b>Sum</b>	4	31	179	516	469	295	142	76	59	1	2	<b>1774</b>

# C Results from modified all sea state

## C.1 Airgap

Table 24: Characteristic crest height values from the long term analysis in modified all sea state approach. The characteristic values are found in q-probabilities ULS and ALS.

ULS [m]	ALS [m]
18.61	24.33

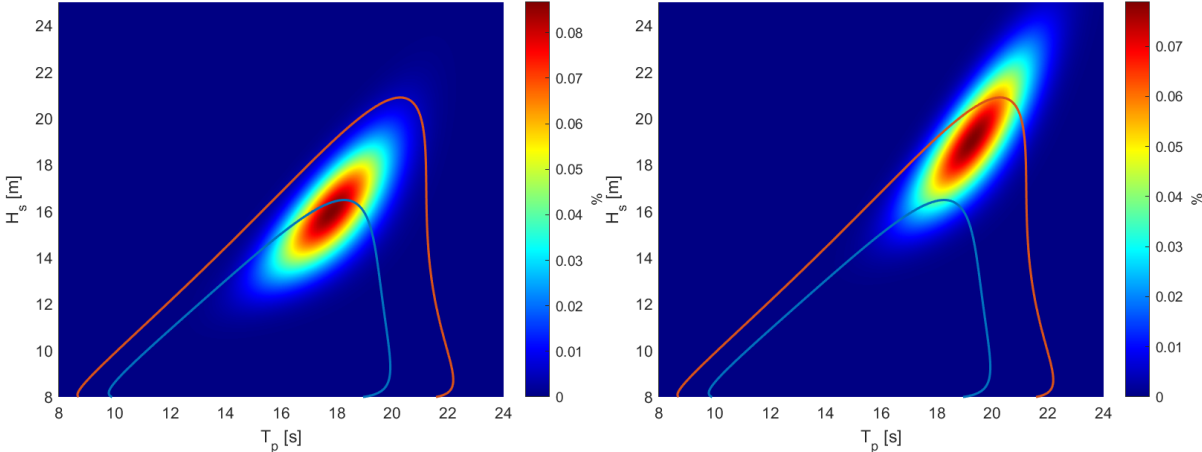


Figure 46: Relative contribution for the crest height to exceed ULS (left figure) and ALS (right figure) probabilities given the sea states in the modified all sea state approach.



## C.2 Deck displacement

Table 25: Characteristic deck displacement values from the long term analysis in modified all sea state approach. The characteristic values are found in  $q$ -probabilities ULS and ALS.

ULS [m]	ALS [m]
0.0792	0.1272

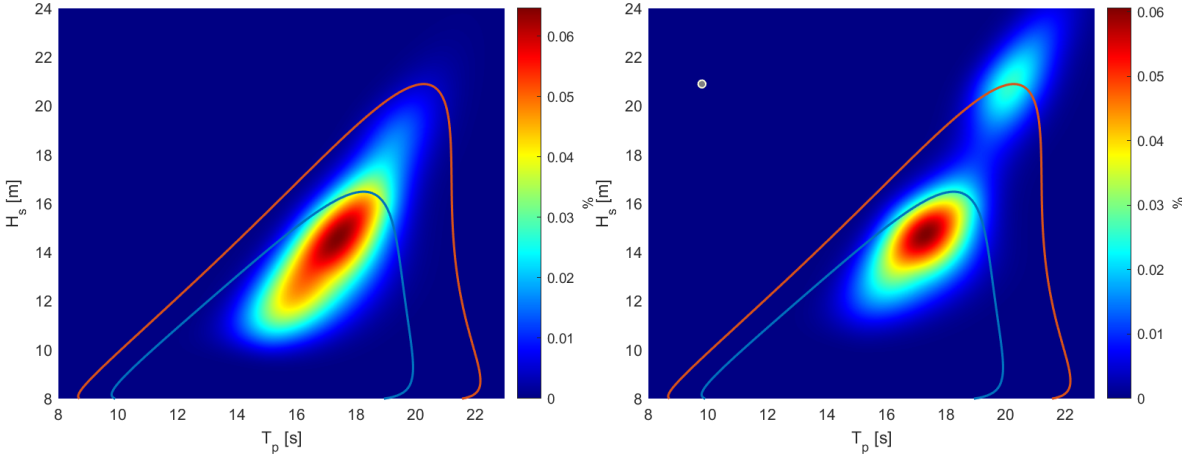


Figure 47: Relative contribution for the deck displacement exceeded ULS (left figure) and ALS (right figure) probabilities given the sea states in the modified all sea state approach.

### C.3 Overturning moment

Table 26: Characteristic overturning moment values from the long term analysis in modified all sea state approach. The characteristic values are found in q-probabilities ULS and ALS.

ULS [Nm]	ALS [Nm]
6.2214e+09	1.0530e+10

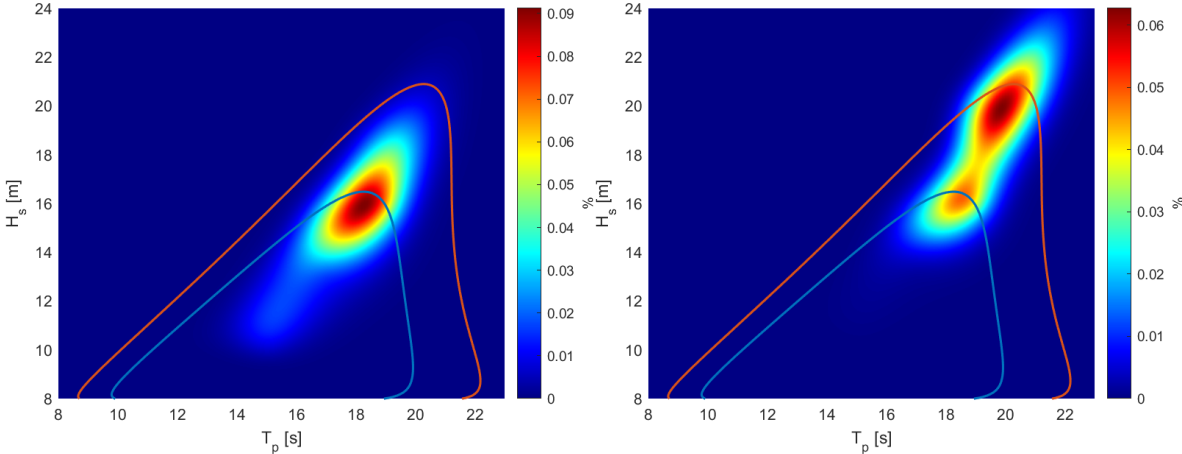


Figure 48: Relative contribution for the overturning moment to exceed ULS (left figure) and ALS (right figure) probabilities given the sea states in the modified all sea state approach.

### C.3 Base shear

Table 27: Characteristic base shear values from the long term analysis in modified all sea state approach. The characteristic values are found in  $q$ -probabilities ULS and ALS.

ULS [N]	ALS [N]
4.2389e+07	7.7881e+07

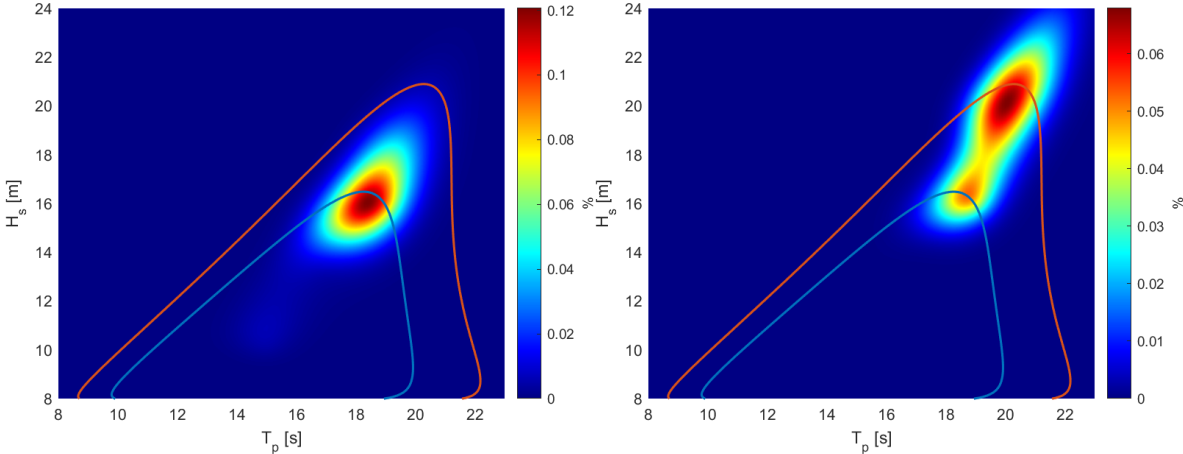


Figure 49: Relative contribution for the base shear to exceed ULS (left figure) and ALS (right figure) probabilities given the sea states in the modified all sea state approach.

## D Results from POT

### D.1 Airgap

Table 28: Summary of crest response values in a POT approach.

<b>Mpm 3-parameter Weibull fitting</b>			
<b>Threshold</b>	$\alpha$	$\beta$	$\lambda$
<b>8</b>	2.2674	1.3820	7.8390
<b>9</b>	2.2471	1.4461	8.8845
<b>10</b>	2.6045	1.6708	9.4800
<b>Mpm long term distribution</b>			
<b>Threshold</b>	ULS [m]	ALS [m]	
<b>8</b>	16.69	20.84	
<b>9</b>	16.56	20.31	
<b>10</b>	16.46	19.69	
<b>Beta</b>			
<b>Threshold</b>	$\beta_v$		
<b>8</b>	0.0636		
<b>9</b>	0.0639		
<b>10</b>	0.0654		
<b>Long term distribution crest height</b>			
<b>Threshold</b>	ULS [m]	ALS [m]	
<b>8</b>	18.30	23.91	
<b>9</b>	18.23	23.58	
<b>10</b>	18.25	23.42	

## D.2 Deck displacement

Table 29: Summary of deck displacement response values in a POT approach.

<b>Mpm 3-parameter Weibull fitting</b>			
<b>Threshold</b>	$\alpha$	$\beta$	$\lambda$
<b>8</b>	0.0099	1.2091	0.0087
<b>9</b>	0.0113	1.3544	0.0125
<b>10</b>	0.0147	1.5785	0.0128
<b>Mpm long term distribution</b>			
<b>Threshold</b>	ULS [m]	ALS [m]	
<b>8</b>	0.0561	0.0823	
<b>9</b>	0.0548	0.0772	
<b>10</b>	0.0551	0.0758	
<b>Beta</b>			
<b>Threshold</b>	$\beta_v$		
<b>8</b>	0.2201		
<b>9</b>	0.2638		
<b>10</b>	0.2900		
<b>Long term distribution of deck displacement</b>			
<b>Threshold</b>	ULS [m]	ALS [m]	
<b>8</b>	0.0781	0.1351	
<b>9</b>	0.0838	0.1459	
<b>10</b>	0.0876	0.1553	

### D.3 Overturning moment

Table 30: Summary of overturning moment response values in a POT approach.

<b>Mpm 3-parameter Weibull fitting</b>			
<b>Threshold</b>	$\alpha$	$\beta$	$\lambda$
<b>8</b>	8.0522e+08	1.3284	9.2876e+08
<b>9</b>	8.4543e+08	1.4372	1.2598e+09
<b>10</b>	9.6618e+09	1.5126	1.3890e+09
<b>Mpm long term distribution</b>			
<b>Threshold</b>	ULS [Nm]	ALS [Nm]	
<b>8</b>	4.2509e+09	5.8838e+09	
<b>9</b>	4.1686e+09	5.6041e+09	
<b>10</b>	4.2603e+09	5.7576e+09	
<b>Beta</b>			
<b>Threshold</b>	$\beta_v$		
<b>8</b>	0.1758		
<b>9</b>	0.2104		
<b>10</b>	0.2334		
<b>Long term distribution of overturning moment</b>			
<b>Threshold</b>	ULS [Nm]	ALS [Nm]	
<b>8</b>	5.6203e+09	9.0127e+09	
<b>9</b>	5.9846e+09	9.7211e+09	
<b>10</b>	6.2547e+09	1.0506e+10	

## D.4 Base shear

Table 31: Summary of base shear response values in a POT approach.

<b>Mpm 3-parameter Weibull fitting</b>			
<b>Threshold</b>	$\alpha$	$\beta$	$\lambda$
<b>8</b>	5.9516e+06	1.4481	4.6660e+06
<b>9</b>	6.0604e+06	1.5597	7.0309e+06
<b>10</b>	6.1300e+06	1.4755	8.3115e+06
<b>Mpm long term distribution</b>			
<b>Threshold</b>	ULS [N]	ALS [N]	
<b>8</b>	2.6507e+07	3.6183e+07	
<b>9</b>	2.5953e+07	3.4415e+07	
<b>10</b>	2.7050e+07	3.7132e+07	
<b>Beta</b>			
<b>Threshold</b>	$\beta_v$		
<b>8</b>	0.2002		
<b>9</b>	0.2258		
<b>10</b>	0.2456		
<b>Long term distribution of base shear</b>			
<b>Threshold</b>	ULS [N]	ALS [N]	
<b>8</b>	3.7136e+07	6.0348e+07	
<b>9</b>	3.8829e+07	6.3423e+07	
<b>10</b>	4.0358e+07	6.9012e+07	